Electronic Supplementary Information (ESI) II – structures, CV, UV-vis spectroscopy and DFT calculations

for

Isoelectronic Pt(II) Complexes of Cyclometalating C^N^N Ligands with Phenyl/(Benzo)thiophenyl/Pyridyl/(Benzo)thiazole Moieties

Maren Krause,[a] Joshua Nicolas Friedel,[a] Stefan Buss,[b] Dana Brünink,[c] Annemarie Berger,[a] Cristian A. Strassert,[b,*] Nikos L. Doltsinis,[c,*]Axel Klein[a,*]

* to whom the correspondence should be addressed: e-mail: axel.klein@uni-koeln.de

Contents

Fig. S33 UV-vis absorption spectra of [Pt(ph(tbppy)btz)Cl] **(8)**, [Pt(ph(tbppy)btz)(CCPh)] **(9)**, [Pt(bth(tbppy)py)Cl] **(15)**, and [Pt(bth(tbppy)py)(CCPh)] **(16)**.

Fig. S34 UV-vis absorption spectra of [Pt(th(tbppy)tz)Cl] **(17)**, [Pt(th(tbppy)tz)(CCPh)] **(18)**, and [Pt(na(tbppy)tz)(CCPh)] **(6)**.

Fig. S35 TD-DFT-calculated UV-vis absorption spectra (THEO, red) compared to experimental spectra (EXP, black) of [Pt(ph(ppy)tz)Cl] (**1**) and [Pt(ph(tbppy)tz)Cl] (**2**).

Fig. S36 TD-DFT-calculated UV-vis absorption spectra (THEO, red) of compared to experimental spectra (EXP, black) of [Pt(th(tbppy)py)C≡CPh] (**12**), [Pt(ph(tbppy)tz)Cl] (**2**), and [Pt(th(tbppy)py)C≡CC$_6$F$_5$] (**13**).

Fig. S37 UV-vis absorption and emission spectra of [Pt(th(tbppy)py)(CCPh)] **(12)** and [Pt(bth(tbppy)py)(CCPh] **(16)** in CH_2Cl_2 at 298 K.

Fig. S38 UV-vis absorption and emission spectra of [Pt(th(ppy)py)Cl] **(10)** and [Pt(ph(ppy)py)Cl] in CH_2Cl_2 at 298 K.

Fig. S39 UV-vis absorption and emission spectra of [Pt(th(tbppy)py)Cl] **(11)** and [Pt(bth(tbppy)py)Cl] **(15)** in CH_2Cl_2 at 298 K.

Fig. S40 UV-vis absorption and emission spectra of [Pt(th(tbppy)py)X] **(11, 12, 13)** with X = Cl, CCPh, or CCC$_6$F$_5$ in CH_2Cl_2 at 298 K.

Fig. S41 UV-vis absorption and emission spectra of [Pt(ph(tbppy)tz)X] **(2, 3, 4)** with X = Cl, CCPh, or CCC$_6$F$_5$ in CH_2Cl_2 at 298 K.

Fig. S42 UV-vis absorption and emission spectra of [Pt(ph(ppy)py)Cl] and [Pt(ph(ppy)tz)Cl] **(1)** in CH_2Cl_2 at 298 K.

Fig. S43 UV-vis absorption and emission spectra of [Pt(ph(tbppy)tz)Cl] **(2)** and [Pt(na(tbppy)tz)Cl] **(5)** in CH_2Cl_2 at 298 K.

Fig. S44 UV-vis absorption and emission spectra of [Pt(ph(tbppy)tz)Cl] **(2)** and [Pt(ph(tbppy)btz)Cl] **(8)** in CH_2Cl_2 at 298 K.

Fig. S45 Normalised photoluminescence spectra of [Pt(th(tbppy)py)Cl] **(11)**, [Pt(ph(tbppy)tz)Cl] **(2)**, [Pt(th(tbppy)tz)Cl] **(17)**, [Pt(th(tbppy)py)CCPh] **(12)**, [Pt(ph(tbppy)tz)CCPh] **(3)** and [Pt(th(tbppy)tz)CCPh] **(18)** in CH_2Cl_2 at 298 K or frozen glassy CH_2Cl_2/MeOH matrices at 77 K.

Fig. S46 Normalised photoluminescence spectra of [Pt(ph(tbppy)tz)CCPh] **(3)**, [Pt(na(tbppy)tz)CCPh] **(6)** and [Pt(ph(tbppy)btz)CCPh] **(9)** in CH_2Cl_2 at 298 K and in frozen glassy CH_2Cl_2/MeOH matrices (V:V = 1:1) at 77 K.

Fig. S47 Normalised photoluminescence spectra of [Pt(th(tbppy)py)CCPh] **(12)** and [Pt(bth(tbppy)py)CCPh] **(16)** in CH_2Cl_2 at 298 K and in frozen glassy CH_2Cl_2/MeOH matrices (V:V = 1:1) at 77 K.

Fig. S48 Normalised photoluminescence spectra of [Pt(th(tbppy)py)CCPh] **(12)**, [Pt(ph(tbppy)tz)CCPh] **(3)** and [Pt(th(tbppy)tz)CCPh] **(18)** in CH_2Cl_2 at 298 K and in frozen glassy CH_2Cl_2/MeOH matrices (V:V = 1:1) at 77 K.

Fig. S49 Normalised emission spectra of [Pt(ph(ppy)tz)Cl] **(1)**, [Pt(th(ppy)py)Cl] **(10)** and [Pt(th(ppy)tz)Cl] in CH_2Cl_2 at 298 K.

Fig. S50 Normalised emission spectra of, [Pt(bth(tbppy)py)Cl] **(15)**, [Pt(bth(ppy)py)Cl] **(14)**, and [Pt(ph(ppy)btz)Cl] **(7)** and [Pt(na(ppy)tz)Cl] in CH_2Cl_2 at 298 K.

Fig. S51 Normalised emission spectra of [Pt(ph(tbppy)btz)(CCPh)] **(9)**, [Pt(ph(tbppy)btz)Cl] **(8)** , [Pt(na(tbppy)tz)Cl] **(5)** and [Pt(na(tbppy)tz)(CCPh)] **(6)** in CH_2Cl_2 at 298 K.

Fig. S52 Normalised emission spectra of [Pt(ph(tbppy)tz)X] with X = Cl, CCPh, or CCC$_6$F$_5$ **(2), (3)** and **(4)** in glassy frozen CH_2Cl_2/MeOH (1:1) matrix at 77 K.

Fig. S53 Excitation and emission spectra of [Pt(ph(tbppy)tz)(CCPh)] **(3)** at 298 K in CH_2Cl_2 and at 77 K in a frozen glassy CH_2Cl_2/MeOH matrix (V:V = 1:1).

Fig. S54 Time-resolved photoluminescence decay of [Pt(ph(tbppy)tz)CCPh] **(3)** in CH_2Cl_2 at 298 K (air-equilibrated).

Fig. S55 Time-resolved photoluminescence decay of [Pt(ph(tbppy)tz)CCPh] **(3)** in CH_2Cl_2 at 298 K (Ar-purged).

Fig. S56 Time-resolved photoluminescence decay of [Pt(ph(tbppy)tz)CCPh] **(3)** in a frozen glassy CH_2Cl_2/MeOH matrix (V:V = 1:1) at 77 K.

Fig. S57 Excitation and emission spectra of [Pt(ph(tbppy)tz)(CCC$_6$F$_5$)] **(4)** at 298 K in CH_2Cl_2 and at 77 K in a frozen glassy CH_2Cl_2/MeOH matrix (V:V = 1:1).

Fig. S58 Time-resolved photoluminescence decay of [Pt(ph(tbppy)tz)CC$_6$F$_5$] **(4)** in CH_2Cl_2 at 298 K (air-equilibrated).

Fig. S59 Time-resolved photoluminescence decay of [Pt(ph(tbppy)tz)CC$_6$F$_5$] **(4)** in CH_2Cl_2 at 298 K (Ar-purged).

Fig. S60 Time-resolved photoluminescence decay of [Pt(ph(tbppy)tz)CC$_6$F$_5$] **(4)** in a frozen glassy CH_2Cl_2/MeOH matrix (V:V = 1:1) at 77 K.

Fig. S61 Excitation and emission spectra of [Pt(na(tbppy)tz)(CCPh)] **(6)** at 298 K in CH_2Cl_2 and at 77 K in a frozen glassy CH_2Cl_2/MeOH matrix (V:V = 1:1).

Fig. S62 Time-resolved photoluminescence decay of [Pt(na(tbppy)tz)CCPh] **(6)** in CH_2Cl_2 at 298 K (air-equilibrated).

Fig. S63 Time-resolved photoluminescence decay of [Pt(na(tbppy)tz)CCPh] **(6)** in CH_2Cl_2 at 298 K (Ar-purged).

Fig. S64 Time-resolved photoluminescence decay of [Pt(na(tbppy)tz)CCPh] **(6)** in a frozen glassy CH_2Cl_2/MeOH matrix (V:V = 1:1) at 77 K.

Fig. S65 Excitation and emission spectra of [Pt(ph(tbppy)btz)Cl] **(8)** at 298 K in CH_2Cl_2 and at 77 K in a frozen glassy CH_2Cl_2/MeOH matrix (V:V = 1:1).

Supporting Tables

Photophysical characterisation

Steady-state excitation and emission spectra were recorded on a FluoTime300 spectrometer from PicoQuant equipped with a 300 W ozone-free Xe lamp (250-900 nm), a 10 W Xe flash-lamp (250-900 nm, pulse width < 10 μs) with repetition rates of 0.1 to 300 Hz, an excitation monochromator (Czerny-Turner 2.7 nm/mm dispersion, 1200 grooves/mm, blazed at 300 nm), diode lasers (pulse width < 80 ps) operated by a computer-controlled laser driver PDL-820 (repetition rate up to 80 MHz, burst mode for slow and weak decays), two emission monochromators (Czerny-Turner, selectable gratings blazed at 500 nm with 2.7 nm/mm dispersion and 1200 grooves/mm, or blazed at 1250 nm with 5.4 nm/mm dispersion and 600 grooves/mm), Glan-Thompson polarisers for excitation (Xe-lamps) and emission, a Peltier-thermostatised sample holder from Quantum Northwest (–40 °C to 105 °C), and two detectors, a PMA Hybrid 40 (transit time spread FWHM < 120 ps, 300 to 720 nm) and a R5509-42 NIR-photomultiplier tube (transit time spread FWHM 1.5 ns, 300-1400 nm) with external cooling (–80 °C) from Hamamatsu.

Steady-state and fluorescence lifetimes were recorded in TCSPC mode by a PicoHarp 300 (minimum base resolution 4 ps).

Phosphorescence lifetimes were recorded in MCS mode by a TimeHarp 300 (minimum base resolution 250 ps). Emission and excitation spectra were corrected for source intensity (lamp and grating) by standard correction curves.

Lifetime analysis was performed using the commercial FluoFit software. The quality of the fit was assessed by minimizing the reduced chi squared function (χ^2) and visual inspection of the weighted residuals and their autocorrelation.

Luminescence quantum yields (PLQY) were measured with a Hamamatsu Photonics absolute PL quantum yield measurement system (C9920-02) equipped with a L9799-01 CW Xenon light source (150 W), monochromator, C7473 photonic multi-channel analyser, integrating sphere and employing U6039-05 PLQY measurement software (Hamamatsu Photonics, Ltd., Shizuoka, Japan). The used dichloromethane was of spectroscopic grade (Uvasol®).

Supporting Figures

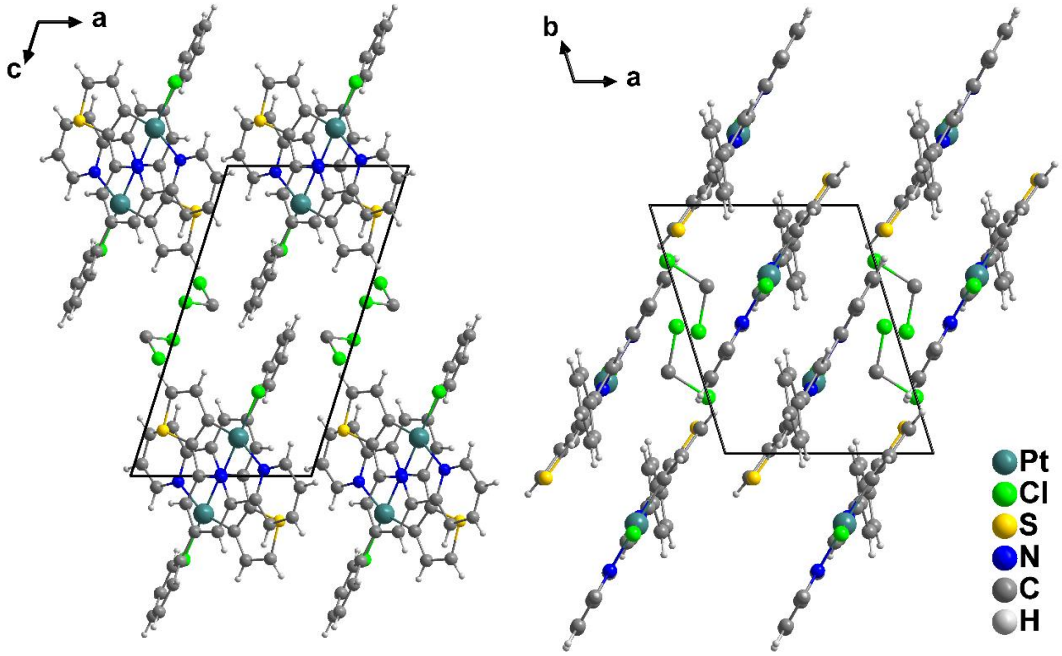

Fig. S1 Crystal structure of [Pt(th(ppy)py)Cl]·CD_2Cl_2 (**10**·CH_2Cl_2) viewed along the crystallographic *b* (left) and *c* (right) axes.

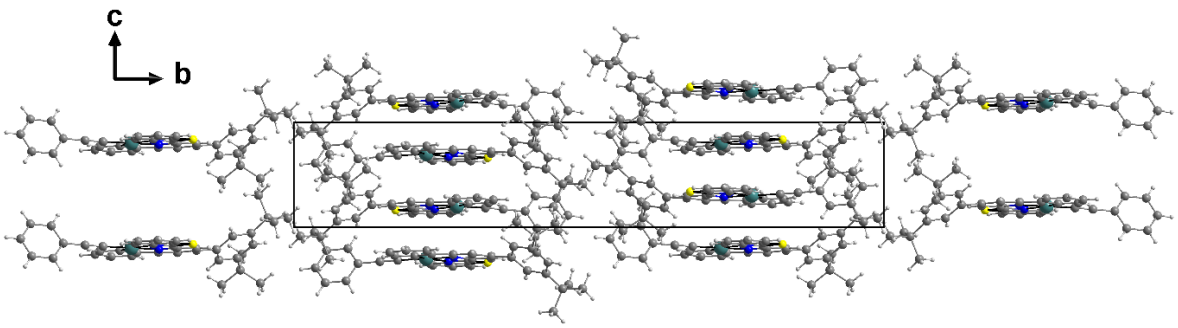

Fig. S2 Crystal structure of [Pt(ph(tbppy)bzt)CCPh] (**9**) viewed along the crystallographic *a* axis.

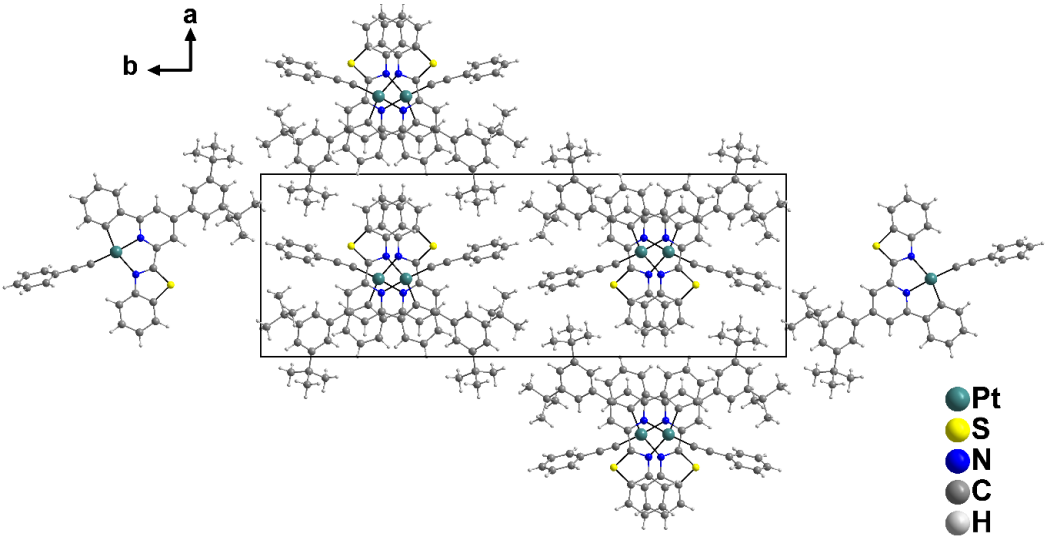

Fig. S3 Crystal structure of [Pt(ph(tbppy)bzt)CCPh] (**9**) viewed along the crystallographic *c* axis.

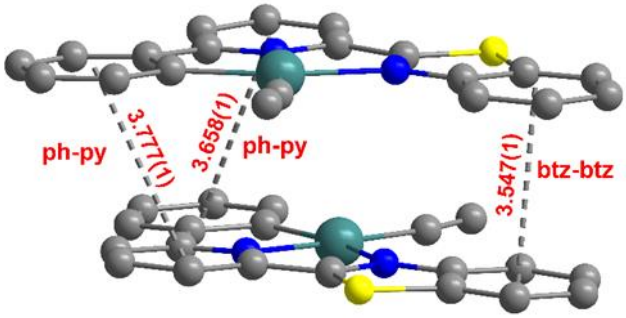

Fig. S4 Intermolecular π-stacking interactions in [Pt(ph(tbppy)bzt)CCPh] (**9**).

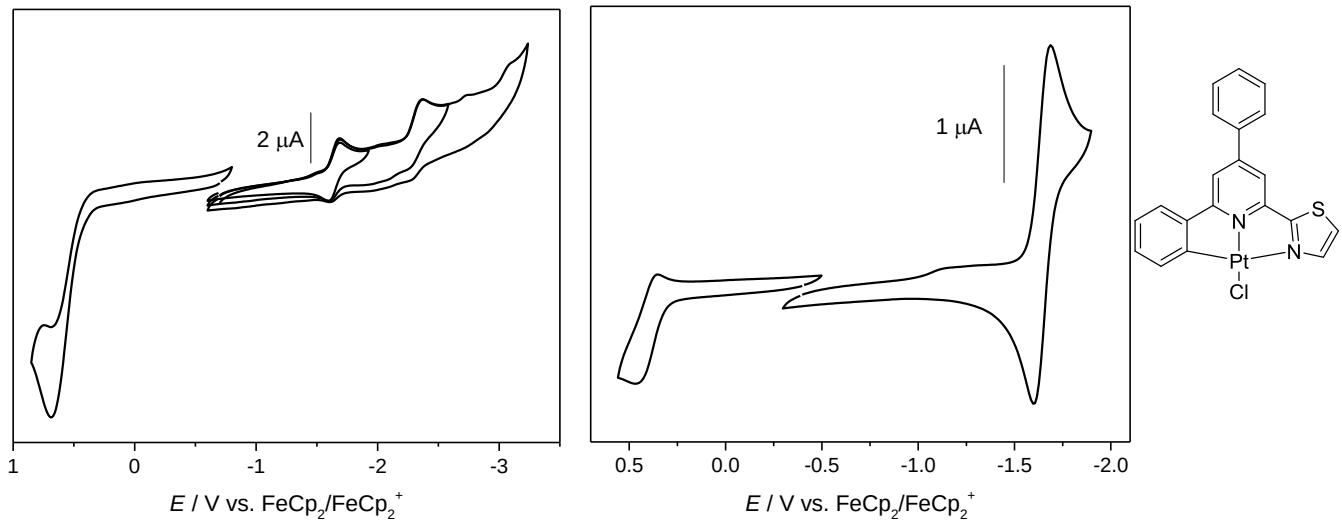

Fig. S5 Cyclic voltammograms of [Pt(ph(ppy)tz)Cl] **(1)** in 0.1 M *n*Bu$_4$NPF$_6$/THF (left) and 0.1 M /CH_2Cl_2 (right, Pt working electrode).

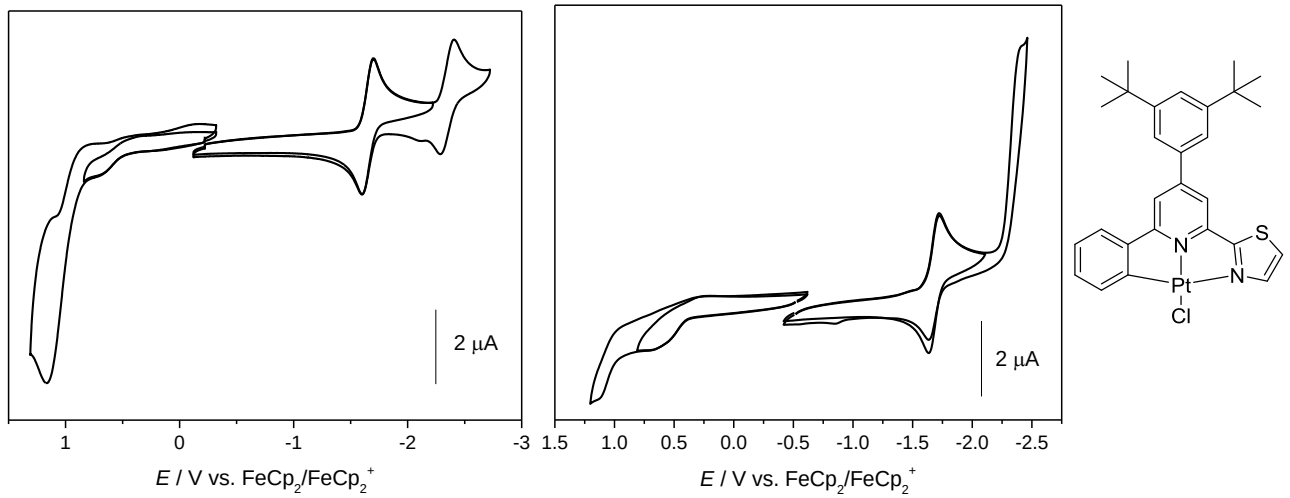

Fig. S6 Cyclic voltammograms of [Pt(ph(tbppy)tz)Cl] **(2)** in 0.1 M *n*Bu$_4$NPF$_6$/THF (left) and /CH_2Cl_2 (right).

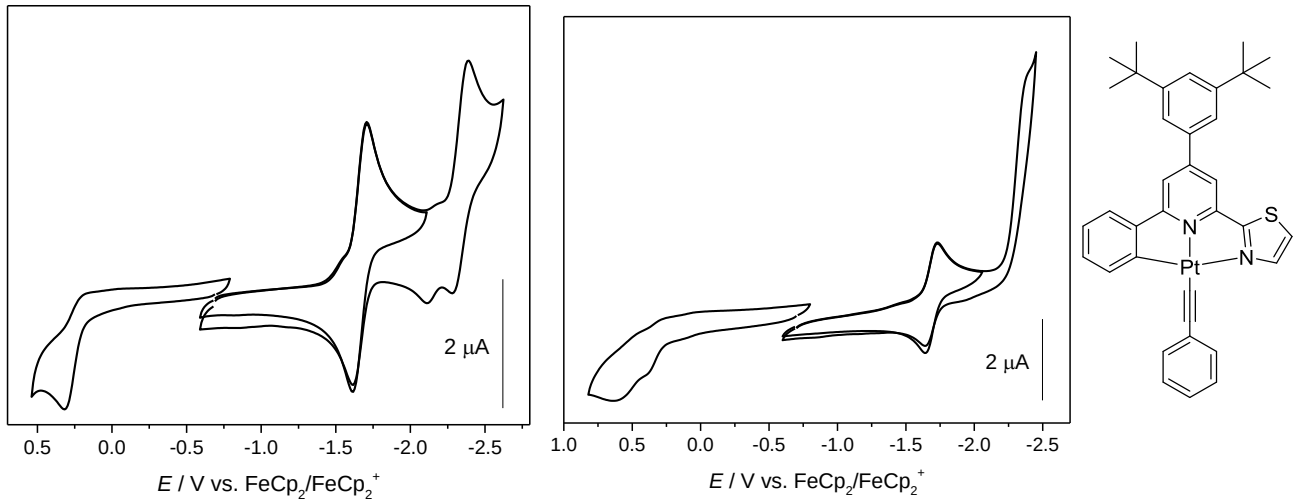

Fig. S7 Cyclic voltammograms of [Pt(ph(tbppy)tz)(CCPh)] **(3)** in 0.1 M *n*Bu$_4$NPF$_6$/THF (left) and /CH_2Cl_2 (right).

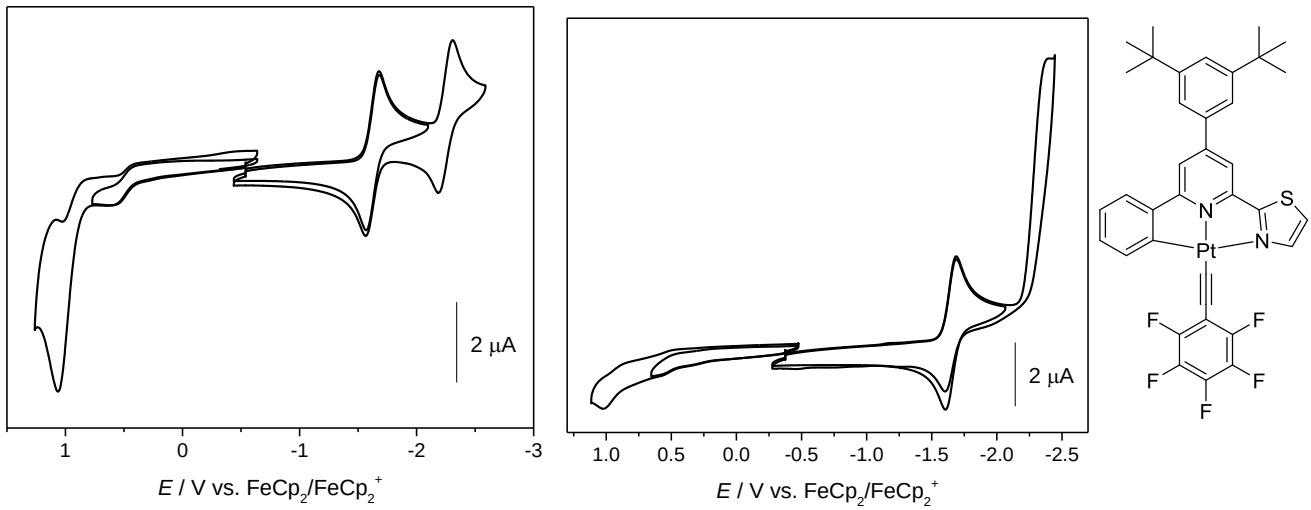

Fig. S8 Cyclic voltammograms of [Pt(ph(tbppy)tz)(CCC$_6$F$_5$)] **(4)** in 0.1 M *n*Bu$_4$NPF$_6$/THF (left) and /CH$_2$Cl$_2$ (right).

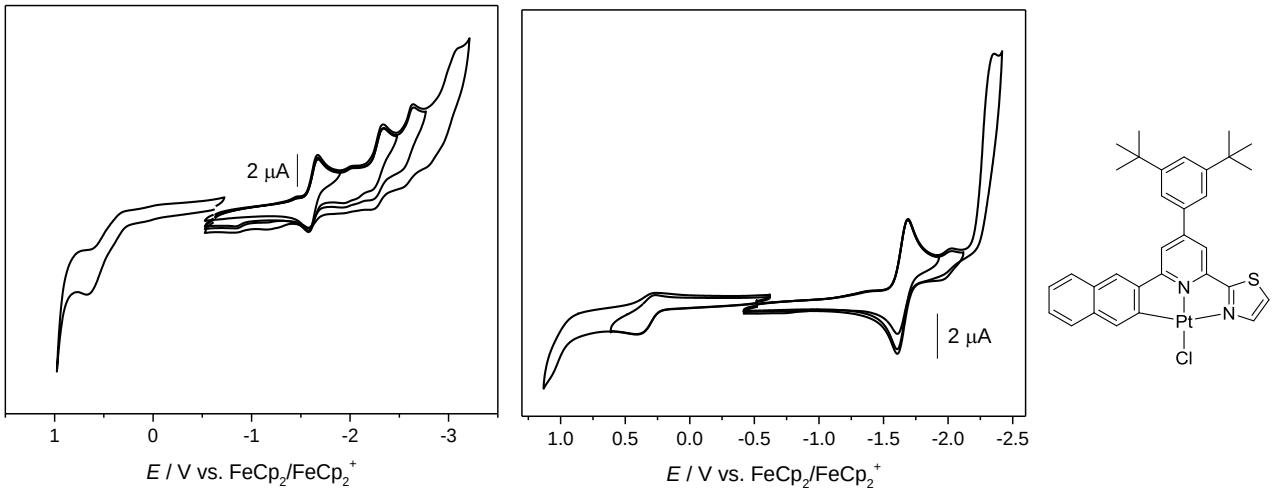

Fig. S9 Cyclic voltammograms of [Pt(na(tbppy)tz)Cl] **(5)** in 0.1 M *n*Bu$_4$NPF$_6$/THF (left) and /CH$_2$Cl$_2$ (right).

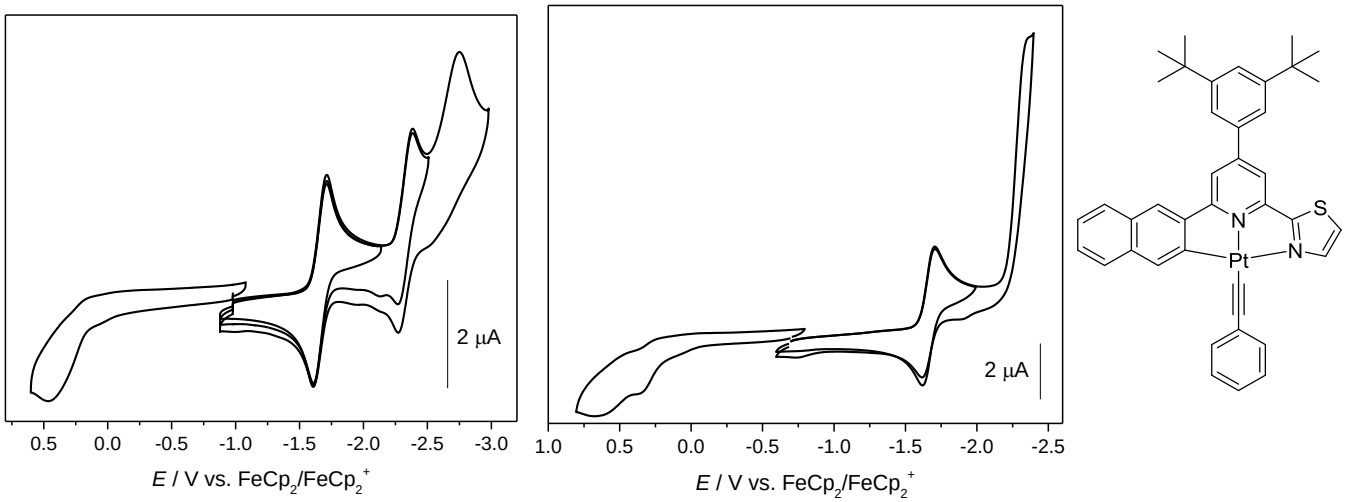

Fig. S10 Cyclic voltammograms of [Pt(na(tbppy)tz)(CCPh)] **(6)** in 0.1 M *n*Bu$_4$NPF$_6$/THF (left) and /CH$_2$Cl$_2$ (right).

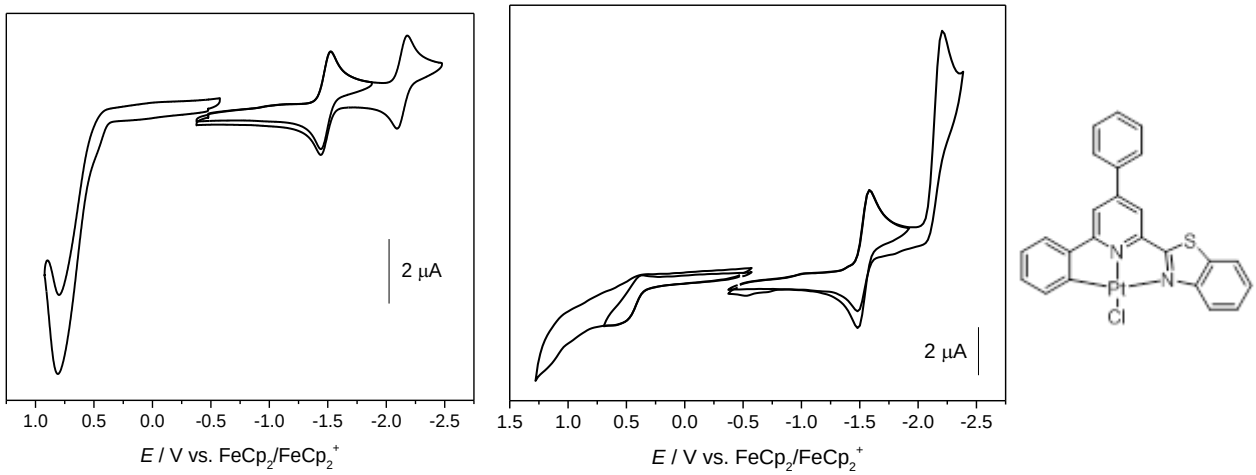

Fig. S11 Cyclic voltammograms of [Pt(ph(ppy)btz)Cl] **(7)** in 0.1 M nBu$_4$NPF$_6$/THF (left) and /CH_2Cl_2 (right).

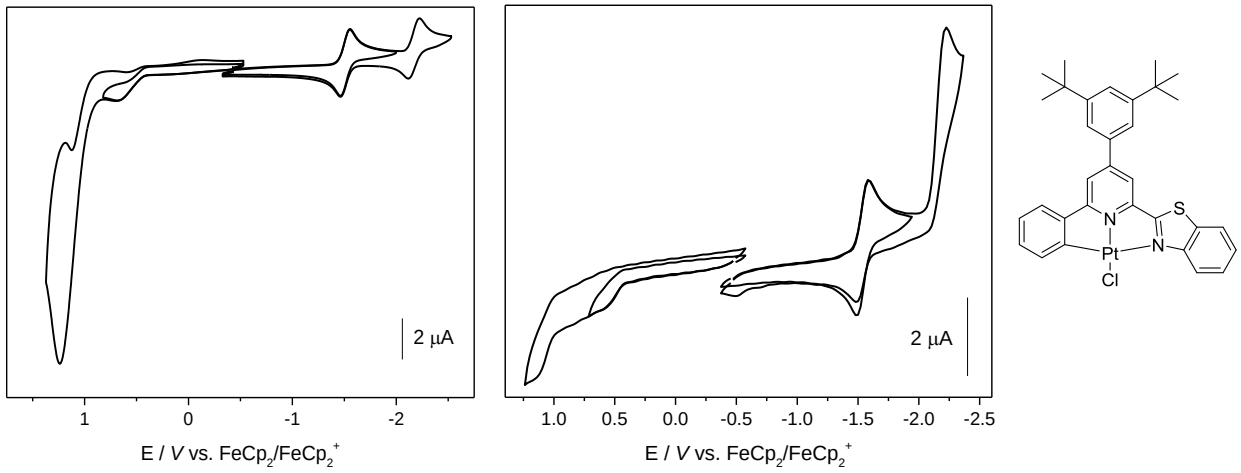

Fig. S12 Cyclic voltammograms of [Pt(ph(tbppy)btz)Cl] **(8)** in 0.1 M nBu$_4$NPF$_6$/THF (left) and /CH_2Cl_2 (right).

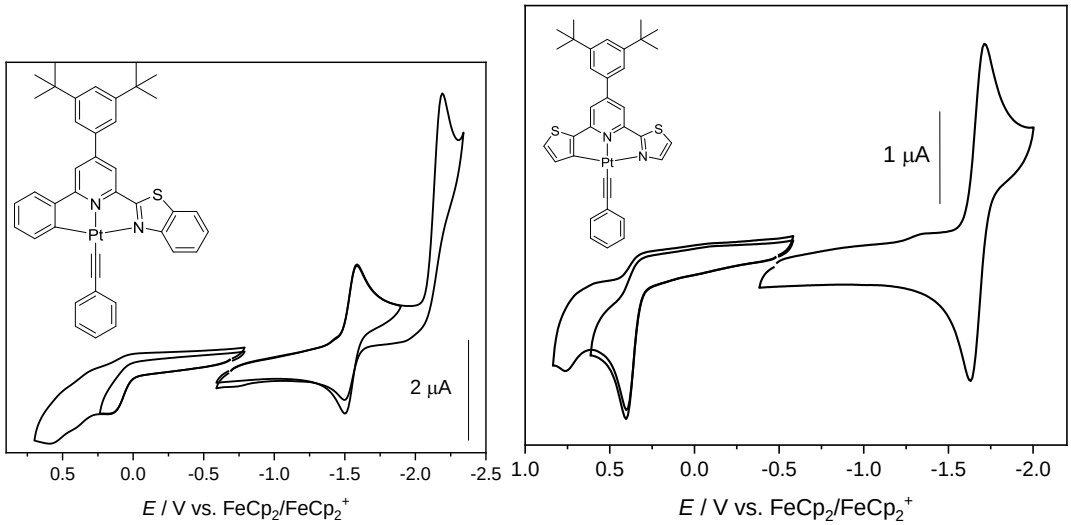

Fig. S13 Cyclic voltammograms of [Pt(ph(tbppy)btz)(CCPh)] **(9)** (left) and [Pt(th(tbppy)tz)(CCPh)] **(18)** (right) in 0.1 M nBu$_4$NPF$_6$/CH_2Cl_2.

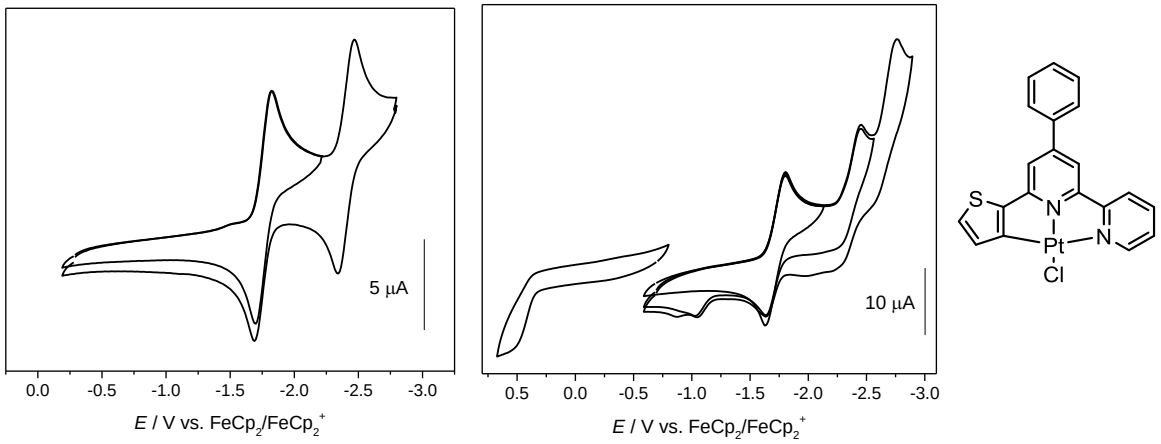

Fig. S14 Cyclic voltammograms of [Pt(th(ppy)py)Cl] (**10**) in 0.1 M nBu$_4$NPF$_6$/THF (left) and /DMF (right).

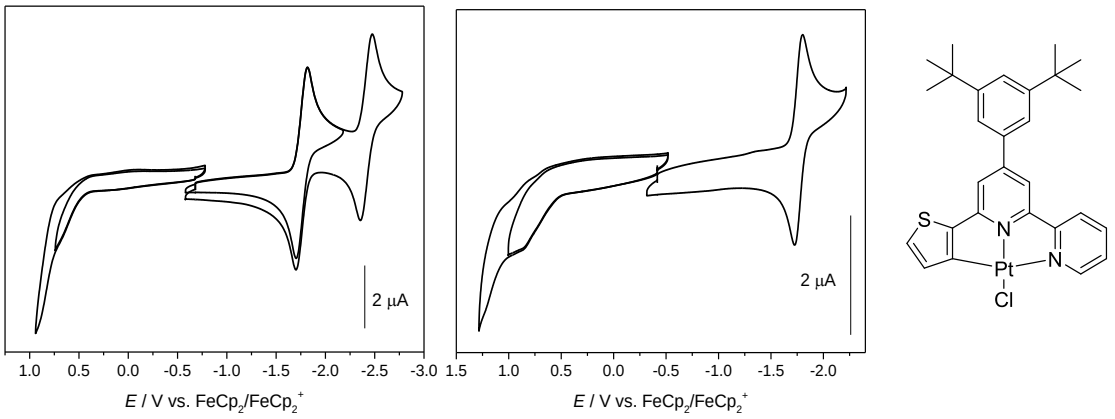

Fig. S15 Cyclic voltammograms of [Pt(th(tbppy)py)Cl] (**11**) in 0.1 M nBu$_4$NPF$_6$/THF (left) and 0.1 M /CH_2Cl_2 (right).

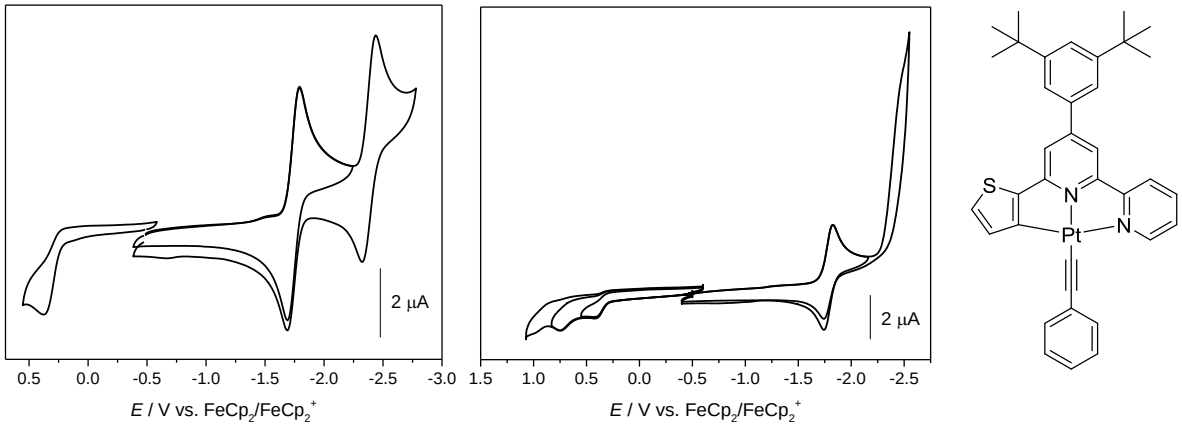

Fig. S16 Cyclic voltammograms of [Pt(th(tbppy)py)CCPh] (**12**) in 0.1 M nBu$_4$NPF$_6$/THF (left) and /CH_2Cl_2 (right).

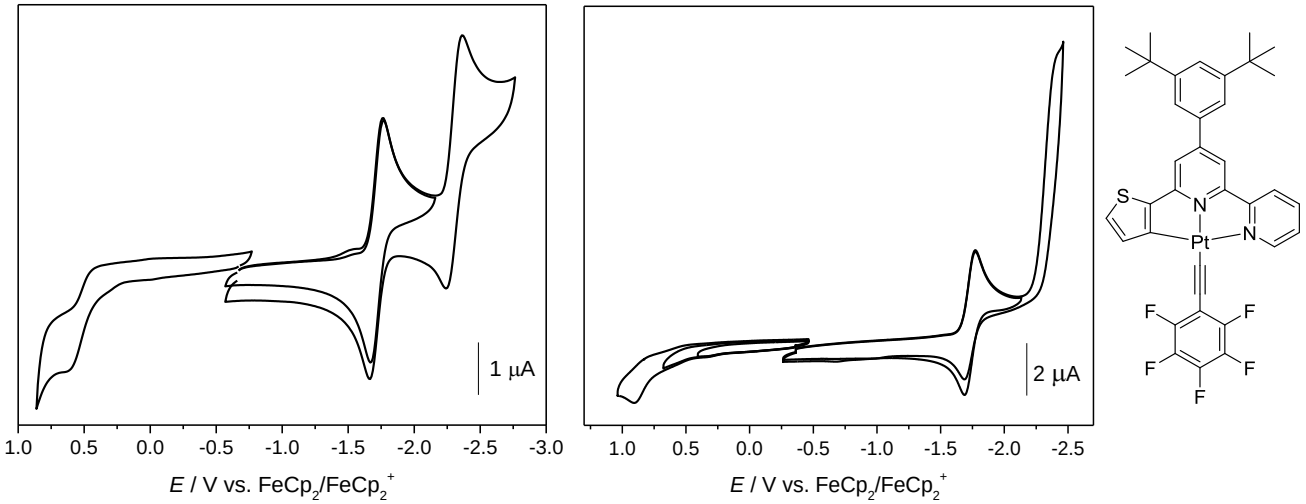

Fig. S17 Cyclic voltammograms of [Pt(th(tbppy)py)CCC$_6$F$_5$] (**13**) in 0.1 M *n*Bu$_4$NPF$_6$/THF (left) and /CH$_2$Cl$_2$ (right).

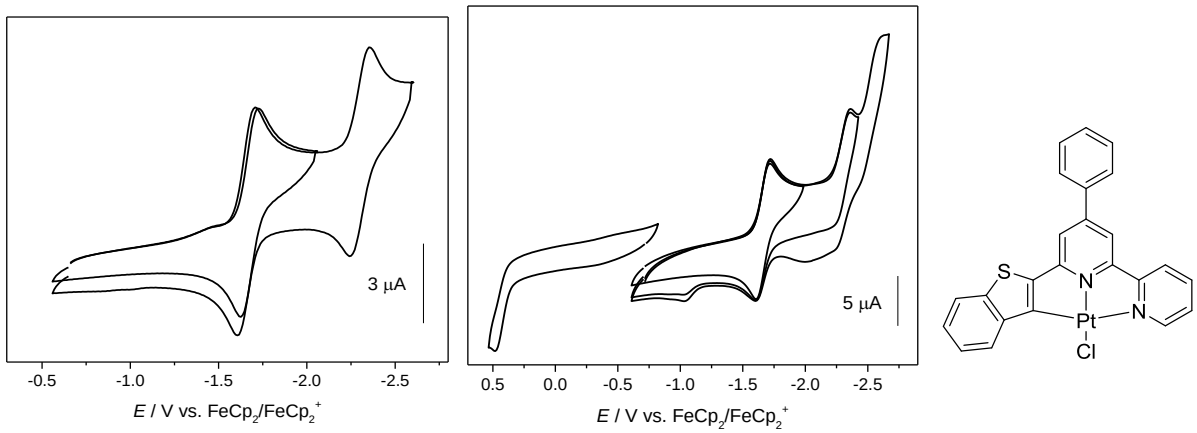

Fig. S18 Cyclic voltammograms of [Pt(bth(ppy)py)Cl] **(14)** in 0.1 M *n*Bu$_4$NPF$_6$/THF (left) and /DMF (right).

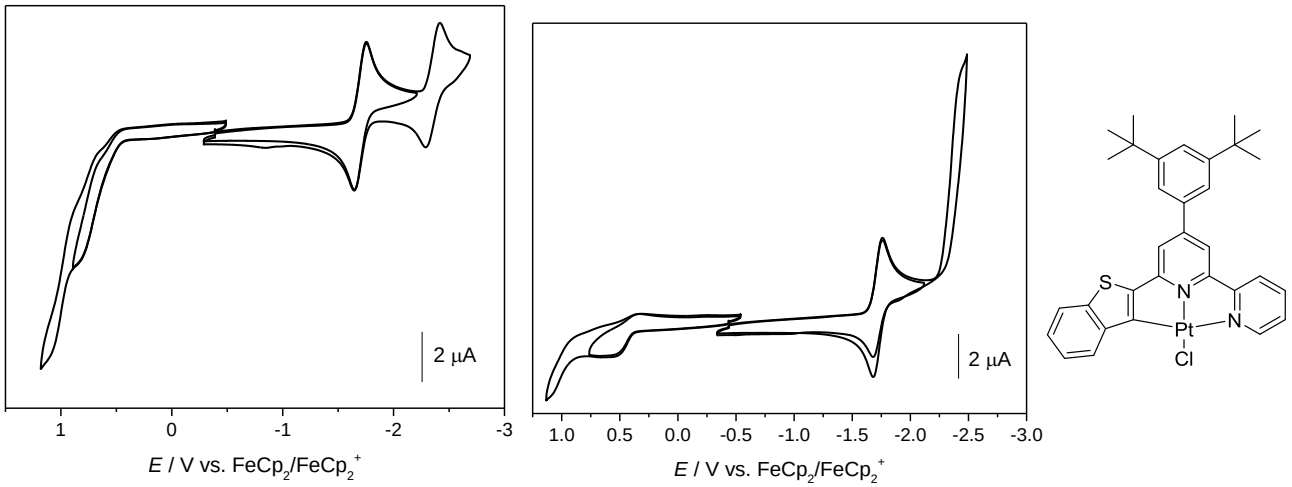

Fig. S19 Cyclic voltammograms of [Pt(bth(tbppy)py)Cl] **(15)** in 0.1 M *n*Bu$_4$NPF$_6$/THF (left) and /CH$_2$Cl$_2$ (right).

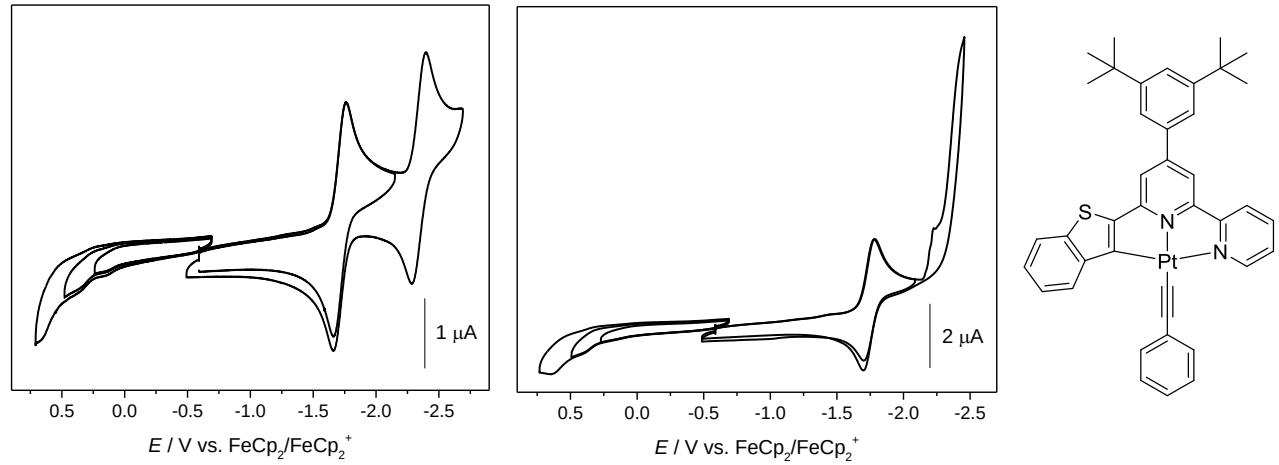

Fig. S20 Cyclic voltammograms of [Pt(bth(tbppy)py)CCPh] **(16)** in 0.1 M nBu$_4$NPF$_6$/THF (left) and /CH_2Cl_2 (right).

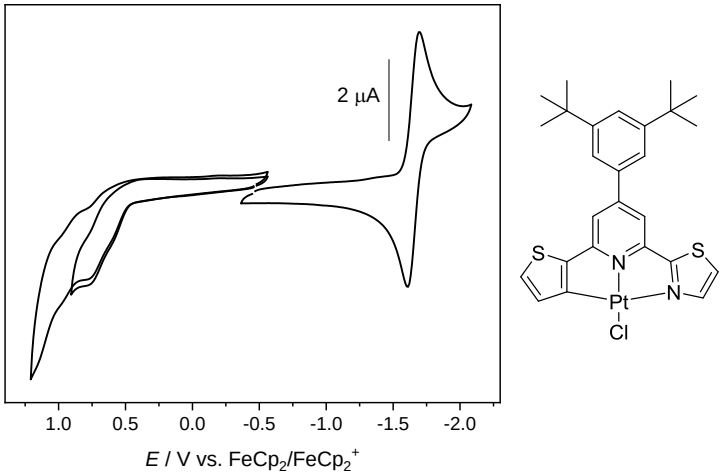

Fig. S21 Cyclic voltammograms of [Pt(th(tbppy)tz)Cl] **(17)** in 0.1 M nBu$_4$NPF$_6$/CH_2Cl_2.

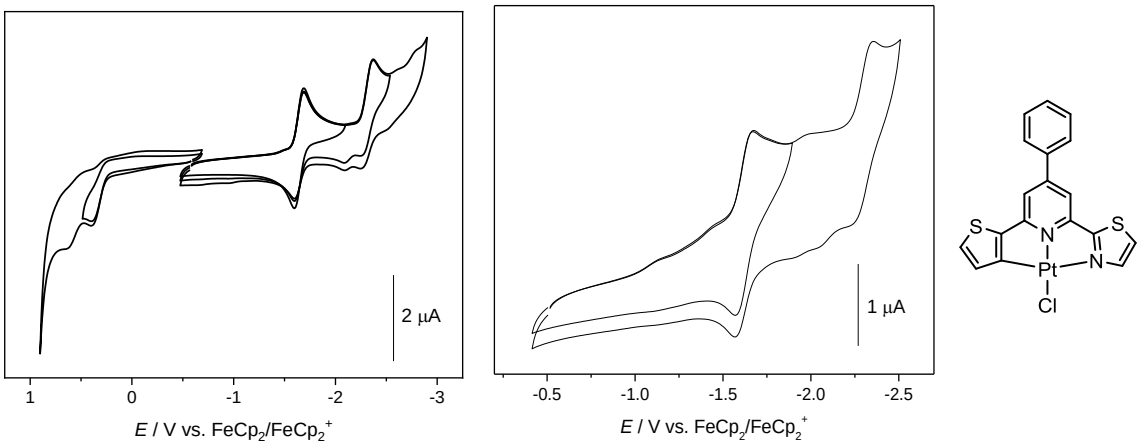

Fig. S22 Cyclic voltammograms of [Pt(th(ppy)tz)Cl] in 0.1 M nBu$_4$NPF$_6$/THF (left) and /CH_2Cl_2 (right).

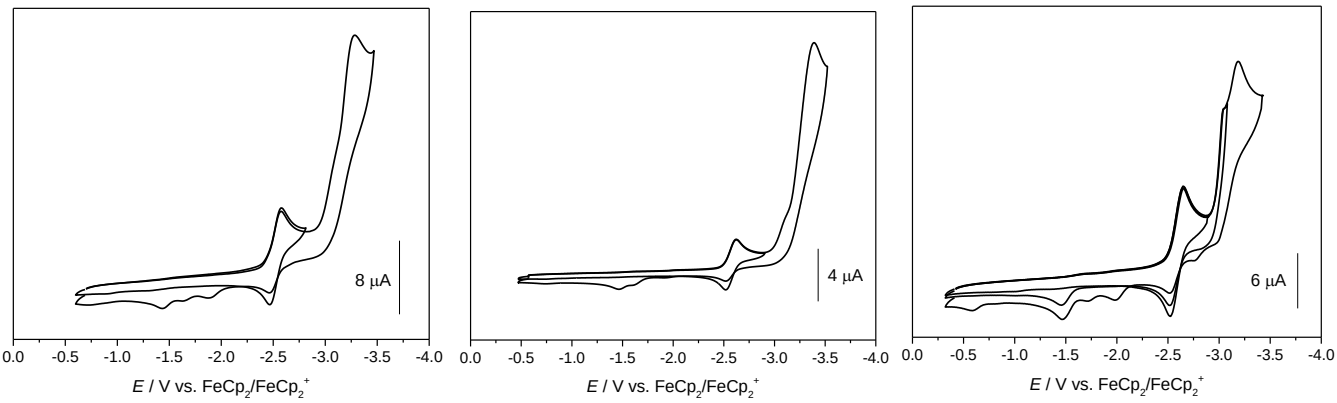

Fig. S23 Cyclic voltammograms of Hth(ppy)py (left), Hth(tbppy)py (middle), and Hbth(ppy)py (right) in 0.1 M nBu$_4$NPF$_6$/THF.

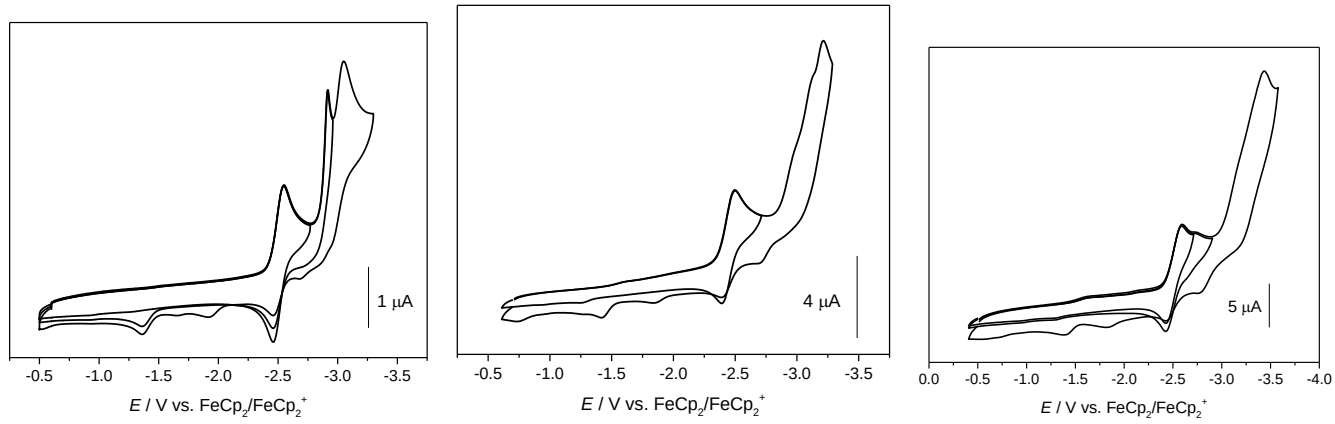

Fig. S24 Cyclic voltammograms of Hbth(tbppy)py (left), Hph(ppy)tz (middle), and Hph(tbppy)tz (right) in 0.1 M nBu$_4$NPF$_6$/THF.

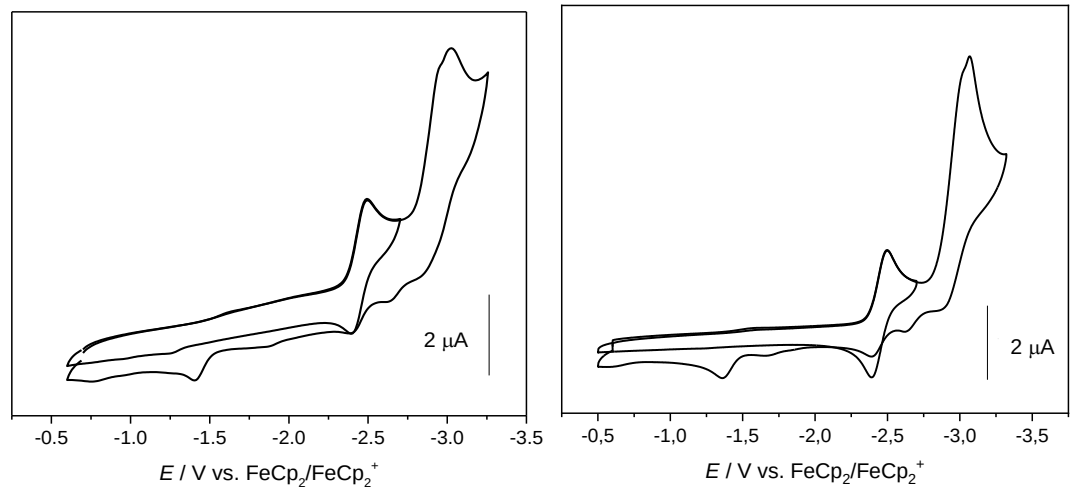

Fig. S25 Cyclic voltammograms of Hna(ppy)tz (left) and Hna(tbppy)tz (right) in 0.1 M nBu$_4$NPF$_6$/THF.

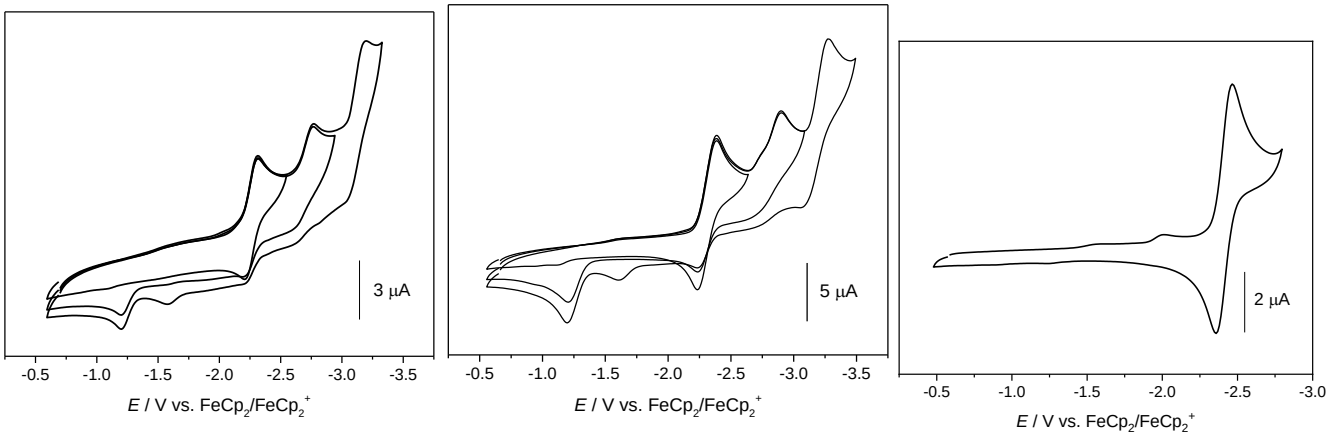

Fig. S26 Cyclic voltammograms of Hph(ppy)btz (left), Hph(tbppy)btz (middle), and Hth(tbppy)tz (right) in 0.1 M nBu$_4$NPF$_6$/THF.

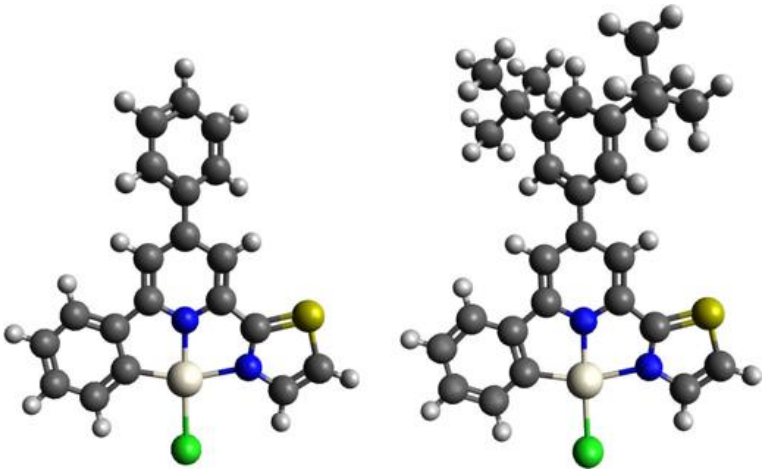

Fig. S27 DFT-optimised geometries of complexes from **class A** with coligand X = Cl and R^1 = H (left) and R^1 = 3,5-tBu$_2$ (right).

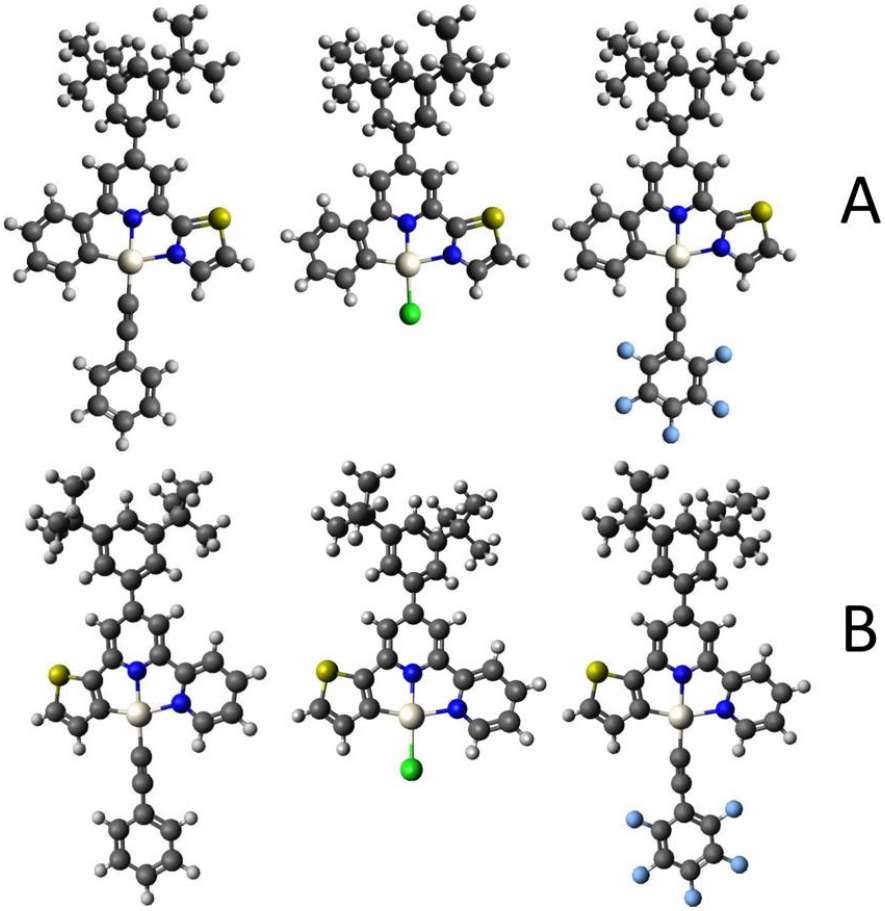

Fig. S28 DFT-optimised geometries of complexes from **classes A** and **B** with coligands X = CCPh, Cl, CCC_6F_5 (from left to right) and R^1 =3,5-*t*Bu_2.

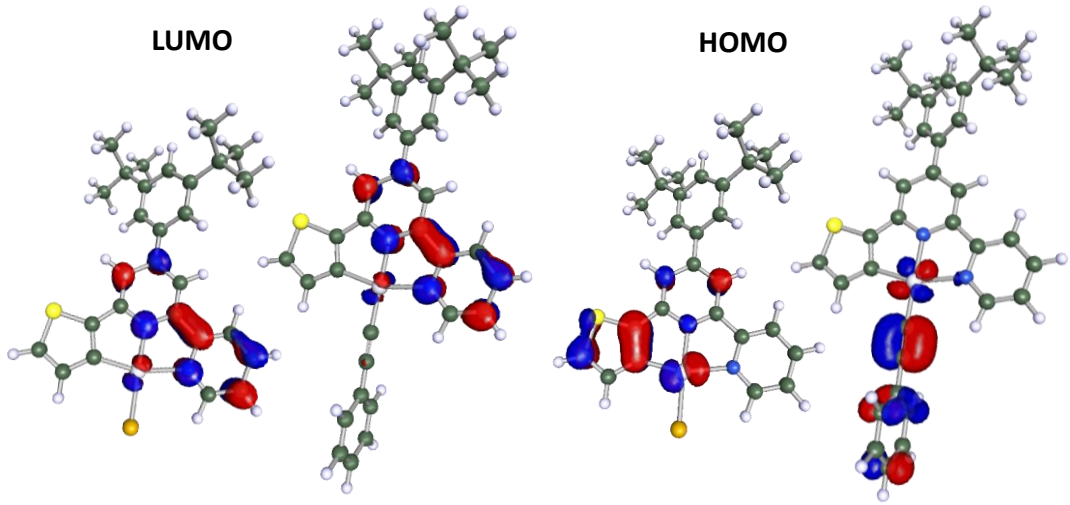

Fig. S29 DFT-calculated compositions of the lowest unoccupied molecular orbitals (LUMO) and highest occupied molecular orbitals (HOMO) of [Pt(th(tbppy)py)Cl] **(11)** and [Pt(th(tbppy)py)(CCPh)] **(12)** calculated on B3LYP level using def2-TZV(P) for C, H, N, S und LAN-L2DZ basis sets for Pt (ECP: Hay/Wadt (n = 1)), isosurface at 0.05.

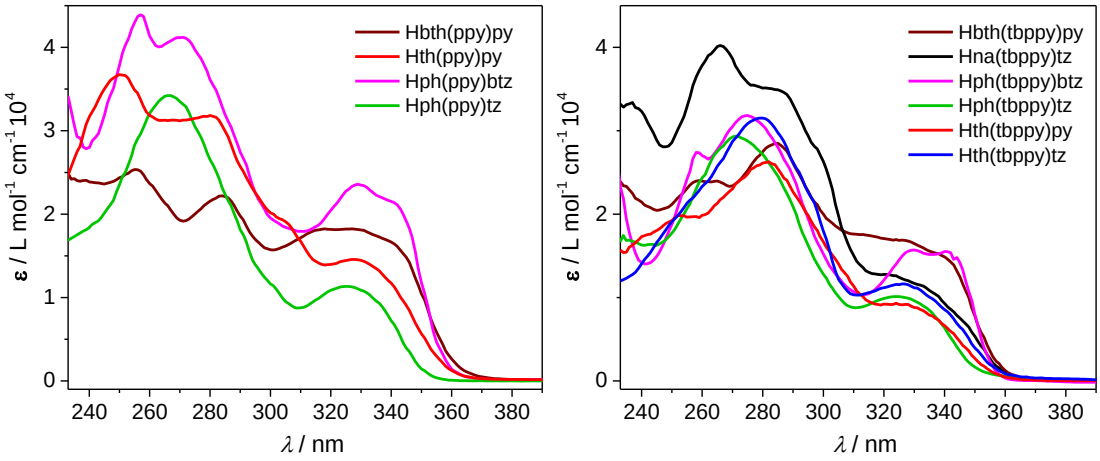

Fig. S30 UV-vis absorption spectra of HC^N^N protoligands with 4-phenyl-pyridyl (Hppy) (left) and 3,5-*t*Bu$_2$-phenyl-pyridyl (Htbppy) (right) in CH_2Cl_2 (298 K).

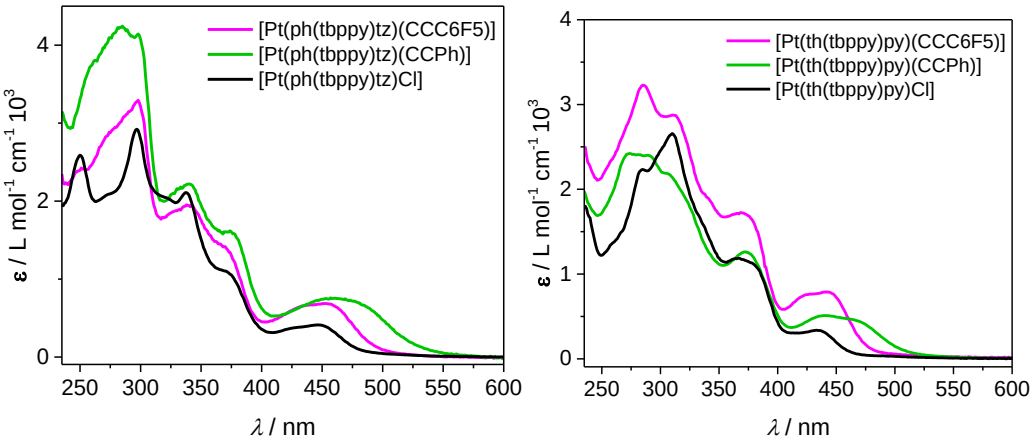

Fig. S31 UV-vis absorption spectra of [Pt(ph(tbppy)tz)(Cl/R)] (R = CCPh, CCC$_6$F$_5$) (**2**, **3**, **4**) (left) and [Pt(th(tbppy)py)(Cl/R)] (R = CCPh, CCC$_6$F$_5$) (**11**, **12**, **13**) (right) in CH_2Cl_2 (298 K).

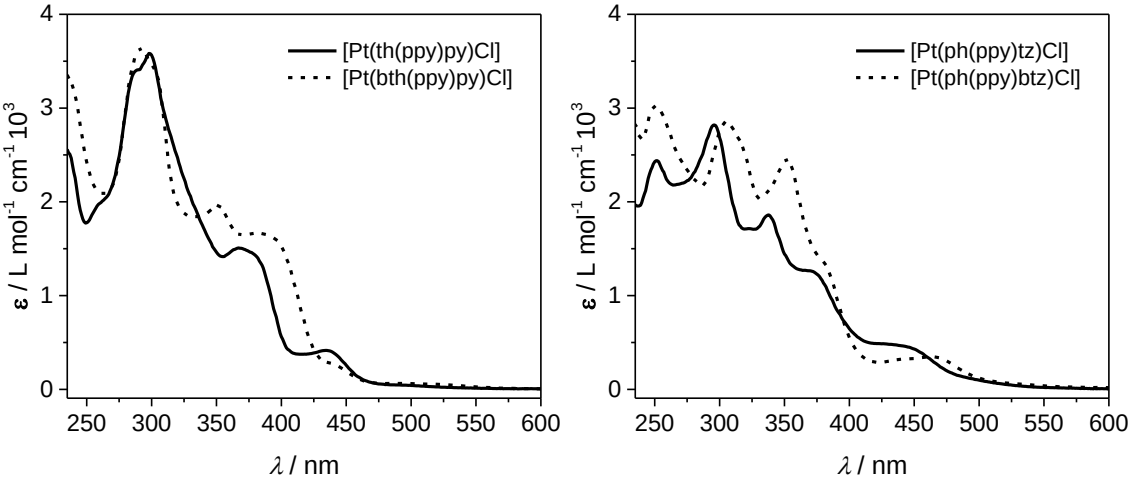

Fig. S32 UV-vis absorption spectra of [Pt(th(ppy)py)Cl] **(10)** and [Pt(bth(ppy)py)Cl] **(14)** (left) and [Pt(ph(ppy)tz)Cl] **(1)** and [Pt(ppy)btz)Cl] **(7)** (right) in CH_2Cl_2 (298 K).

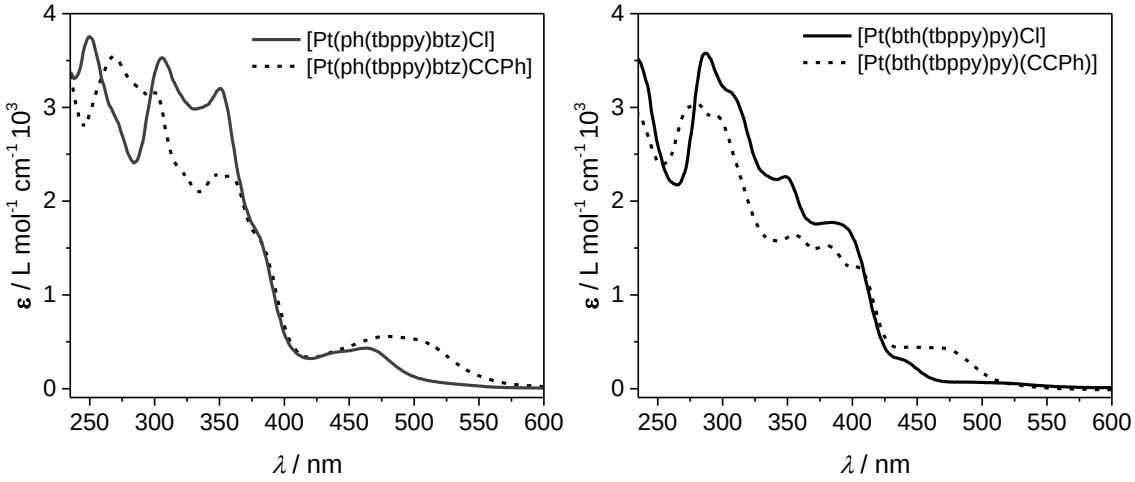

Fig. **S33** UV-vis absorption spectra of [Pt(ph(tbppy)btz)Cl] **(8)** and [Pt(ph(tbppy)btz)(CCPh)] **(9)** (left) and [Pt(bth(tbppy)py)Cl] **(15)** and [Pt(bth(tbppy)py)(CCPh)] **(16)** (right) in CH_2Cl_2 (298 K).

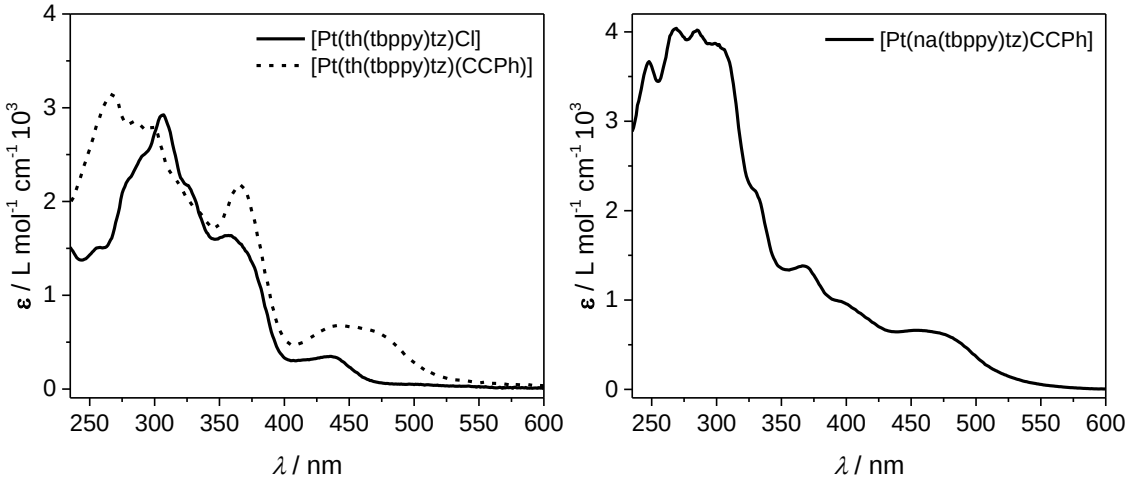

Fig. S34 UV-vis absorption spectra of [Pt(th(tbppy)tz)Cl] **(17)** and [Pt(th(tbppy)tz)(CCPh)] **(18)** (left) and [Pt(na(tbppy)tz)(CCPh)] **(6)** (right) in CH_2Cl_2 (298 K).

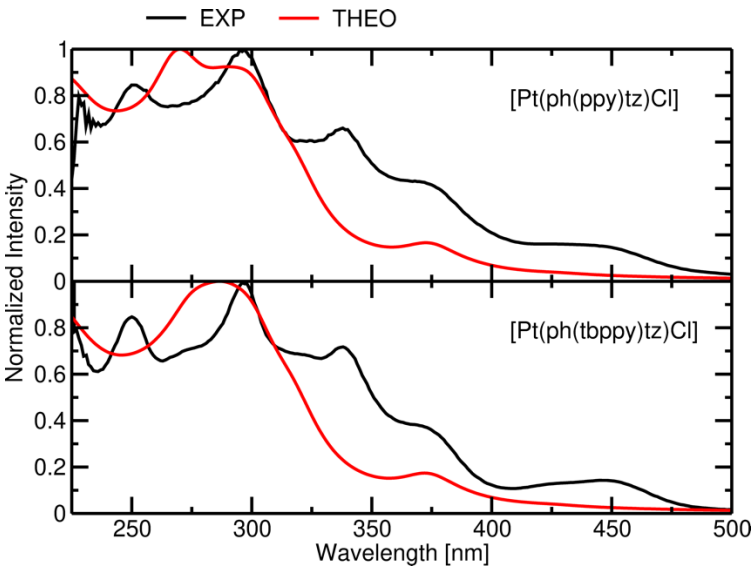

Fig. S35 TD-DFT-calculated UV-vis absorption spectra (THEO, red) compared to experimental spectra (EXP, black) of [Pt(ph(ppy)tz)Cl] (**1**) and [Pt(ph(tbppy)tz)Cl] (**2**).

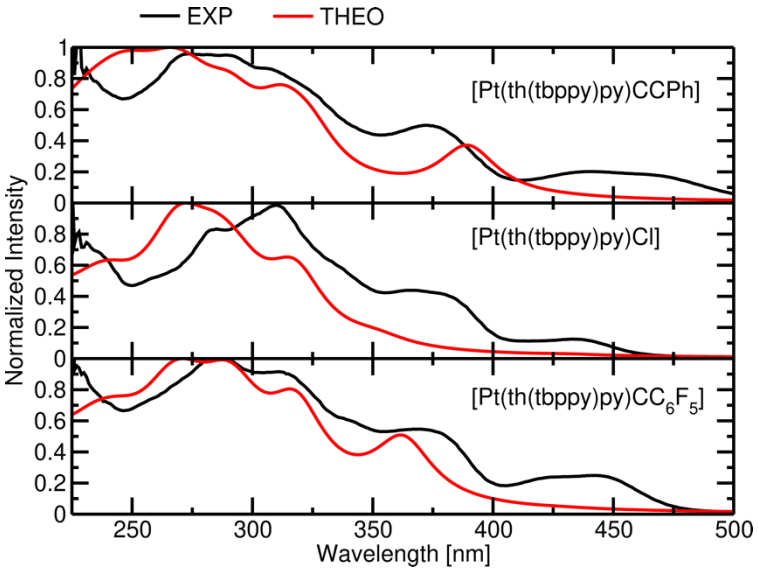

Fig. S36 TD-DFT-calculated UV-vis absorption spectra (THEO, red) of compared to experimental spectra (EXP, black) of [Pt(th(tbppy)py)C≡CPh] (**12**), [Pt(ph(tbppy)tz)Cl] (**2**), and [Pt(th(tbppy)py)C≡CC$_6$F$_5$] (**13**).

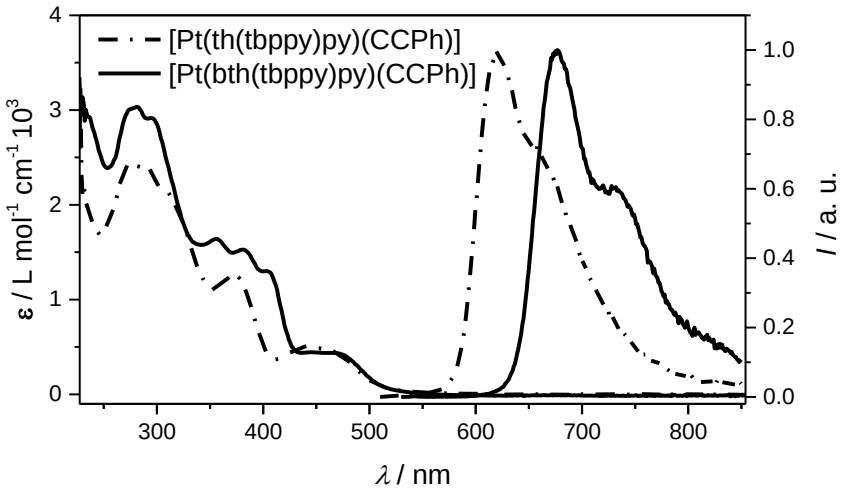

Fig. S37 UV-vis absorption spectra (left) and normalised emission spectra (right) of [Pt(th(tbppy)py)CCPh] **(12)** and [Pt(bth(tbppy)py)CCPh] **(16)** in CH_2Cl_2 at 298 K upon excitation at 350 nm.

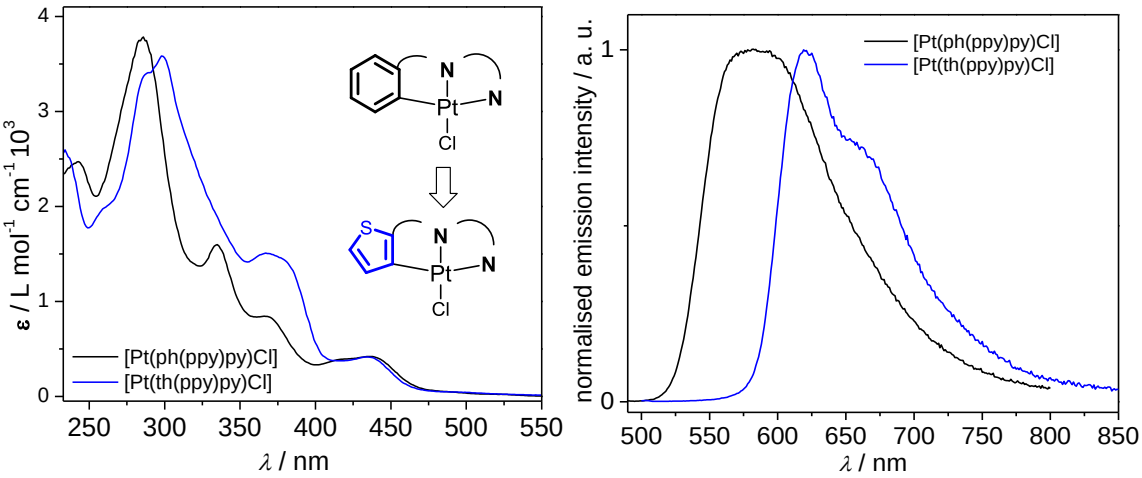

Fig. S38 UV-vis absorption spectra (left) and normalised emission spectra (right) of [Pt(th(ppy)py)Cl] **(10)** and [Pt(ph(ppy)py)Cl] in CH_2Cl_2 at 298 K upon excitation at 350 nm.

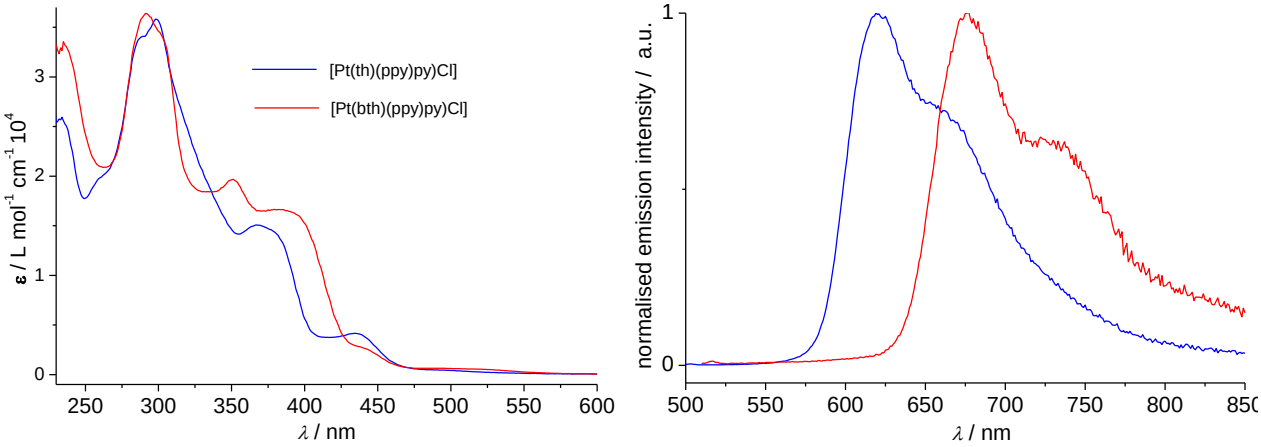

Fig. S39 UV-vis absorption spectra (left) and normalised emission spectra (right) of [Pt(th(tbppy)py)Cl] **(11)** and [Pt(bth(tbppy)py)Cl] **(15)** in CH_2Cl_2 at 298 K upon excitation at 350 nm.

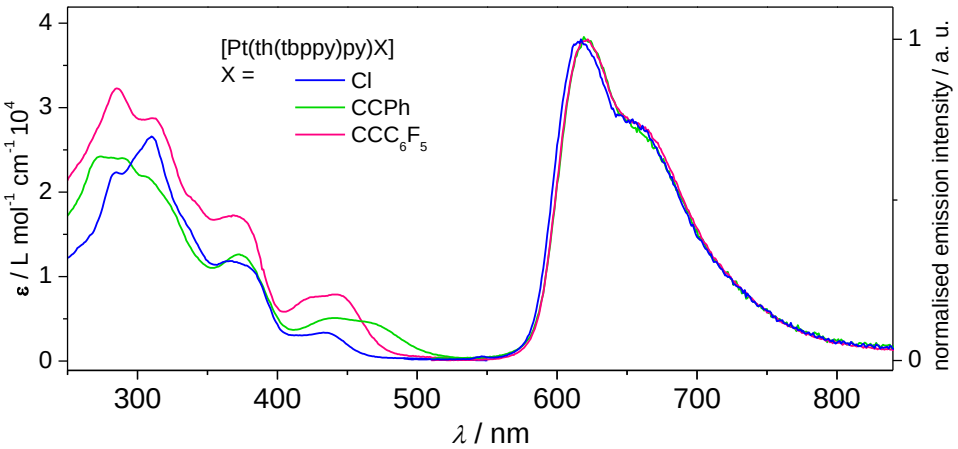

Fig. S40 UV-vis absorption spectra (left) and normalised emission spectra (right) of [Pt(th(tbppy)py)X] with X = Cl, CCPh, or CCC_6F_5 **(11, 12, 13)** in CH_2Cl_2 at 298 K upon excitation at 350 nm.

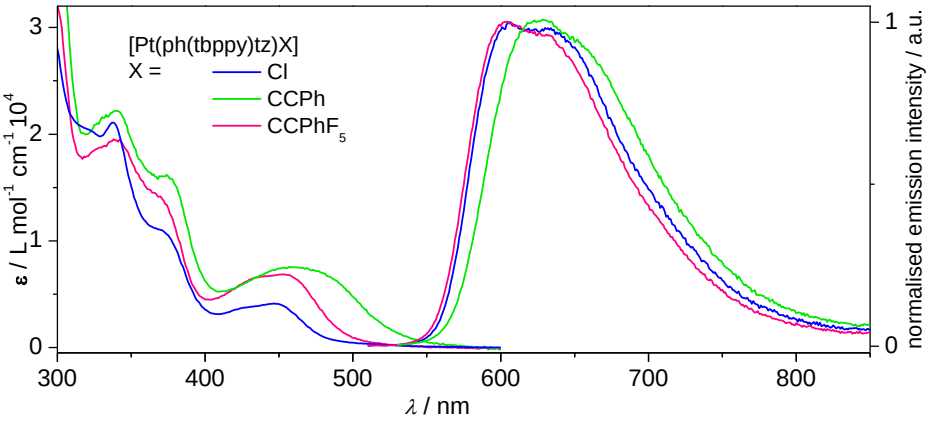

Fig. S41 UV-vis absorption spectra (left) and normalised emission spectra (right) of [Pt(ph(tbppy)tz)X] with X = Cl, CCPh, or CCC_6F_5 **(2, 3, 4)** in CH_2Cl_2 at 298 K upon excitation at 350 nm.

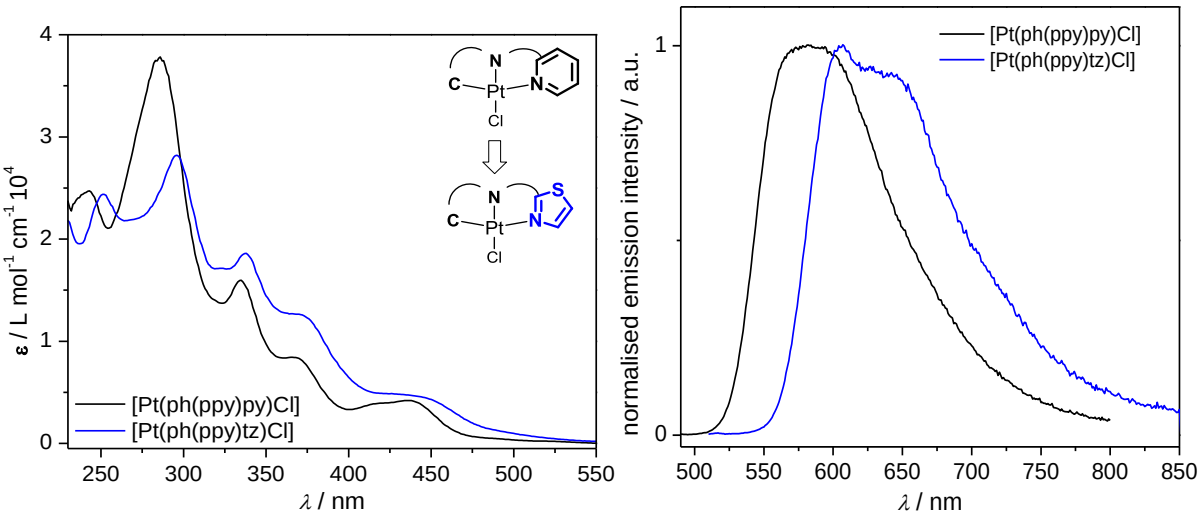

Fig. S42 UV-vis absorption spectra (left) and normalised emission spectra (right) of [Pt(ph(ppy)py)Cl] and [Pt(ph(ppy)tz)Cl] **(1)** in CH_2Cl_2 at 298 K upon excitation at 350 nm.

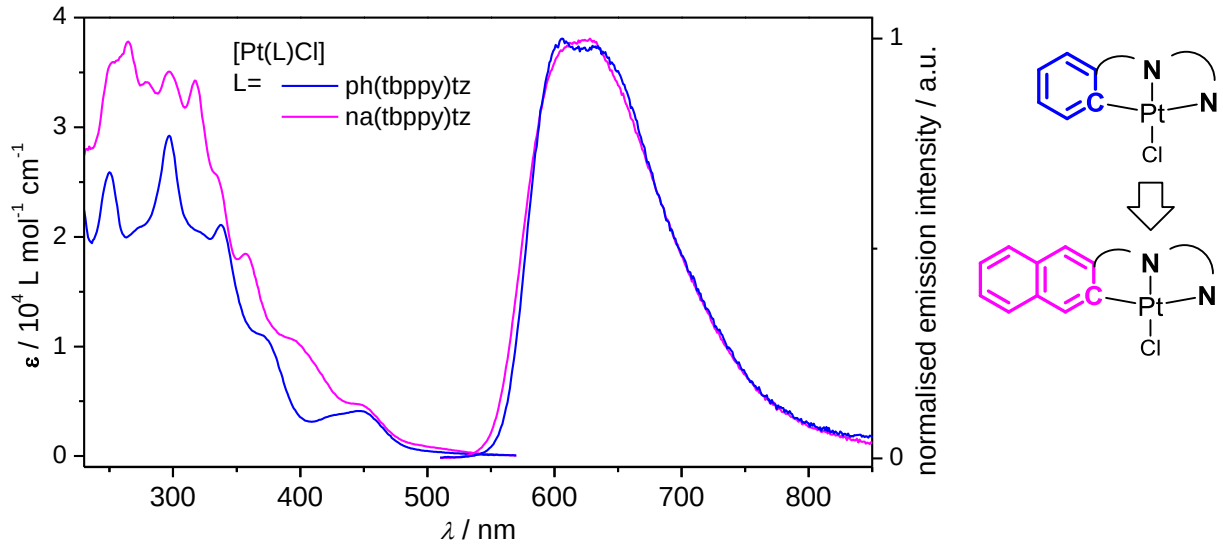

Fig. S43 UV-vis absorption spectra (left) and normalised emission spectra (right) of [Pt(ph(tbppy)tz)Cl] **(2)** and [Pt(na(tbppy)tz)Cl] **(5)** in CH_2Cl_2 at 298 K upon excitation at 350 nm.

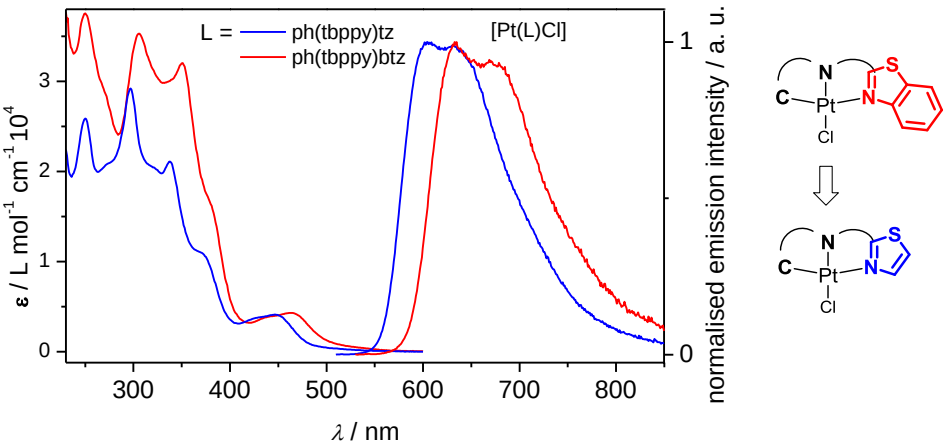

Fig. S44 UV-vis absorption spectra (left) and normalised emission spectra (right) of [Pt(ph(tbppy)tz)Cl] **(2)** and [Pt(ph(tbppy)btz)Cl] **(8)** in CH_2Cl_2 at 298 K upon excitation at 350 nm.

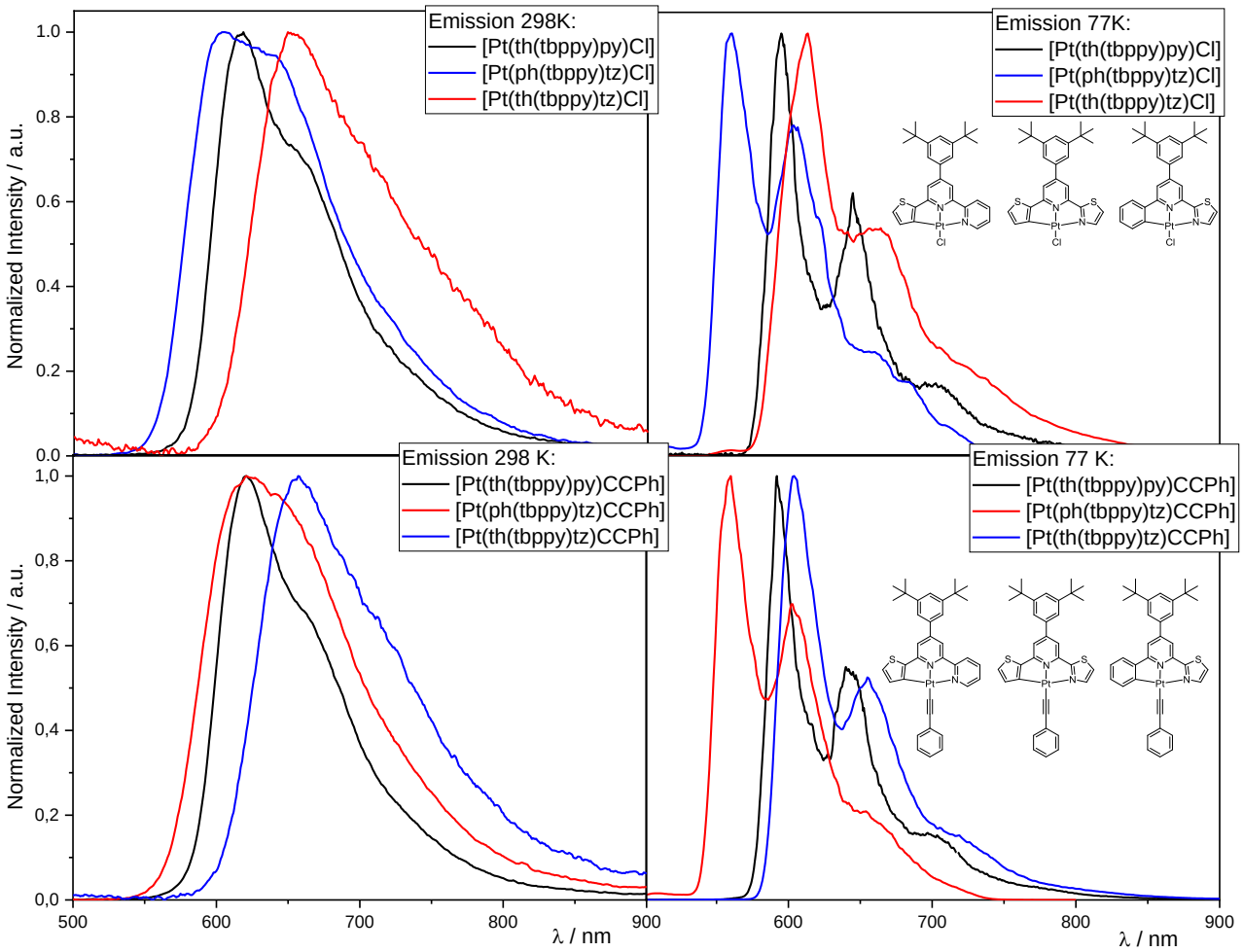

Fig. S45 Normalised photoluminescence spectra (λ_{exc} = 350 nm) with focus on the influence of the periphal ring; top: [Pt(th(tbppy)py)Cl] **(11)** (black), [Pt(ph(tbppy)tz)Cl] **(2)** (blue) and [Pt(th(tbppy)tz)Cl] **(17)** (red); bottom: [Pt(th(tbppy)py)CCPh] **(12)** (black), [Pt(ph(tbppy)tz)CCPh] **(3)** (red) and [Pt(th(tbppy)tz)CCPh] **(18)** (blue). Measured in CH_2Cl_2 at 298 K (left) or frozen glassy CH_2Cl_2/MeOH matrices at 77 K (right).

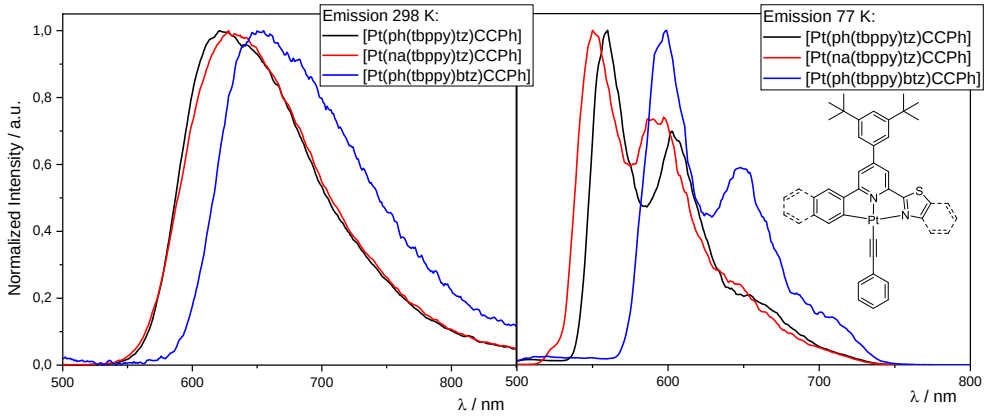

Fig. S46 Normalised photoluminescence spectra (λ_{exc} = 350 nm) involving the main ligands used for **class A** complexes (see Table 1); [Pt(ph(tbppy)tz)CCPh] **(3)** (black), [Pt(na(tbppy)tz)CCPh] **(6)** (red) and [Pt(ph(tbppy)btz)CCPh] **(9)** (blue) in CH_2Cl_2 at 298 K (left) and in frozen glassy CH_2Cl_2/MeOH matricx (V:V = 1:1) at 77 K (right).

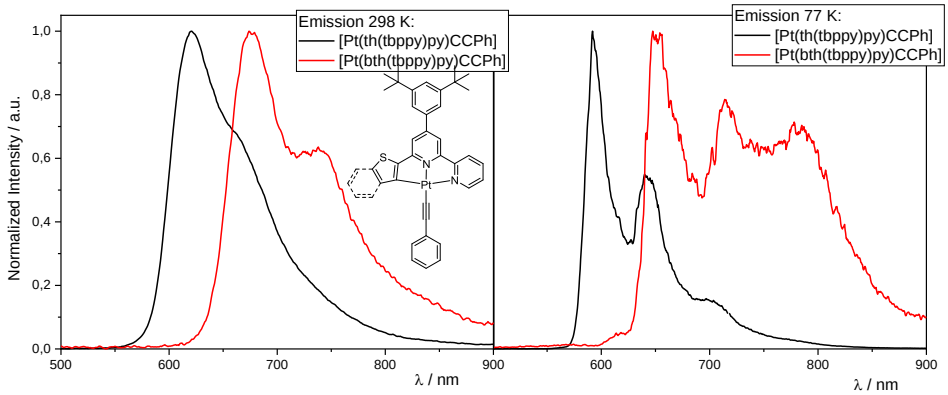

Fig. S47 Normalised photoluminescence spectra (λ_{exc} = 350 nm) involving the main ligands used for **class B** complexes (see Table 1) [Pt(th(tbppy)py)CCPh] **(12)** (black) and [Pt(bth(tbppy)py)CCPh] **(16)** (red) in fluid CH_2Cl_2 at 298 K (left) and in frozen glassy CH_2Cl_2/MeOH matrices (V:V = 1:1) at 77 K (right).

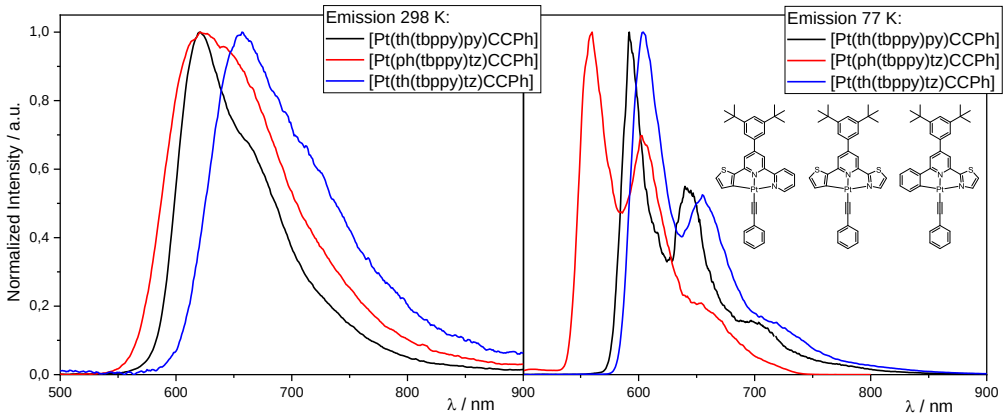

Fig. S48 Normalised photoluminescence spectra (λ_{exc} = 350 nm) of [Pt(th(tbppy)py)CCPh] **(12)** (black), [Pt(ph(tbppy)tz)CCPh] **(3)** (red) and [Pt(th(tbppy)tz)CCPh] **(18)** (blue) in CH_2Cl_2 at 298 K (left) and in frozen glassy CH_2Cl_2/MeOH matrices (V:V = 1:1) (right) at 77 K.

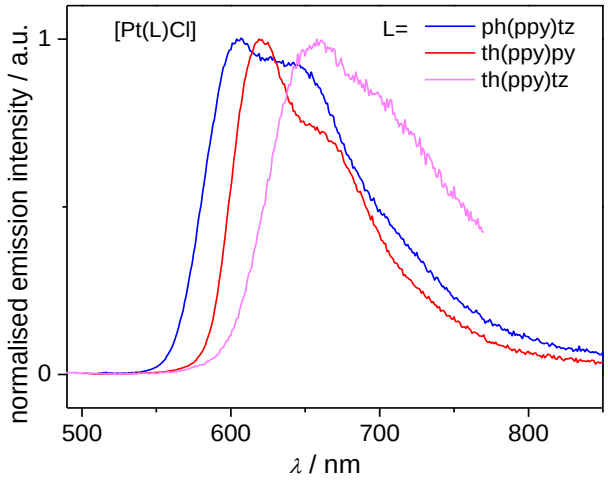

Fig. S49 Normalised emission spectra of [Pt(ph(ppy)tz)Cl] **(1)** (blue), [Pt(th(ppy)py)Cl] **(10)** (red) and [Pt(th(ppy)tz)Cl] (violet) in CH_2Cl_2 at 298 K upon excitation at 350 nm.

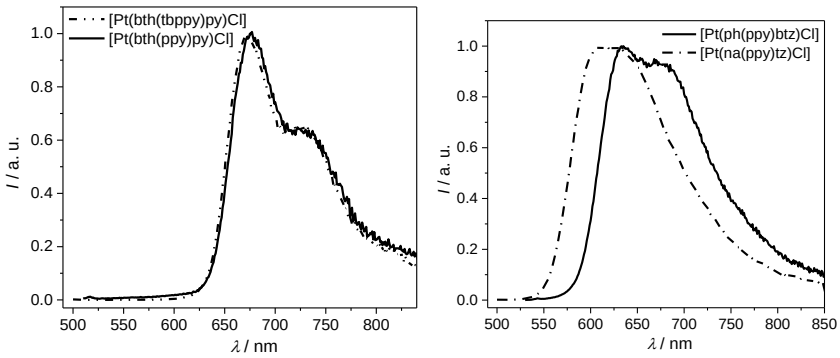

Fig. S50 Normalised emission spectra of, [Pt(bth(tbppy)py)Cl] **(15)**, [Pt(bth(ppy)py)Cl] **(14)** (left), and [Pt(ph(ppy)btz)Cl] **(7)**, [Pt(na(ppy)tz)Cl] (right), in CH_2Cl_2 at 298 K upon excitation with 350 nm.

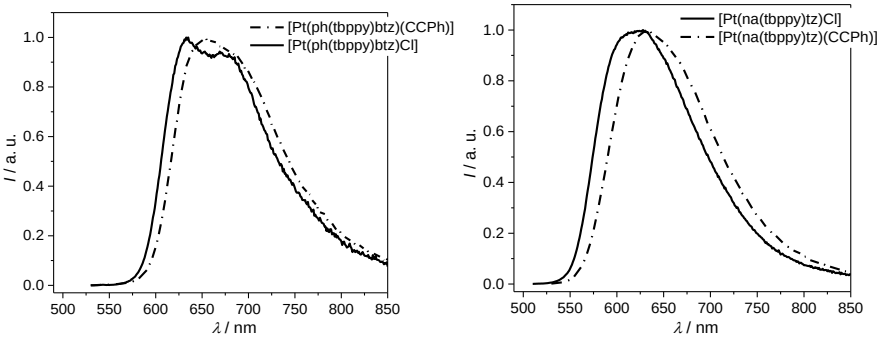

Fig. S51 Normalised emission spectra of (left), [Pt(ph(tbppy)btz)(CCPh)] **(9)**, [Pt(ph(tbppy)btz)Cl] **(8)** (left), and [Pt(na(tbppy)tz)Cl] **(5)**, [Pt(na(tbppy)tz)(CCPh)] **(6)** (right), in CH_2Cl_2 at 298 K upon excitation with 350 nm.

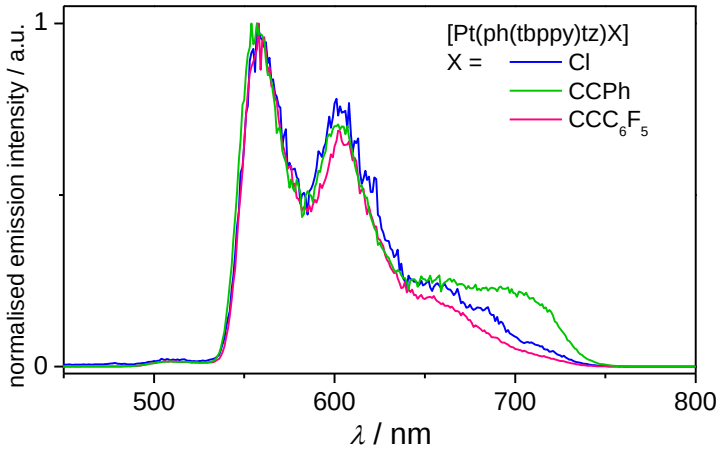

Fig. S52 Normalised emission spectra of [Pt(ph(tbppy)tz)X] with X = Cl, CCPh, or CCC_6F_5 **(2), (3)** and **(4)** in glassy frozen CH_2Cl_2/MeOH (1:1) matrix at 77 K upon excitation at 350 nm.

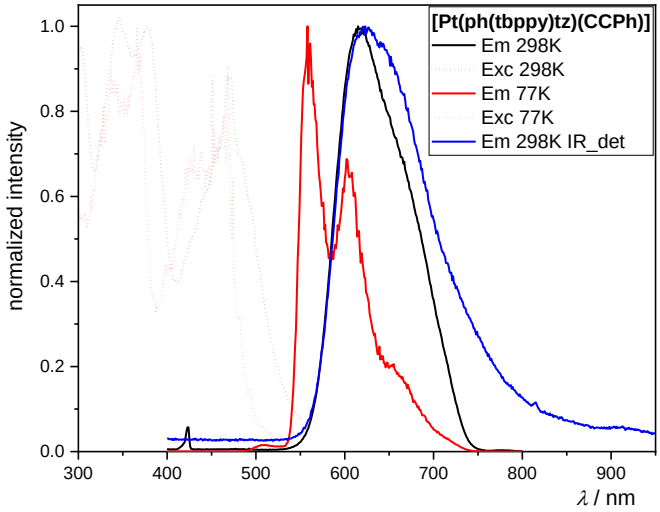

Fig. S53 Excitation (dotted line) and emission spectra (solid line) of [Pt(ph(tbppy)tz)(CCPh)] **(3)** (λ_{exc} = 350 nm; λ_{em} = 590 nm at 298 K, λ_{em} = 560 nm at 77 K) at 298 K with the UV/Vis-detector (black) and with IR-detector (blue) in CH_2Cl_2 and at 77 K (red) in a frozen glassy CH_2Cl_2/MeOH matrix (V:V = 1:1). All solutions were optically diluted (A < 0.1). Spectra normalised to the highest intensity.

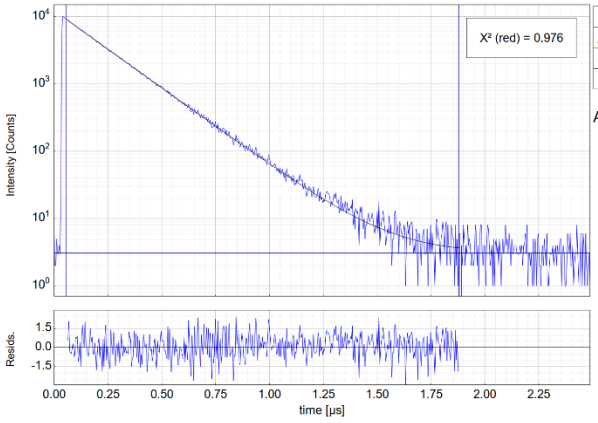

Parameter	Value	Conf. Lower	Conf. Upper	Conf. Estimation
A_1 [Cnts]	8914.7	-45.5	+45.5	Fitting
τ_1 [µs]	0.189084	-0.000701	+0.000701	Fitting
Bkgr. Dec [Cnts]	3.049	-0.695	+0.695	Fitting

Average Lifetime:

$\tau_{Av.1}$=0.189084 µs (intensity weighted)

$\tau_{Av.2}$=0.189084 µs (amplitude weighted)

Fig. S54 Left: Raw (experimental) time-resolved photoluminescence decay of [Pt(ph(tbppy)tz)CCPh] **(3)** in CH_2Cl_2 at 298 K (air-equilibrated), including the residuals (λ_{exc} = 376.7 nm, λ_{em} = 630 nm). Right: Fitting parameters including pre-exponential factors and confidence limits.

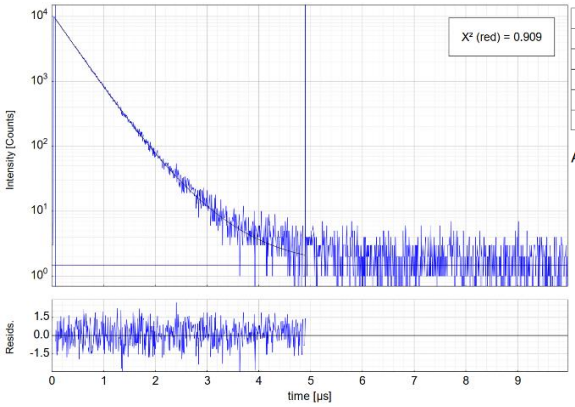

Parameter	Value	Conf. Lower	Conf. Upper	Conf. Estimation
A_1 [Cnts]	304.0	-20.7	+20.7	Fitting
τ_1 [µs]	0.7759	-0.0201	+0.0201	Fitting
A_2 [Cnts]	8805.0	-52.1	+52.1	Fitting
τ_2 [µs]	0.37483	-0.00170	+0.00170	Fitting
Bkgr. Dec [Cnts]	1.480	-0.531	+0.531	Fitting

Average Lifetime:

$\tau_{Av.1}$=0.4016 µs (intensity weighted)

$\tau_{Av.2}$=0.3882 µs (amplitude weighted)

Fig. S55 Left: Raw (experimental) time-resolved photoluminescence decay of [Pt(ph(tbppy)tz)CCPh] **(3)** in CH_2Cl_2 at 298 K (Ar-purged), including the residuals (λ_{exc} = 376.7 nm, λ_{em} = 630 nm). Right: Fitting parameters including pre-exponential factors and confidence limits.

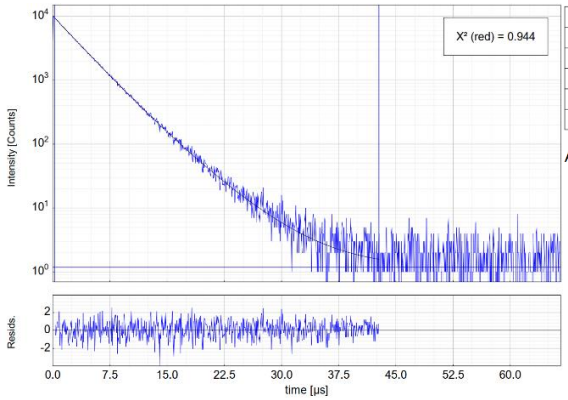

Parameter	Value	Conf. Lower	Conf. Upper	Conf. Estimation
A_1 [Cnts]	737.5	-27.1	+27.1	Fitting
τ_1 [µs]	5.594	-0.120	+0.120	Fitting
A_2 [Cnts]	8497.0	-53.5	+53.5	Fitting
τ_2 [µs]	3.3131	-0.0159	+0.0159	Fitting
Bkgr. Dec [Cnts]	1.183	-0.506	+0.506	Fitting

Average Lifetime:

$\tau_{Av.1}$=3.605 µs (intensity weighted)

$\tau_{Av.2}$=3.495 µs (amplitude weighted)

Fig. S56 Left: Raw (experimental) time-resolved photoluminescence decay of [Pt(ph(tbppy)tz)CCPh] **(3)** in a frozen glassy CH_2Cl_2/MeOH matrix (V:V = 1:1) at 77 K, including the residuals (λ_{exc} = 376.7 nm, λ_{em} = 560 nm). Right: Fitting parameters including pre-exponential factors and confidence limits.

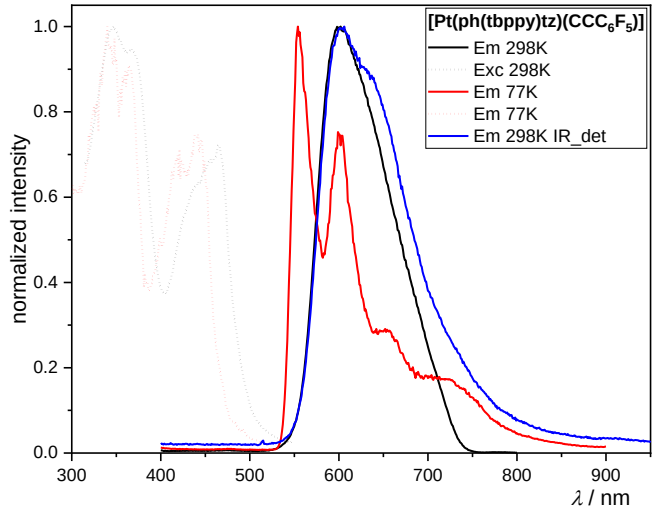

Fig. S57 Excitation (dotted line) and emission spectra (solid line) of [Pt(ph(tbppy)tz)(CCC_6F_5)] **(4)** (λ_{exc} = 350 nm; λ_{em} = 580 nm at 298 K, λ_{em} = 560 nm at 77 K) at 298 K with the UV/Vis-detector (black) and with IR-detector (blue) in CH_2Cl_2 and at 77 K (red) in a frozen glassy CH_2Cl_2/MeOH matrix (V:V = 1:1). All solutions were optically diluted (A < 0.1). Spectra normalised to the highest intensity.

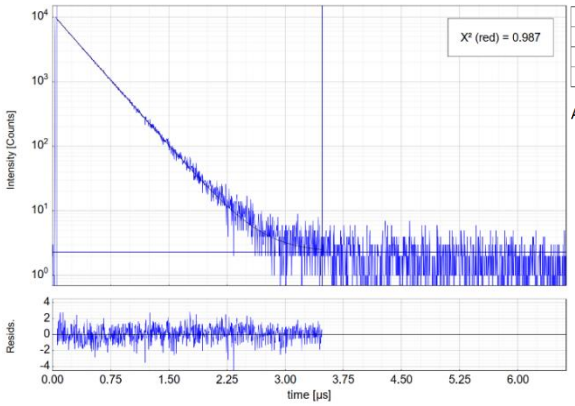

Parameter	Value	Conf. Lower	Conf. Upper	Conf. Estimation
A_1 [Cnts]	9215.6	-49.2	+49.2	Fitting
τ_1 [µs]	0.31946	-0.00123	+0.00123	Fitting
Bkgr. Dec [Cnts]	2.306	-0.574	+0.574	Fitting

Average Lifetime:

$\tau_{Av.1}$=0.31946 µs (intensity weighted)

$\tau_{Av.2}$=0.31946 µs (amplitude weighted)

Fig. S58 Left: Raw (experimental) time-resolved photoluminescence decay of [Pt(ph(tbppy)tz)CC$_6$F$_5$] **(4)** in CH_2Cl_2 at 298 K (air-equilibrated), including the residuals (λ_{exc} = 376.7 nm, λ_{em} = 600 nm). Right: Fitting parameters including pre-exponential factors and confidence limits.

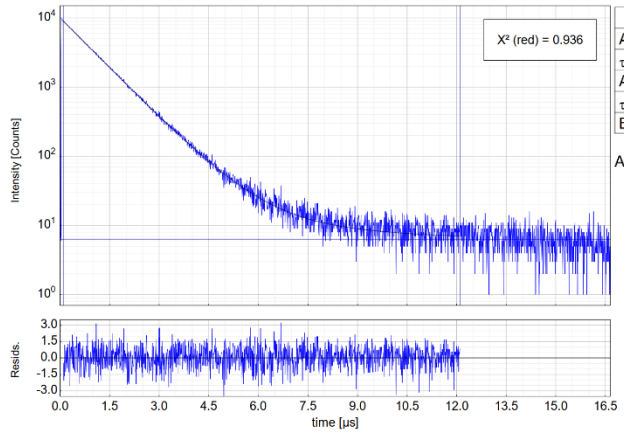

Parameter	Value	Conf. Lower	Conf. Upper	Conf. Estimation
A_1 [Cnts]	57.64	-9.97	+9.97	Fitting
τ_1 [µs]	2.722	-0.217	+0.217	Fitting
A_2 [Cnts]	8876.9	-53.0	+53.0	Fitting
τ_2 [µs]	0.89900	-0.00400	+0.00400	Fitting
Bkgr. Dec [Cnts]	6.324	-0.702	+0.702	Fitting

Average Lifetime:

$\tau_{Av.1}$=0.934 µs (intensity weighted)

$\tau_{Av.2}$=0.911 µs (amplitude weighted)

Fig. S59 Left: Raw (experimental) time-resolved photoluminescence decay of [Pt(ph(tbppy)tz)CC$_6$F$_5$] **(4)** in CH_2Cl_2 at 298 K (Ar-purged), including the residuals (λ_{exc} = 376.7 nm, λ_{em} = 600 nm). Right: Fitting parameters including pre-exponential factors and confidence limits.

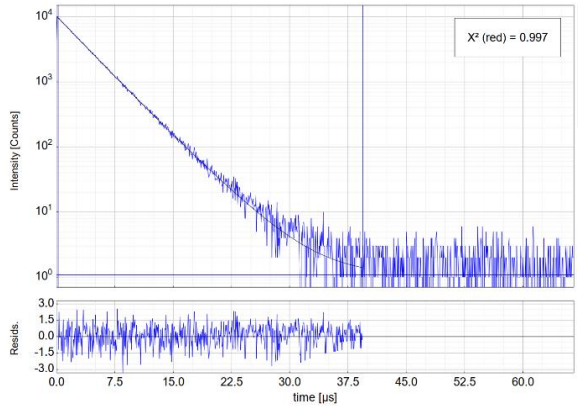

Parameter	Value	Conf. Lower	Conf. Upper	Conf. Estimation
A_1 [Cnts]	1223.9	-38.9	+38.9	Fitting
τ_1 [µs]	4.6095	-0.0696	+0.0696	Fitting
A_2 [Cnts]	8291.5	-53.5	+53.5	Fitting
τ_2 [µs]	3.3670	-0.0170	+0.0170	Fitting
Bkgr. Dec [Cnts]	1.080	-0.526	+0.526	Fitting

Average Lifetime:

$\tau_{Av.1}$=3.5758 µs (intensity weighted)

$\tau_{Av.2}$=3.5268 µs (amplitude weighted)

Fig. S60 Left: Raw (experimental) time-resolved photoluminescence decay of [Pt(ph(tbppy)tz)CC$_6$F$_5$] **(4)** in a frozen glassy CH_2Cl_2/MeOH matrix (V:V = 1:1) at 77 K, including the residuals (λ_{exc} = 376.7 nm, λ_{em} = 560 nm). Right: Fitting parameters including pre-exponential factors and confidence limits.

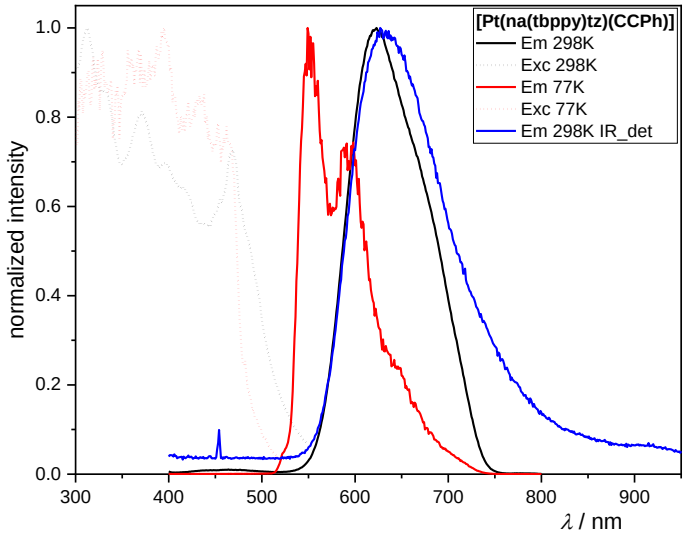

Fig. S61 Excitation (dotted line) and emission spectra (solid line) of [Pt(na(tbppy)tz)(CCPh)] **(6)** (λ_{exc} = 350 nm; λ_{em} = 590 nm at 298 K, λ_{em} = 550 nm at 77 K) at 298 K with the UV/Vis-detector (black) and with IR-detector (blue) in CH_2Cl_2 and at 77 K (red) in a frozen glassy CH_2Cl_2/MeOH matrix (V:V = 1:1). All solutions were optically diluted (A < 0.1). Spectra normalised to the highest intensity.

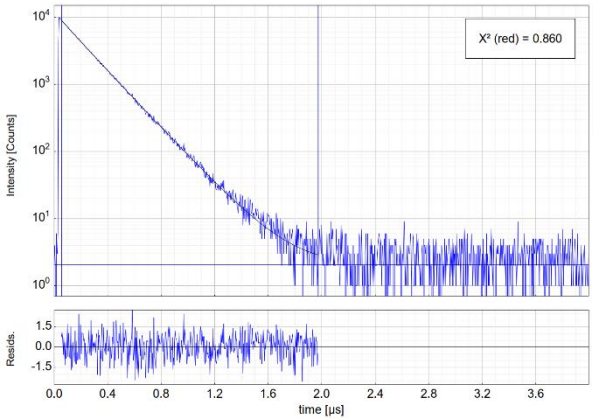

Parameter	Value	Conf. Lower	Conf. Upper	Conf. Estimation
A_1 [Cnts]	7497.0	-40.5	+40.5	Fitting
τ_1 [µs]	0.210466	-0.000797	+0.000797	Fitting
A_2 [Cnts]	1432.9	-55.7	+55.7	Fitting
τ_2 [µs]	0.14696	-0.00529	+0.00529	Fitting
Bkgr. Dec [Cnts]	2.052	-0.645	+0.645	Fitting

Average Lifetime:

$\tau_{Av.1}$=0.202989 µs (intensity weighted)

$\tau_{Av.2}$=0.200276 µs (amplitude weighted)

Fig. S62 Left: Raw (experimental) time-resolved photoluminescence decay of [Pt(na(tbppy)tz)CCPh] **(6)** in CH_2Cl_2 at 298 K (air-equilibrated), including the residuals (λ_{exc} = 376.7 nm, λ_{em} = 620 nm). Right: Fitting parameters including pre-exponential factors and confidence limits.

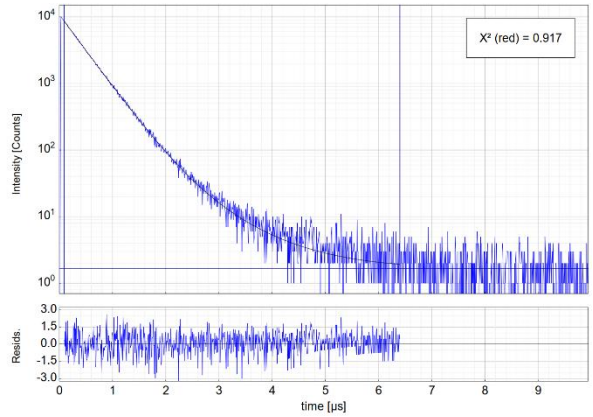

Parameter	Value	Conf. Lower	Conf. Upper	Conf. Estimation
A_1 [Cnts]	184.4	-15.4	+15.4	Fitting
τ_1 [µs]	0.9662	-0.0354	+0.0354	Fitting
A_2 [Cnts]	8347.9	-56.2	+56.2	Fitting
τ_2 [µs]	0.39502	-0.00202	+0.00202	Fitting
Bkgr. Dec [Cnts]	1.655	-0.449	+0.449	Fitting

Average Lifetime:

$\tau_{Av.1}$=0.4243 µs (intensity weighted)

$\tau_{Av.2}$=0.4074 µs (amplitude weighted)

Fig. S63 Left: Raw (experimental) time-resolved photoluminescence decay of [Pt(na(tbppy)tz)CCPh] **(6)** in CH_2Cl_2 at 298 K (Ar-purged), including the residuals (λ_{exc} = 376.7 nm, λ_{em} = 620 nm). Right: Fitting parameters including pre-exponential factors and confidence limits.

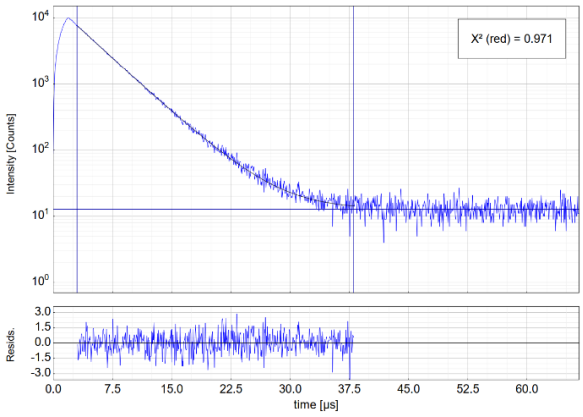

Parameter	Value	Conf. Lower	Conf. Upper	Conf. Estimation
A_1 [Cnts]	5005.0	-37.4	+37.4	Fitting
τ_1 [µs]	4.2865	-0.0210	+0.0210	Fitting
A_2 [Cnts]	2504.3	-47.9	+47.9	Fitting
τ_2 [µs]	3.3332	-0.0634	+0.0634	Fitting
Bkgr. Dec [Cnts]	12.81	-1.11	+1.11	Fitting

Average Lifetime:

$\tau_{Av.1}$=4.0194 µs (intensity weighted)

$\tau_{Av.2}$=3.9685 µs (amplitude weighted)

Fig. S64 Left: Raw (experimental) time-resolved photoluminescence decay of [Pt(na(tbppy)tz)CCPh] **(6)** in a frozen glassy CH_2Cl_2/MeOH matrix (V:V = 1:1) at 77 K, including the residuals (λ_{exc} = 376.7 nm, λ_{em} = 550 nm). Right: Fitting parameters including pre-exponential factors and confidence limits.

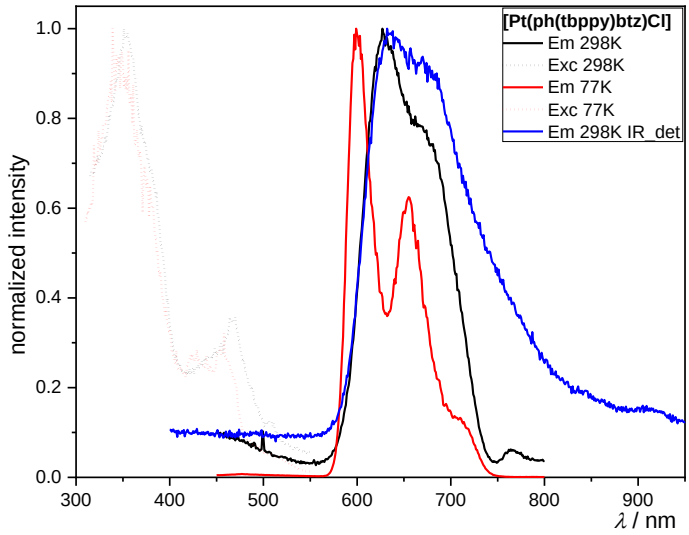

Fig. S65 Excitation (dotted line) and emission spectra (solid line) of [Pt(ph(tbppy)btz)Cl] **(8)** (λ_{exc} = 350 nm; λ_{em} = 600 nm) at 298 K with the UV/Vis-detector (black) and with IR-detector (blue) in CH_2Cl_2 and at 77 K (red) in a frozen glassy CH_2Cl_2/MeOH matrix (V:V = 1:1). All solutions were optically diluted (A < 0.1). Spectra normalised to the highest intensity.

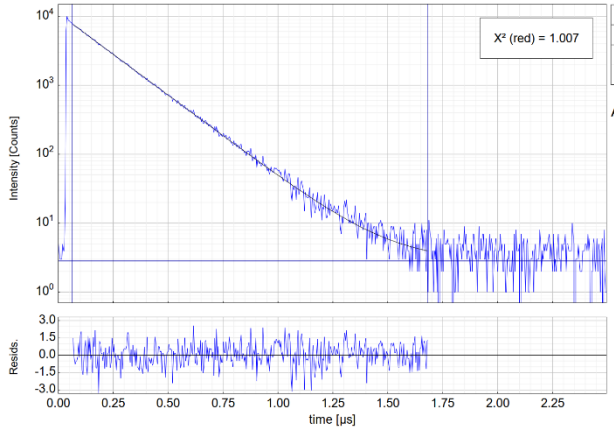

Parameter	Value	Conf. Lower	Conf. Upper	Conf. Estimation
A_1 [Cnts]	7584.0	-40.7	+40.7	Fitting
τ_1 [µs]	0.183228	-0.000717	+0.000717	Fitting
Bkgr. Dec [Cnts]	2.841	-0.789	+0.789	Fitting

Average Lifetime:

$\tau_{Av.1}$=0.183228 µs (intensity weighted)

$\tau_{Av.2}$=0.183228 µs (amplitude weighted)

Fig. S66 Left: Raw (experimental) time-resolved photoluminescence decay of [Pt(ph(tbppy)btz)Cl] **(8)** in CH_2Cl_2 at 298 K (air-equilibrated), including the residuals (λ_{exc} = 376.7 nm, λ_{em} = 630 nm). Right: Fitting parameters including pre-exponential factors and confidence limits.

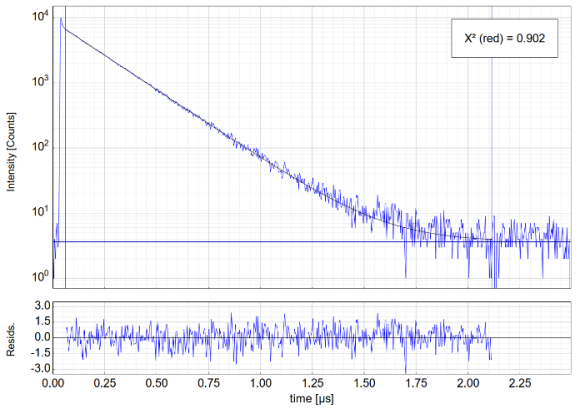

Parameter	Value	Conf. Lower	Conf. Upper	Conf. Estimation
A_1 [Cnts]	6491.2	-38.0	+38.0	Fitting
τ_1 [µs]	0.205726	-0.000883	+0.000883	Fitting
Bkgr. Dec [Cnts]	3.648	-0.634	+0.634	Fitting

Average Lifetime:

$\tau_{Av.1}$=0.205726 µs (intensity weighted)

$\tau_{Av.2}$=0.205726 µs (amplitude weighted)

Fig. S67 Left: Raw (experimental) time-resolved photoluminescence decay of [Pt(ph(tbppy)btz)Cl] **(8)** in CH_2Cl_2 at 298 K (Ar-purged), including the residuals (λ_{exc} = 376.7 nm, λ_{em} = 630 nm). Right: Fitting parameters including pre-exponential factors and confidence limits.

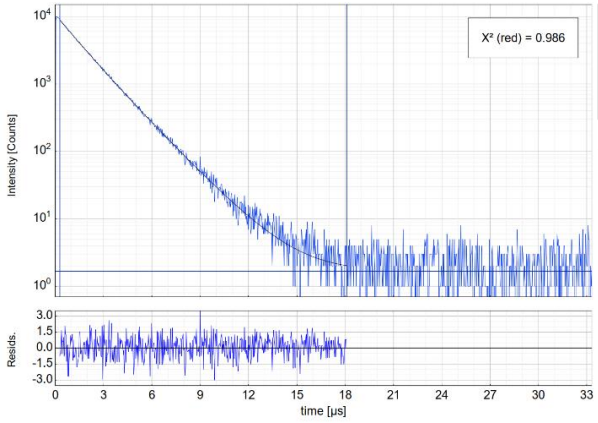

Parameter	Value	Conf. Lower	Conf. Upper	Conf. Estimation
A_1 [Cnts]	4648.3	-41.3	+41.3	Fitting
τ_1 [µs]	1.8705	-0.0110	+0.0110	Fitting
A_2 [Cnts]	4197.2	-59.1	+59.1	Fitting
τ_2 [µs]	1.2793	-0.0154	+0.0154	Fitting
Bkgr. Dec [Cnts]	1.681	-0.563	+0.563	Fitting

Average Lifetime:

$\tau_{Av.1}$=1.6448 µs (intensity weighted)

$\tau_{Av.2}$=1.5900 µs (amplitude weighted)

Fig. S68 Left: Raw (experimental) time-resolved photoluminescence decay of [Pt(ph(tbppy)btz)Cl] **(8)** in a frozen glassy CH_2Cl_2/MeOH matrix (V:V = 1:1) at 77 K, including the residuals (λ_{exc} = 376.7 nm, λ_{em} = nm). Right: Fitting parameters including pre-exponential factors and confidence limits.

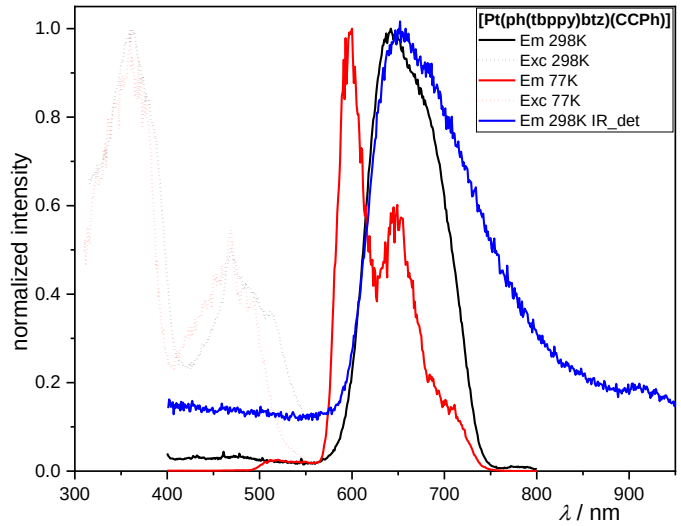

Fig. S69 Excitation (dotted line) and emission spectra (solid line) of [Pt(ph(tbppy)btz)CCPh] **(9)** (λ_{exc} = 350 nm; λ_{em} = 610 nm at 298 K, λ_{em} = 600 nm at 77 K) at 298 K with the UV/Vis-detector (black) and with IR-detector (blue) in CH_2Cl_2 and at 77 K (red) in a frozen glassy CH_2Cl_2/MeOH matrix (V:V = 1:1). All solutions were optically diluted (A < 0.1). Spectra normalised to the highest intensity.

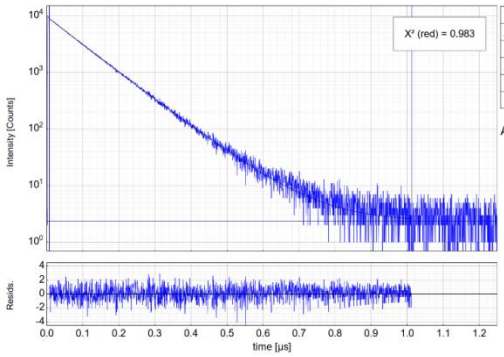

Parameter	Value	Conf. Lower	Conf. Upper	Conf. Estimation
A_1 [Cnts]	1222.4	-37.1	+37.1	Fitting
τ_1 [µs]	0.11554	-0.00200	+0.00200	Fitting
A_2 [Cnts]	7668.6	-52.1	+52.1	Fitting
τ_2 [µs]	0.084409	-0.000437	+0.000437	Fitting
Bkgr. Dec [Cnts]	2.367	-0.574	+0.574	Fitting

Average Lifetime:

$\tau_{Av.1}$=0.08998 µs (intensity weighted)

$\tau_{Av.2}$=0.08869 µs (amplitude weighted)

Fig. S70 Left: Raw (experimental) time-resolved photoluminescence decay of [Pt(ph(tbppy)btz)CCPh] **(9)** in CH_2Cl_2at 298 K (air-equilibrated), including the residuals (λ_{exc} = 376.7 nm, λ_{em} = 640 nm). Right: Fitting parameters including pre-exponential factors and confidence limits.

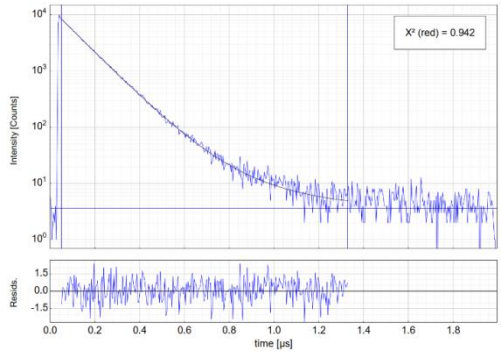

Parameter	Value	Conf. Lower	Conf. Upper	Conf. Estimation
A_1 [Cnts]	8120.9	-47.9	+47.9	Fitting
τ_1 [µs]	0.108487	-0.000487	+0.000487	Fitting
A_2 [Cnts]	164.5	-14.7	+14.7	Fitting
τ_2 [µs]	0.26200	-0.00942	+0.00942	Fitting
Bkgr. Dec [Cnts]	3.611	-0.703	+0.703	Fitting

Average Lifetime:

$\tau_{Av.1}$=0.115646 µs (intensity weighted)

$\tau_{Av.2}$=0.111535 µs (amplitude weighted)

Fig. S71 Left: Raw (experimental) time-resolved photoluminescence decay of [Pt(ph(tbppy)btz)CCPh] **(9)** in CH_2Cl_2 at 298 K (Ar-purged), including the residuals (λ_{exc} = 376.7 nm, λ_{em} = 640 nm). Right: Fitting parameters including pre-exponential factors and confidence limits.

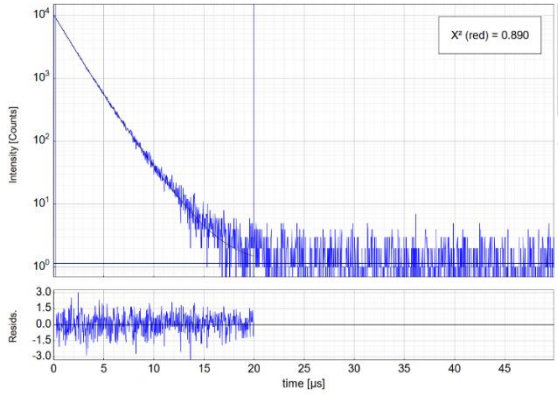

Parameter	Value	Conf. Lower	Conf. Upper	Conf. Estimation
A_1 [Cnts]	2167.3	-35.7	+35.7	Fitting
τ_1 [µs]	2.2446	-0.0189	+0.0189	Fitting
A_2 [Cnts]	6635.4	-52.9	+52.9	Fitting
τ_2 [µs]	1.5215	-0.0102	+0.0102	Fitting
Bkgr. Dec [Cnts]	1.151	-0.496	+0.496	Fitting

Average Lifetime:

$\tau_{Av.1}$=1.7566 µs (intensity weighted)

$\tau_{Av.2}$=1.6995 µs (amplitude weighted)

Fig. S72 Left: Raw (experimental) time-resolved photoluminescence decay of [Pt(ph(tbppy)btz)CCPh] **(9)** in a frozen glassy CH_2Cl_2/MeOH matrix (V:V = 1:1) at 77 K, including the residuals (λ_{exc} = 376.7 nm, λ_{em} = 600 nm). Right: Fitting parameters including pre-exponential factors and confidence limits.

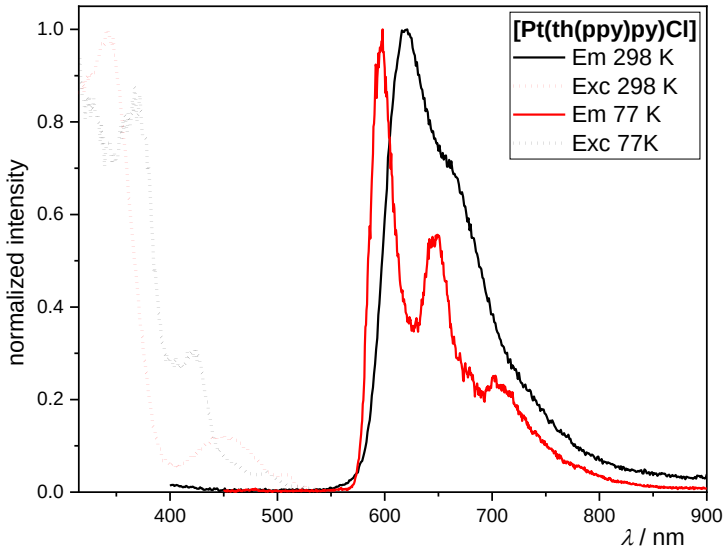

Fig. S73 Excitation (dotted line) and emission spectra (solid line) of [Pt(th(ppy)py)Cl] **(10)** (λ_{exc} = 350 nm; λ_{em} = 600 nm) at 298 K (black) in CH_2Cl_2 and at 77 K (red) in a frozen glassy CH_2Cl_2/MeOH matrix (V:V = 1:1). All solutions were optically diluted (A < 0.1). Normalised to the highest intensity.

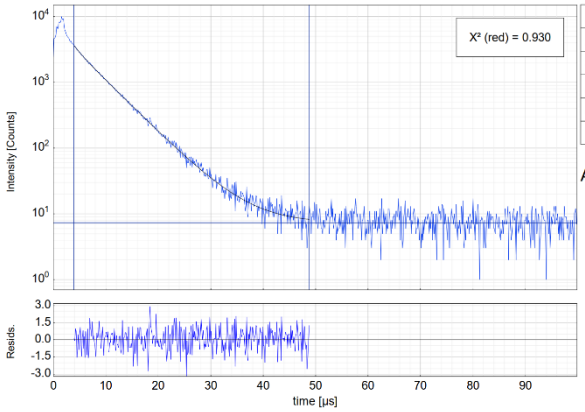

Parameter	Value	Conf. Lower	Conf. Upper	Conf. Estimation
A_1 [Cnts]	3214.7	-25.0	+25.0	Fitting
τ_1 [µs]	5.4940	-0.0317	+0.0317	Fitting
A_2 [Cnts]	392.4	-67.3	+67.3	Fitting
τ_2 [µs]	1.295	-0.282	+0.282	Fitting
Bkgr. Dec [Cnts]	7.319	-0.849	+0.849	Fitting

Average Lifetime:

$\tau_{Av.1}$=5.3766 µs (intensity weighted)

$\tau_{Av.2}$=5.0372 µs (amplitude weighted)

Fig. S74 Left: Raw (experimental) time-resolved photoluminescence decay of [Pt(th(ppy)py)Cl] **(10)** in CH_2Cl_2 at 298 K (Ar-purged), including the residuals (λ_{exc} = 376.7 nm, λ_{em} = 620 nm). Right: Fitting parameters including pre-exponential factors and confidence limits.

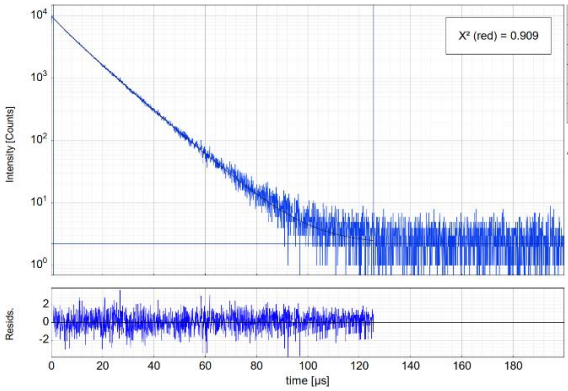

Parameter	Value	Conf. Lower	Conf. Upper	Conf. Estimation
A_1 [Cnts]	7225.8	-43.2	+43.2	Fitting
τ_1 [µs]	12.3431	-0.0512	+0.0512	Fitting
A_2 [Cnts]	1912.0	-77.2	+77.2	Fitting
τ_2 [µs]	6.133	-0.255	+0.255	Fitting
Bkgr. Dec [Cnts]	2.213	-0.573	+0.573	Fitting

Average Lifetime:

$\tau_{Av.1}$=11.6215 µs (intensity weighted)

$\tau_{Av.2}$=11.0437 µs (amplitude weighted)

Fig. S75 Left: Raw (experimental) time-resolved photoluminescence decay of [Pt(th(ppy)py)Cl] **(10)** in a frozen glassy CH_2Cl_2/MeOH matrix (V:V = 1:1) at 77 K, including the residuals (λ_{exc} = 376.7 nm, λ_{em} = 600 nm). Right: Fitting parameters including pre-exponential factors and confidence limits.

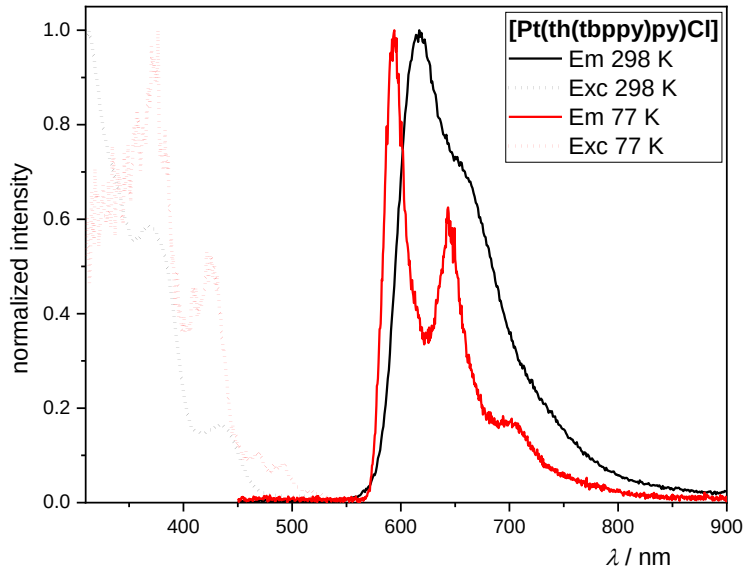

Fig. S76 Excitation (dotted line) and emission spectra (solid line) of [Pt(th(tbppy)py)Cl] **(11)** (λ_{exc} = 350 nm; λ_{em} = 600 nm) at 298 K (black) in CH_2Cl_2 and at 77 K (red) in a frozen glassy CH_2Cl_2/MeOH matrix (V:V = 1:1). All solutions were optically diluted (A < 0.1). Spectra normalised to the highest intensity.

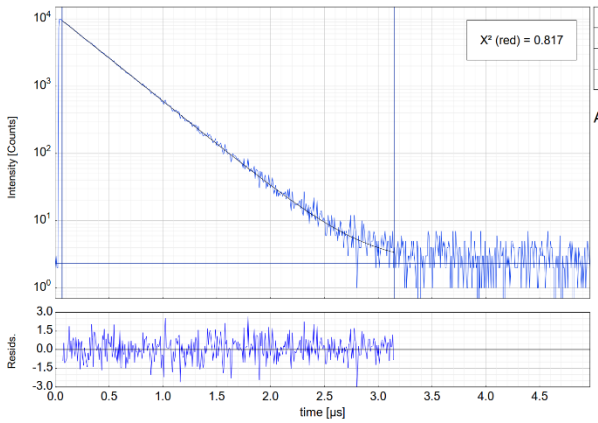

Parameter	Value	Conf. Lower	Conf. Upper	Conf. Estimation
A_1 [Cnts]	9213.8	-41.0	+41.0	Fitting
τ_1 [µs]	0.33930	-0.00109	+0.00109	Fitting
Bkgr. Dec [Cnts]	2.332	-0.688	+0.688	Fitting

Average Lifetime:

$\tau_{Av.1}$=0.33930 µs (intensity weighted)

$\tau_{Av.2}$=0.33930 µs (amplitude weighted)

Fig. S77 Left: Raw (experimental) time-resolved photoluminescence decay of [Pt(th(tbppy)py)Cl] **(11)** in CH_2Cl_2 at 298 K (air-equilibrated), including the residuals (λ_{exc} = 376.7 nm, λ_{em} = 620 nm). Right: Fitting parameters including pre-exponential factors and confidence limits.

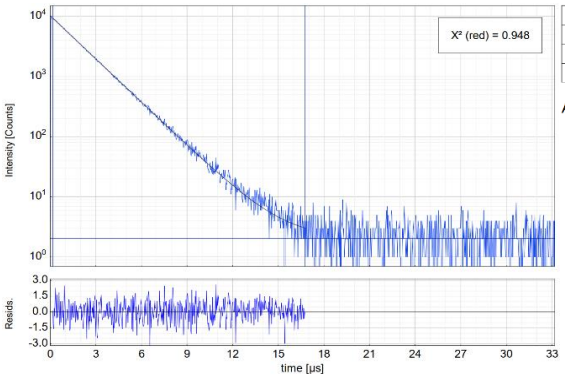

Parameter	Value	Conf. Lower	Conf. Upper	Conf. Estimation
A_1 [Cnts]	9382.0	-44.9	+44.9	Fitting
τ_1 [µs]	1.80919	-0.00627	+0.00627	Fitting
Bkgr. Dec [Cnts]	2.066	-0.708	+0.708	Fitting

Average Lifetime:

$\tau_{Av.1}$=1.80919 µs (intensity weighted)

$\tau_{Av.2}$=1.80919 µs (amplitude weighted)

Fig. S78 Left: Raw (experimental) time-resolved photoluminescence decay of [Pt(th(tbppy)py)Cl] **(11)** in CH_2Cl_2 at 298 K (Ar-purged), including the residuals (λ_{exc} = 376.7 nm, λ_{em} = 620 nm). Right: Fitting parameters including pre-exponential factors and confidence limits.

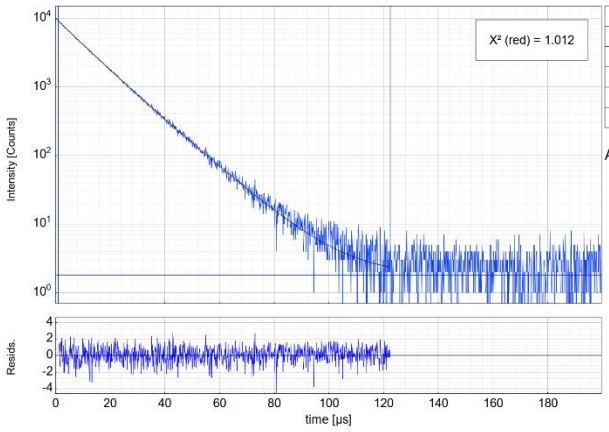

Parameter	Value	Conf. Lower	Conf. Upper	Conf. Estimation
A_1 [Cnts]	3712.9	-59.6	+59.6	Fitting
τ_1 [µs]	9.323	-0.131	+0.131	Fitting
A_2 [Cnts]	5413.0	-43.1	+43.1	Fitting
τ_2 [µs]	13.1675	-0.0690	+0.0690	Fitting
Bkgr. Dec [Cnts]	1.819	-0.632	+0.632	Fitting

Average Lifetime:

$\tau_{Av.1}$=11.911 µs (intensity weighted)

$\tau_{Av.2}$=11.603 µs (amplitude weighted)

Fig. S79 Left: Raw (experimental) time-resolved photoluminescence decay of [Pt(th(tbppy)py)Cl] **(11)** in a frozen glassy CH_2Cl_2/MeOH matrix (V:V = 1:1) at 77 K, including the residuals (λ_{exc} = 376.7 nm, λ_{em} = 600 nm). Right: Fitting parameters including pre-exponential factors and confidence limits.

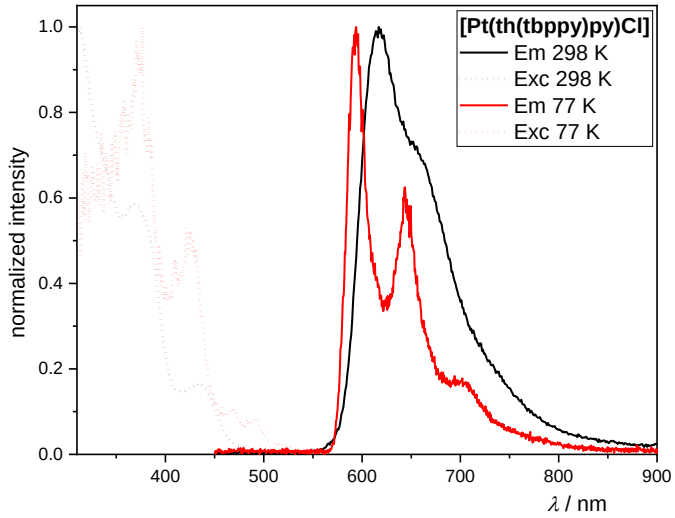

Fig. S80 Excitation (dotted line) and emission spectra (solid line) of [Pt(th(tbppy)py)CCPh] **(12)** (λ_{exc} = 350 nm; λ_{em} = 600 nm) at 298 K (black) in CH_2Cl_2 and at 77 K (red) in a frozen glassy CH_2Cl_2/MeOH matrix (V:V = 1:1). All solutions were optically diluted (A < 0.1). Spectra normalised to the highest intensity.

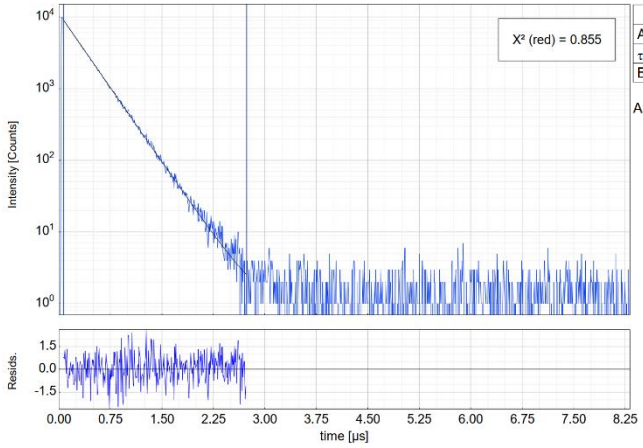

Parameter	Value	Conf. Lower	Conf. Upper	Conf. Estimation
A_1 [Cnts]	8882.2	-39.7	+39.7	Fitting
τ_1 [µs]	0.31461	-0.00102	+0.00102	Fitting
Bkgr. Dec [Cnts]	0.652	-0.712	+0.712	Fitting

Average Lifetime:

$\tau_{Av.1}$=0.31461 µs (intensity weighted)

$\tau_{Av.2}$=0.31461 µs (amplitude weighted)

Fig. S81 Left: Raw (experimental) time-resolved photoluminescence decay of [Pt(th(tbppy)py)CCPh] **(12)** in CH_2Cl_2 at 298 K (air-equilibrated), including the residuals (λ_{exc} = 376.7 nm, λ_{em} = 620 nm). Right: Fitting parameters including pre-exponential factors and confidence limits.

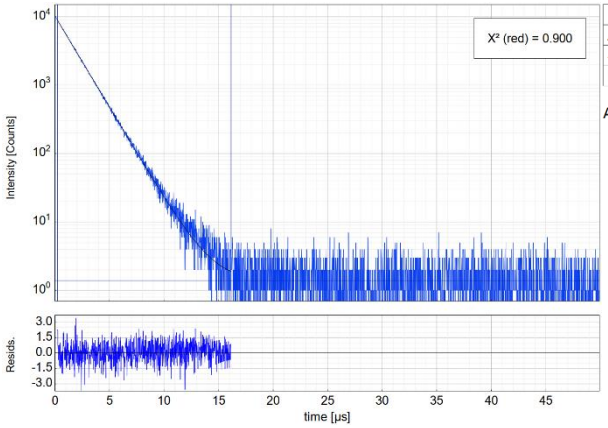

Parameter	Value	Conf. Lower	Conf. Upper	Conf. Estimation
A_1 [Cnts]	8826.6	-43.9	+43.9	Fitting
τ_1 [µs]	1.62822	-0.00584	+0.00584	Fitting
Bkgr. Dec [Cnts]	1.390	-0.566	+0.566	Fitting

Average Lifetime:

$\tau_{Av.1}$=1.62822 µs (intensity weighted)

$\tau_{Av.2}$=1.62822 µs (amplitude weighted)

Fig. S82 Left: Raw (experimental) time-resolved photoluminescence decay of [Pt(th(tbppy)py)CCPh] **(12)** in CH_2Cl_2 at 298 K (Ar-purged), including the residuals (λ_{exc} = 376.7 nm, λ_{em} = 620 nm). Right: Fitting parameters including pre-exponential factors and confidence limits.

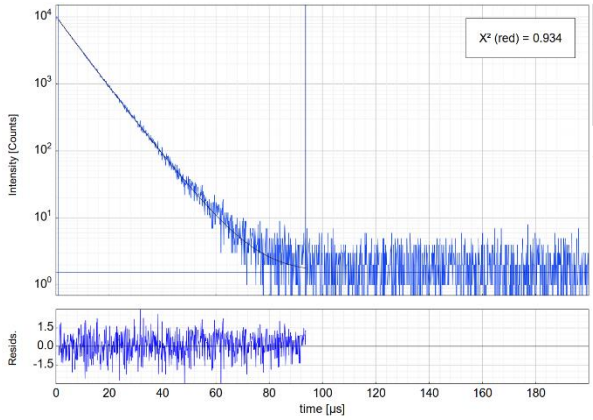

Parameter	Value	Conf. Lower	Conf. Upper	Conf. Estimation
A_1 [Cnts]	3356.0	-40.9	+40.9	Fitting
τ_1 [µs]	9.6866	-0.0733	+0.0733	Fitting
A_2 [Cnts]	5600.4	-53.5	+53.5	Fitting
τ_2 [µs]	7.3876	-0.0573	+0.0573	Fitting
Bkgr. Dec [Cnts]	1.535	-0.521	+0.521	Fitting

Average Lifetime:

$\tau_{Av.1}$=8.3992 µs (intensity weighted)

$\tau_{Av.2}$=8.2491 µs (amplitude weighted)

Fig. S83 Left: Raw (experimental) time-resolved photoluminescence decay of [Pt(th(tbppy)py)CCPh**] (12)** in a frozen glassy CH_2Cl_2/MeOH matrix (V:V = 1:1) at 77 K, including the residuals (λ_{exc} = 376.7 nm, λ_{em} = 600 nm). Right: Fitting parameters including pre-exponential factors and confidence limits.

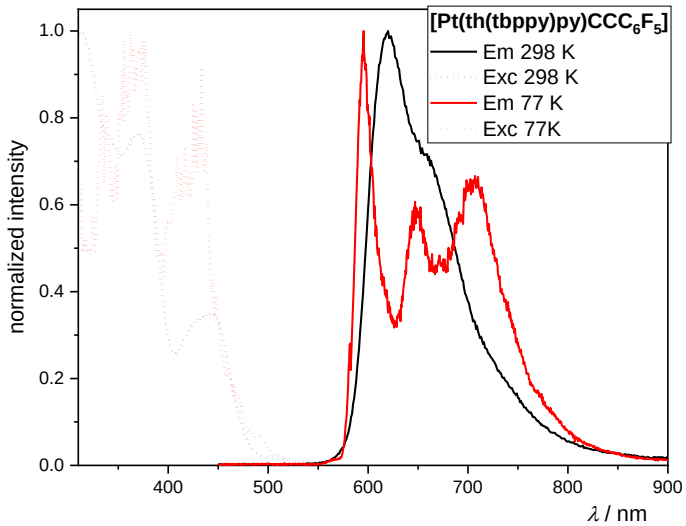

Fig. S84 Excitation (dotted line) and emission spectra (solid line) of [Pt(th(tbppy)py)CCC_6F_5] **(13)** (λ_{exc} = 350 nm; λ_{em} = 600 nm) at 298 K (black) in CH_2Cl_2 and at 77 K (red) in a frozen glassy CH_2Cl_2/MeOH matrix (V:V = 1:1). All solutions were optically diluted (A < 0.1). Spectra normalised to the highest intensity.

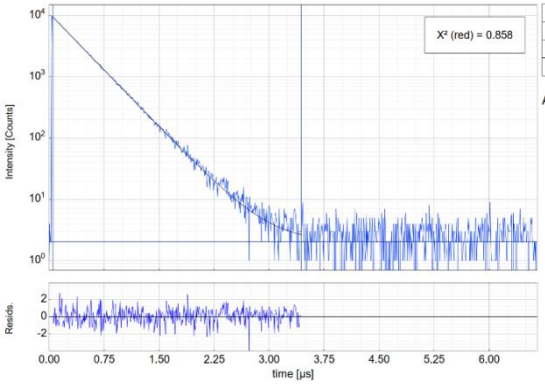

Parameter	Value	Conf. Lower	Conf. Upper	Conf. Estimation
A_1 [Cnts]	9344.2	-43.6	+43.6	Fitting
τ_1 [µs]	0.35130	-0.00119	+0.00119	Fitting
Bkgr. Dec [Cnts]	2.057	-0.621	+0.621	Fitting

Average Lifetime:

$\tau_{Av.1}$=0.35130 µs (intensity weighted)

$\tau_{Av.2}$=0.35130 µs (amplitude weighted)

Fig. S85 Left: Raw (experimental) time-resolved photoluminescence decay of [Pt(th(tbppy)py)CCC$_6$F$_5$] **(13)** in CH_2Cl_2 at 298 K (air-equilibrated), including the residuals (λ_{exc} = 376.7 nm, λ_{em} = 620 nm). Right: Fitting parameters including pre-exponential factors and confidence limits.

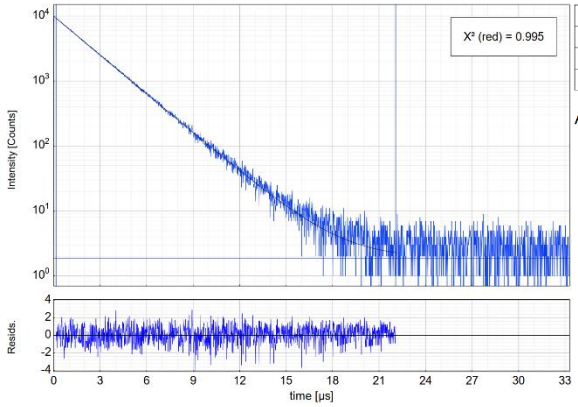

Parameter	Value	Conf. Lower	Conf. Upper	Conf. Estimation
A_1 [Cnts]	9281.3	-48.1	+48.1	Fitting
τ_1 [µs]	2.17770	-0.00813	+0.00813	Fitting
Bkgr. Dec [Cnts]	1.893	-0.614	+0.614	Fitting

Average Lifetime:

$\tau_{Av.1}$=2.17770 µs (intensity weighted)

$\tau_{Av.2}$=2.17770 µs (amplitude weighted)

Fig. S86 Left: Raw (experimental) time-resolved photoluminescence decay of [Pt(th(tbppy)py)CCC$_6$F$_5$] **(13)** in CH_2Cl_2 at 298 K (Ar-purged), including the residuals (λ_{exc} = 376.7 nm, λ_{em} = 620 nm). Right: Fitting parameters including pre-exponential factors and confidence limits.

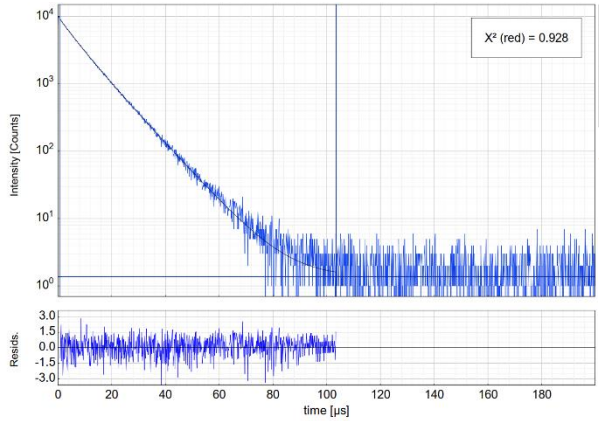

Parameter	Value	Conf. Lower	Conf. Upper	Conf. Estimation
A_1 [Cnts]	6296.3	-42.3	+42.3	Fitting
τ_1 [µs]	10.0762	-0.0459	+0.0459	Fitting
A_2 [Cnts]	2608.6	-71.8	+71.8	Fitting
τ_2 [µs]	5.450	-0.148	+0.148	Fitting
Bkgr. Dec [Cnts]	1.375	-0.507	+0.507	Fitting

Average Lifetime:

$\tau_{Av.1}$=9.2293 µs (intensity weighted)

$\tau_{Av.2}$=8.7210 µs (amplitude weighted)

Fig. S87 Left: Raw (experimental) time-resolved photoluminescence decay of [Pt(th(tbppy)py)CC$_6$F$_5$] **(13)** in a frozen glassy CH_2Cl_2/MeOH matrix (V:V = 1:1) at 77 K, including the residuals (λ_{exc} = 376.7 nm, λ_{em} = 600 nm). Right: Fitting parameters including pre-exponential factors and confidence limits.

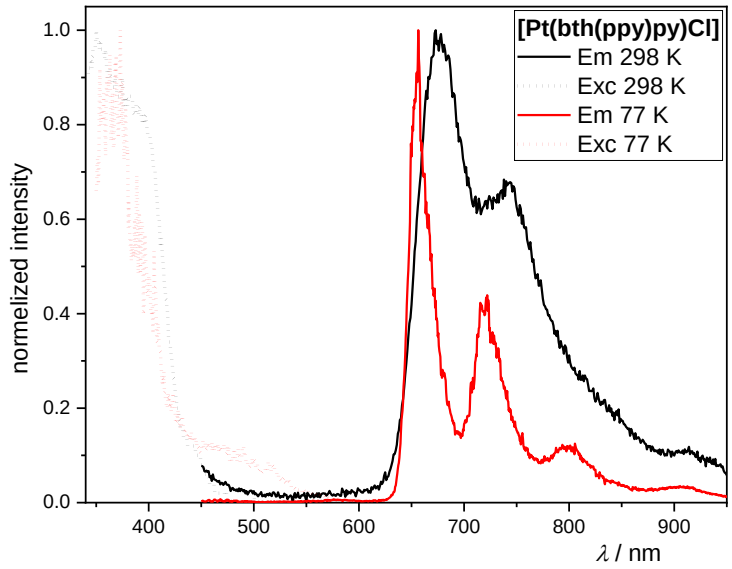

Fig. S88 Excitation (dotted line) and emission spectra (solid line) of [Pt(bth(ppy)py)Cl] **(14)** (λ_{exc} = 350 nm; λ_{em} = 650 nm at 298 K; λ_{em} = 660 nm at 77 K) at 298 K (black) in CH_2Cl_2 and at 77 K (red) in a frozen glassy CH_2Cl_2/MeOH matrix (V:V = 1:1). All solutions were optically diluted (A < 0.1). Spectra normalised to the highest intensity.

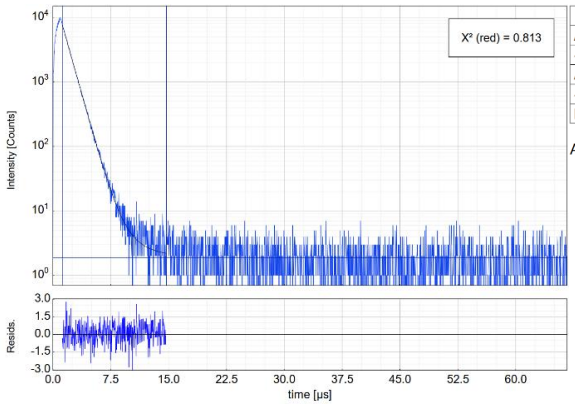

Parameter	Value	Conf. Lower	Conf. Upper	Conf. Estimation
A_1 [Cnts]	28.70	-7.44	+7.44	Fitting
τ_1 [µs]	2.953	-0.366	+0.366	Fitting
A_2 [Cnts]	7538.0	-44.7	+44.7	Fitting
τ_2 [µs]	1.01476	-0.00444	+0.00444	Fitting
Bkgr. Dec [Cnts]	1.886	-0.439	+0.439	Fitting

Average Lifetime:

$\tau_{Av.1}$=1.036 µs (intensity weighted)

$\tau_{Av.2}$=1.022 µs (amplitude weighted)

Fig. S89 Left: Raw (experimental) time-resolved photoluminescence decay of [Pt(bth(ppy)py)Cl] **(14)** in CH_2Cl_2 at 298 K (Ar-purged), including the residuals (λ_{exc} = 376.7 nm, λ_{em} = 670 nm). Right: Fitting parameters including pre-exponential factors and confidence limits.

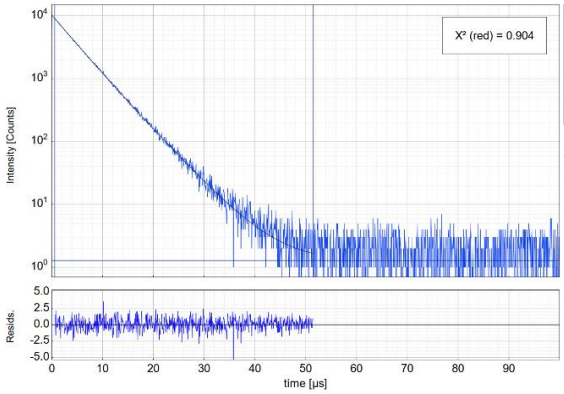

Parameter	Value	Conf. Lower	Conf. Upper	Conf. Estimation
A_1 [Cnts]	5772.7	-50.7	+50.7	Fitting
τ_1 [µs]	4.2264	-0.0276	+0.0276	Fitting
A_2 [Cnts]	3163.0	-37.8	+37.8	Fitting
τ_2 [µs]	5.5961	-0.0494	+0.0494	Fitting
Bkgr. Dec [Cnts]	1.272	-0.530	+0.530	Fitting

Average Lifetime:

$\tau_{Av.1}$=4.8023 µs (intensity weighted)

$\tau_{Av.2}$=4.7112 µs (amplitude weighted)

Fig. S90 Left: Raw (experimental) time-resolved photoluminescence decay of [Pt(bth(ppy)py)Cl] **(14)** in a frozen glassy CH_2Cl_2/MeOH matrix (V:V = 1:1) at 77 K, including the residuals (λ_{exc} = 376.7 nm, λ_{em} = 660 nm). Right: Fitting parameters including pre-exponential factors and confidence limits.

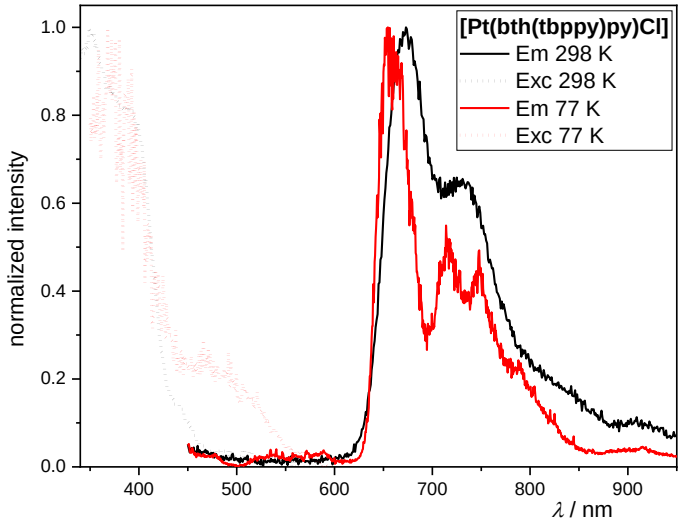

Fig. S91 Excitation (dotted line) and emission spectra (solid line) of [Pt(bth(tbppy)py)Cl] **(15)** (λ_{exc} = 350 nm; λ_{em} = 650 nm at 298 K; λ_{em} = 660 nm at 77 K) at 298 K (black) in CH_2Cl_2 and at 77 K (red) in a frozen glassy CH_2Cl_2/MeOH matrix (V:V = 1:1). All solutions were optically diluted (A < 0.1). Spectra normalised to the highest intensity.

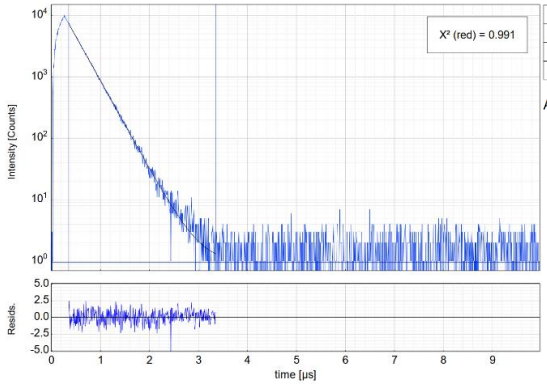

Parameter	Value	Conf. Lower	Conf. Upper	Conf. Estimation
A_1 [Cnts]	7227.4	-41.8	+41.8	Fitting
τ_1 [µs]	0.30185	-0.00126	+0.00126	Fitting
Bkgr. Dec [Cnts]	0.960	-0.539	+0.539	Fitting

Average Lifetime:

$\tau_{Av.1}$=0.30185 µs (intensity weighted)

$\tau_{Av.2}$=0.30185 µs (amplitude weighted)

Fig. S92 Left: Raw (experimental) time-resolved photoluminescence decay of [Pt(bth(tbppy)py)Cl] **(15)** in CH_2Cl_2 at 298 K (air-equilibrated), including the residuals (λ_{exc} = 376.7 nm, λ_{em} = 670 nm). Right: Fitting parameters including pre-exponential factors and confidence limits.

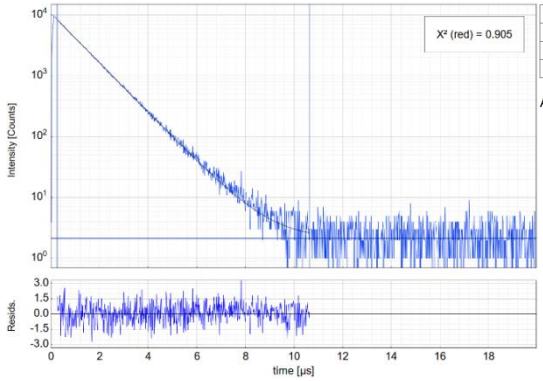

Parameter	Value	Conf. Lower	Conf. Upper	Conf. Estimation
A_1 [Cnts]	8229.8	-42.3	+42.3	Fitting
τ_1 [µs]	1.06880	-0.00398	+0.00398	Fitting
Bkgr. Dec [Cnts]	2.128	-0.604	+0.604	Fitting

Average Lifetime:

$\tau_{Av.1}$=1.06880 µs (intensity weighted)

$\tau_{Av.2}$=1.06880 µs (amplitude weighted)

Fig. S93 Left: Raw (experimental) time-resolved photoluminescence decay of [Pt(bth(tbppy)py)Cl] **(15)** in CH_2Cl_2 at 298 K (Ar-purged), including the residuals (λ_{exc} = 376.7 nm, λ_{em} = 670 nm). Right: Fitting parameters including pre-exponential factors and confidence limits.

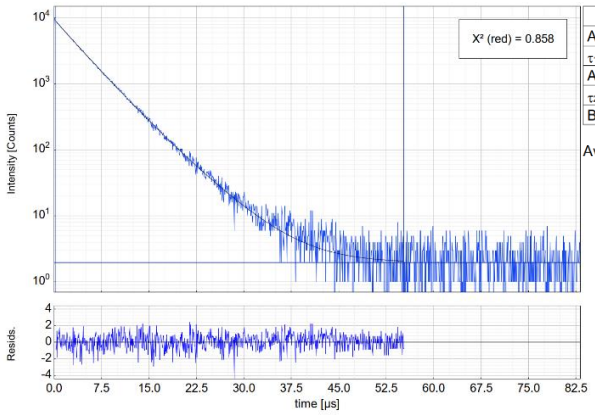

Parameter	Value	Conf. Lower	Conf. Upper	Conf. Estimation
A_1 [Cnts]	1873.4	-35.5	+35.5	Fitting
τ_1 [µs]	5.6366	-0.0606	+0.0606	Fitting
A_2 [Cnts]	6897.8	-54.5	+54.5	Fitting
τ_2 [µs]	3.7567	-0.0239	+0.0239	Fitting
Bkgr. Dec [Cnts]	1.954	-0.460	+0.460	Fitting

Average Lifetime:

$\tau_{Av.1}$=4.3010 µs (intensity weighted)

$\tau_{Av.2}$=4.1582 µs (amplitude weighted)

Fig. S94 Left: Raw (experimental) time-resolved photoluminescence decay of [Pt(bth(tbppy)py)Cl] **(15)** in a frozen glassy CH_2Cl_2/MeOH matrix (V:V = 1:1) at 77 K, including the residuals (λ_{exc} = 376.7 nm, λ_{em} = 660 nm). Right: Fitting parameters including pre-exponential factors and confidence limits.

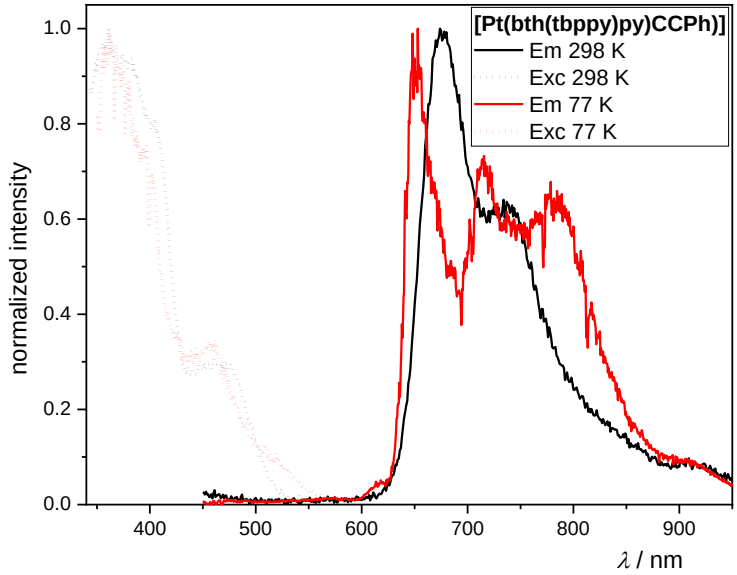

Fig. S95 Excitation (dotted line) and emission spectra (solid line) of [Pt(bth(tbppy)py)CCPh] **(16)** (λ_{exc} = 350 nm; λ_{em} = 650 nm at 298 K; λ_{em} = 660 nm at 77 K) at 298 K (black) in CH_2Cl_2 and at 77 K (red) in a frozen glassy CH_2Cl_2/MeOH matrix (V:V = 1:1). All solutions were optically diluted (A < 0.1). Spectra normalised to the highest intensity.

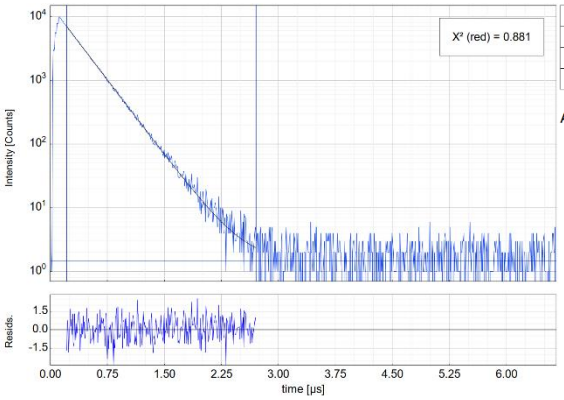

Parameter	Value	Conf. Lower	Conf. Upper	Conf. Estimation
A_1 [Cnts]	7000.6	-36.9	+36.9	Fitting
τ_1 [µs]	0.27722	-0.00106	+0.00106	Fitting
Bkgr. Dec [Cnts]	1.480	-0.626	+0.626	Fitting

Average Lifetime:

$\tau_{Av.1}$=0.27722 µs (intensity weighted)

$\tau_{Av.2}$=0.27722 µs (amplitude weighted)

Fig. S96 Left: Raw (experimental) time-resolved photoluminescence decay of [Pt(bth(tbppy)py)CCPh] **(16)** in CH_2Cl_2 at 298 K (air-equilibrated), including the residuals (λ_{exc} = 376.7 nm, λ_{em} = 675 nm). Right: Fitting parameters including pre-exponential factors and confidence limits.

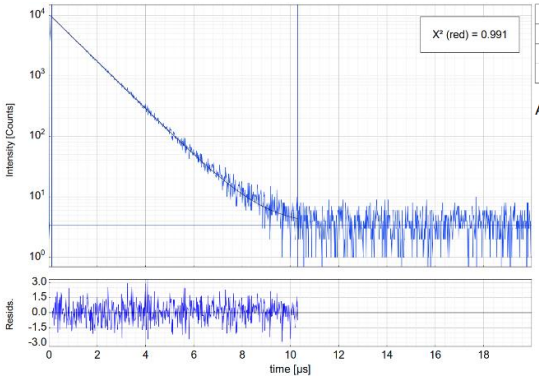

Parameter	Value	Conf. Lower	Conf. Upper	Conf. Estimation
A_1 [Cnts]	9342.3	-45.9	+45.9	Fitting
τ_1 [µs]	1.11035	-0.00396	+0.00396	Fitting
Bkgr. Dec [Cnts]	3.387	-0.790	+0.790	Fitting

Average Lifetime:

$\tau_{Av.1}$=1.11035 µs (intensity weighted)

$\tau_{Av.2}$=1.11035 µs (amplitude weighted)

Fig. S97 Left: Raw (experimental) time-resolved photoluminescence decay of [Pt(bth(tbppy)py)CCPh] **(16)** in CH_2Cl_2 at 298 K (Ar-purged), including the residuals (λ_{exc} = 376.7 nm, λ_{em} = 675 nm). Right: Fitting parameters including pre-exponential factors and confidence limits.

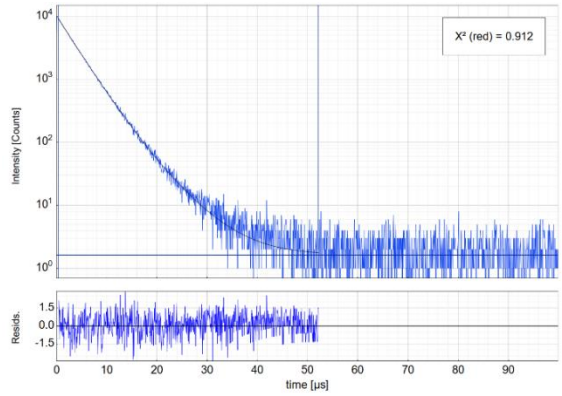

Parameter	Value	Conf. Lower	Conf. Upper	Conf. Estimation
A_1 [Cnts]	750.8	-28.3	+28.3	Fitting
τ_1 [µs]	5.999	-0.113	+0.113	Fitting
A_2 [Cnts]	8197.1	-57.3	+57.3	Fitting
τ_2 [µs]	3.3444	-0.0183	+0.0183	Fitting
Bkgr. Dec [Cnts]	1.636	-0.448	+0.448	Fitting

Average Lifetime:

$\tau_{Av.1}$=3.719 µs (intensity weighted)

$\tau_{Av.2}$=3.567 µs (amplitude weighted)

Fig. S98 Left: Raw (experimental) time-resolved photoluminescence decay of [Pt(bth(tbppy)py)CCPh] **(16)** in a frozen glassy CH_2Cl_2/MeOH matrix (V:V = 1:1) at 77 K, including the residuals (λ_{exc} = 376.7 nm, λ_{em} = 660 nm). Right: Fitting parameters including pre-exponential factors and confidence limits.

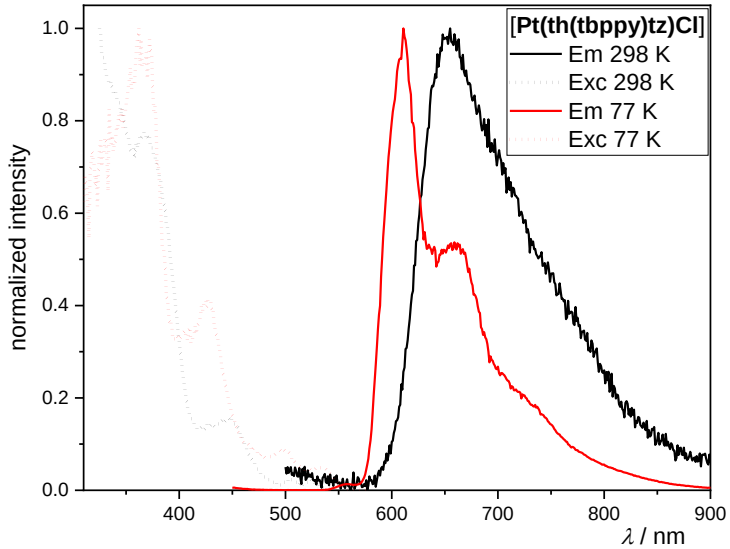

Fig. S99 Excitation (dotted line) and emission spectra (solid line) of [Pt(th(tbppy)tz)Cl] **(17)** (λ_{exc} = 350 nm; λ_{em} = 620 nm at 298 K, λ_{em} = 600 nm at 77 K) at 298 K (black) in CH_2Cl_2 and at 77 K (red) in a frozen glassy CH_2Cl_2/MeOH matrix (V:V = 1:1). All solutions were optically diluted (A < 0.1). Spectra normalised to the highest intensity.

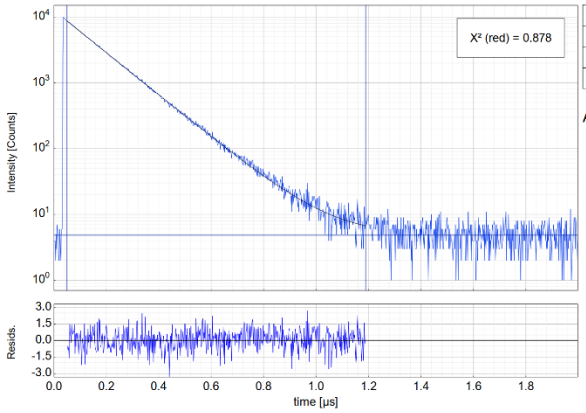

Parameter	Value	Conf. Lower	Conf. Upper	Conf. Estimation
A_1 [Cnts]	8556.4	-39.6	+39.6	Fitting
τ_1 [µs]	0.135102	-0.000457	+0.000457	Fitting
Bkgr. Dec [Cnts]	4.825	-0.897	+0.897	Fitting

Average Lifetime:

$\tau_{Av.1}$=0.135102 µs (intensity weighted)

$\tau_{Av.2}$=0.135102 µs (amplitude weighted)

Fig. S100 Left: Raw (experimental) time-resolved photoluminescence decay of [Pt(th(tbppy)tz)Cl] **(17)** in CH_2Cl_2 at 298 K (air-equilibrated), including the residuals (λ_{exc} = 376.7 nm, λ_{em} = 650 nm). Right: Fitting parameters including pre-exponential factors and confidence limits.

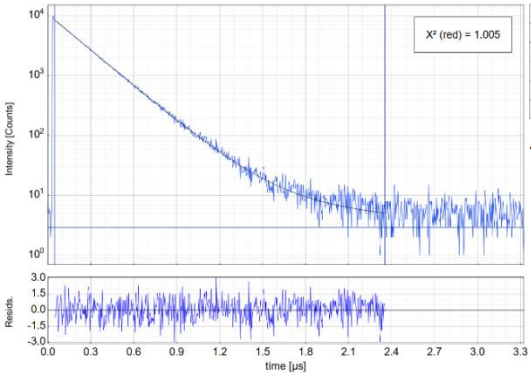

Parameter	Value	Conf. Lower	Conf. Upper	Conf. Estimation
A_1 [Cnts]	36.21	-6.27	+6.27	Fitting
τ_1 [µs]	0.790	-0.484	+0.548	Bootstrap
A_2 [Cnts]	8420.8	-47.4	+47.4	Fitting
τ_2 [µs]	0.21731	-0.00096	+0.00151	Bootstrap
Bkgr. Dec [Cnts]	2.922	-0.758	+0.758	Fitting

Average Lifetime:

$\tau_{Av.1}$=0.226 µs (intensity weighted)

$\tau_{Av.2}$=0.220 µs (amplitude weighted)

Fig. S101 Left: Raw (experimental) time-resolved photoluminescence decay of [Pt(th(tbppy)tz)Cl] **(17)** in CH_2Cl_2 at 298 K (Ar-purged), including the residuals (λ_{exc} = 376.7 nm, λ_{em} = 650 nm). Right: Fitting parameters including pre-exponential factors and confidence limits.

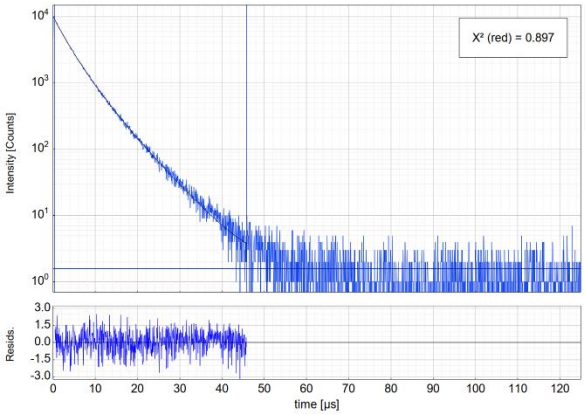

Parameter	Value	Conf. Lower	Conf. Upper	Conf. Estimation
A_1 [Cnts]	3113.2	-29.6	+29.6	Fitting
τ_1 [µs]	6.2508	-0.0360	+0.0360	Fitting
A_2 [Cnts]	5705.9	-59.7	+59.7	Fitting
τ_2 [µs]	3.0401	-0.0294	+0.0294	Fitting
Bkgr. Dec [Cnts]	1.589	-0.760	+0.760	Fitting

Average Lifetime:

$\tau_{Av.1}$=4.7376 µs (intensity weighted)

$\tau_{Av.2}$=4.1735 µs (amplitude weighted)

Fig. S102 Left: Raw (experimental) time-resolved photoluminescence decay of [Pt(th(tbppy)tz)Cl] **(17)** in a frozen glassy CH_2Cl_2/MeOH matrix (V:V = 1:1) at 77 K, including the residuals (λ_{exc} = 376.7 nm, λ_{em} = 600 nm). Right: Fitting parameters including pre-exponential factors and confidence limits.

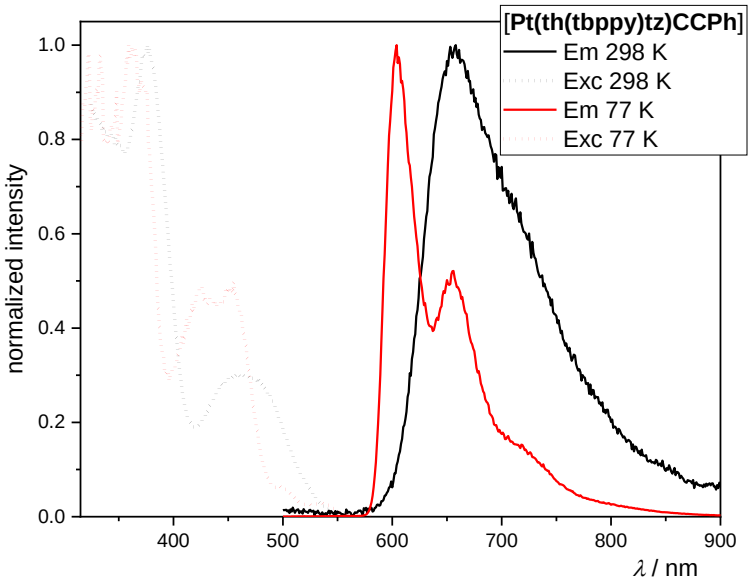

Fig. S103 Excitation (dotted line) and emission spectra (solid line) of [Pt(th(tbppy)tz)CCPh] **(18)** (λ_{exc} = 350 nm; λ_{em} = 620 nm at 298 K, λ_{em} = 600 nm at 77 K) at 298 K (black) in CH_2Cl_2 and at 77 K (red) in a frozen glassy CH_2Cl_2/MeOH matrix (V:V = 1:1). All solutions were optically diluted (A < 0.1). Spectra normalised to the highest intensity.

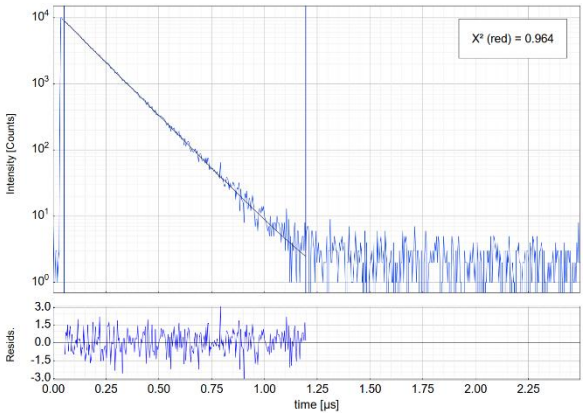

Parameter	Value	Conf. Lower	Conf. Upper	Conf. Estimation
A_1 [Cnts]	8706.9	-41.5	+41.5	Fitting
τ_1 [µs]	0.136143	-0.000469	+0.000469	Fitting
Bkgr. Dec [Cnts]	0.464	-0.760	+0.760	Fitting

Average Lifetime:

$\tau_{Av.1}$=0.136143 µs (intensity weighted)

$\tau_{Av.2}$=0.136143 µs (amplitude weighted)

Fig. S104 Left: Raw (experimental) time-resolved photoluminescence decay of [Pt(th(tbppy)tz)CCPh] **(18)** in CH_2Cl_2 at 298 K (air-equilibrated), including the residuals (λ_{exc} = 376.7 nm, λ_{em} = 650 nm). Right: Fitting parameters including pre-exponential factors and confidence limits.

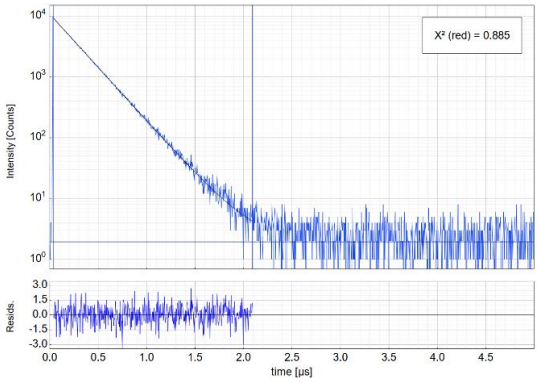

Parameter	Value	Conf. Lower	Conf. Upper	Conf. Estimation
A_1 [Cnts]	9170.7	-40.8	+40.8	Fitting
τ_1 [µs]	0.247380	-0.000797	+0.000797	Fitting
Bkgr. Dec [Cnts]	1.949	-0.838	+0.838	Fitting

Average Lifetime:

$\tau_{Av.1}$=0.247380 µs (intensity weighted)

$\tau_{Av.2}$=0.247380 µs (amplitude weighted)

Fig. S105 Left: Raw (experimental) time-resolved photoluminescence decay of [Pt(th(tbppy)tz)CCPh] **(18)** in CH_2Cl_2 at 298 K (Ar-purged), including the residuals (λ_{exc} = 376.7 nm, λ_{em} = 650 nm). Right: Fitting parameters including pre-exponential factors and confidence limits.

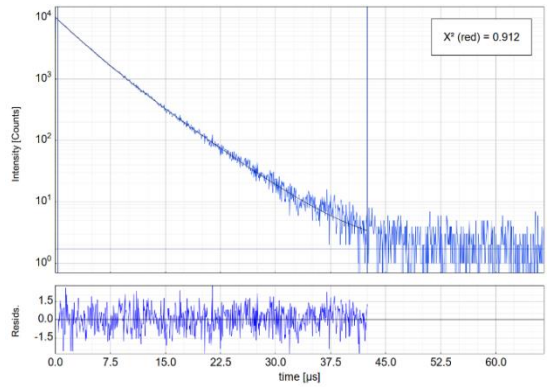

Parameter	Value	Conf. Lower	Conf. Upper	Conf. Estimation
A_1 [Cnts]	4079.4	-34.8	+34.8	Fitting
τ_1 [µs]	5.3992	-0.0290	+0.0290	Fitting
A_2 [Cnts]	5066.7	-57.1	+57.1	Fitting
τ_2 [µs]	3.2150	-0.0324	+0.0324	Fitting
Bkgr. Dec [Cnts]	1.725	-0.742	+0.742	Fitting

Average Lifetime:

$\tau_{Av.1}$=4.4706 µs (intensity weighted)

$\tau_{Av.2}$=4.1892 µs (amplitude weighted)

Fig. S106 Left: Raw (experimental) time-resolved photoluminescence decay of [Pt(th(tbppy)tz)CCPh] **(18)** in a frozen glassy CH_2Cl_2/MeOH matrix (V:V = 1:1) at 77 K, including the residuals (λ_{exc} = 376.7 nm, λ_{em} = 600 nm). Right: Fitting parameters including pre-exponential factors and confidence limits.

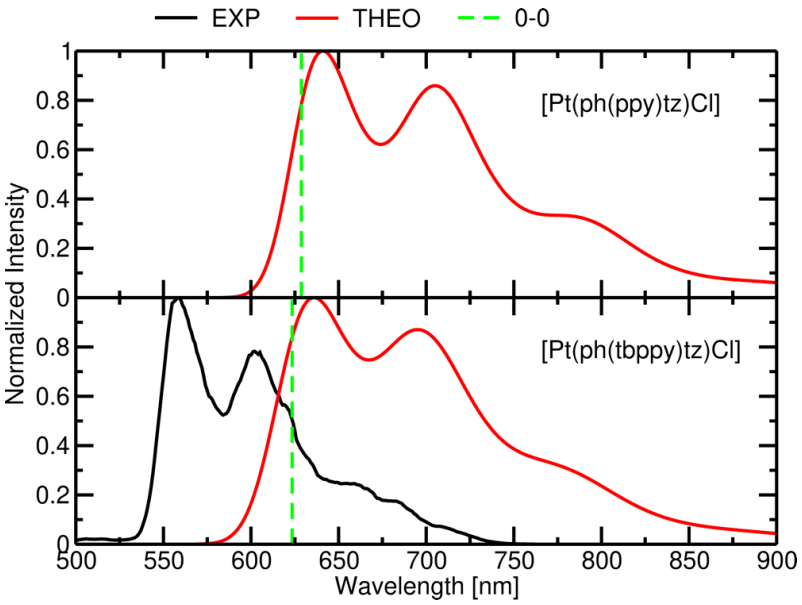

Fig. S107 TD-DFT-calculated emission spectra (THEO, red) compared to experimental spectra at 77 K (EXP, black). Theoretical 0–0 transitions are shown as vertical dashed green lines. Upper panel: complex **1** [Pt(ph(ppy)tz)Cl]. Lower panel complex **2** [Pt(ph(tbppy)tz)Cl].

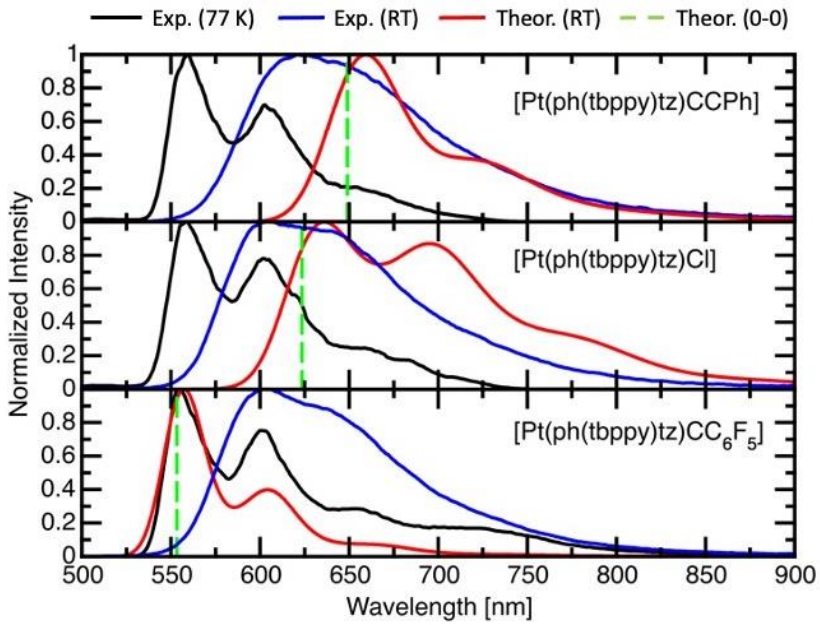

Fig. S108 TD-DFT-calculated emission spectra (Theor, red) compared to experimental spectra (EXP, black) for complexes of **class A** complexes at 77 K. Theoretical 0–0 transitions are shown as vertical dashed green lines. Upper panel: complex **3** [Pt(ph(tbppy)tz)C≡CPh]. Middle panel: complex **2** [Pt(ph(tbppy)tz)Cl]. Lower panel: complex **4** [Pt(ph(tbppy)tz)C≡CC$_6$F$_5$].

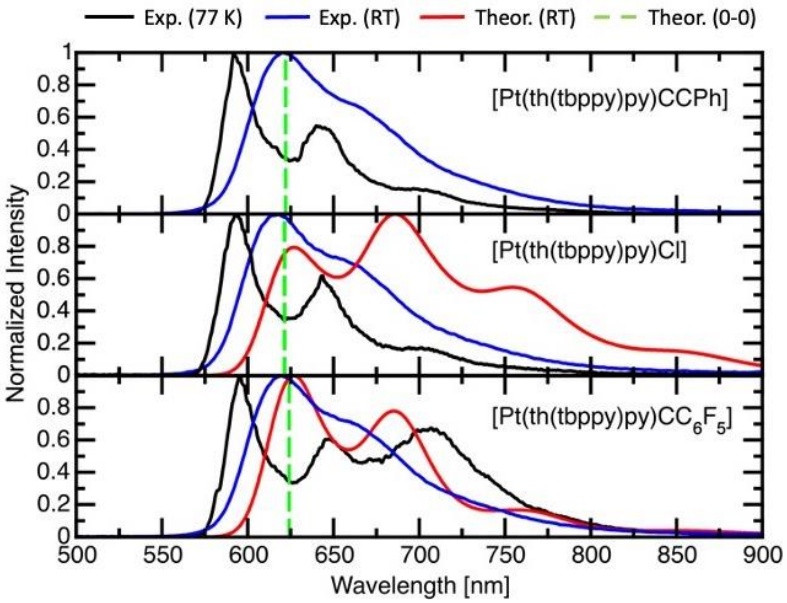

Fig. S109 TD-DFT-calculated emission spectra (Theor, red) of **class B** complexes compared to experimental spectra (EXP, black) at 77 K. Calculated 0–0 transitions are shown as vertical dashed green lines. Upper panel: complex **12** [Pt(th(tbppy)py)C≡CPh]. Middle panel: complex **11** [Pt(th(tbppy)py)Cl]. Lower panel: complex **13** [Pt(th(tbppy)py)C≡CC$_6$F$_5$].

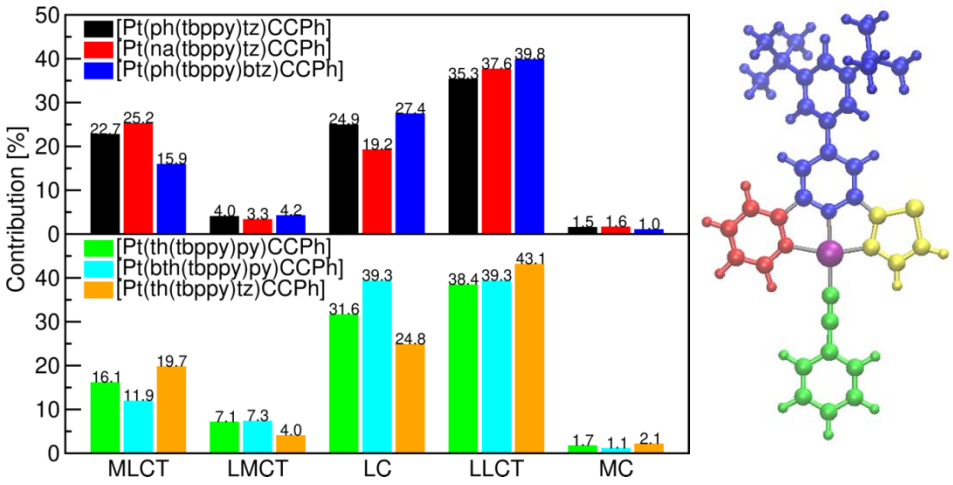

Fig. S110 Left: Decomposition of the emissive T_1 states into MLCT, LMCT, LC, LLCT, and MC contributions of complexes **3**, **6**, **9** (top), and **12**, **16**, **18** (bottom). Right: Molecular partitioning used for the example of complex **3**, all other complexes were partitioned in an analogous manner.

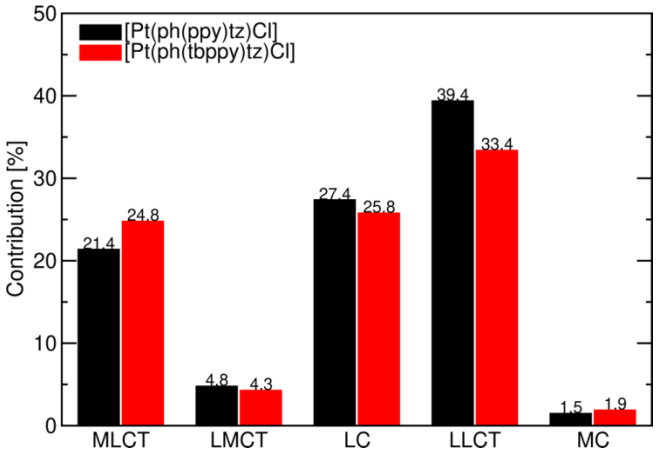

Fig. S111 Decomposition of the emissive T_1 states into MLCT, LMCT, LC, LLCT, and MC contributions of [Pt(ph(ppy)tz)Cl] **(1)** and [Pt(ph(tbppy)tz)Cl] **(2)**.

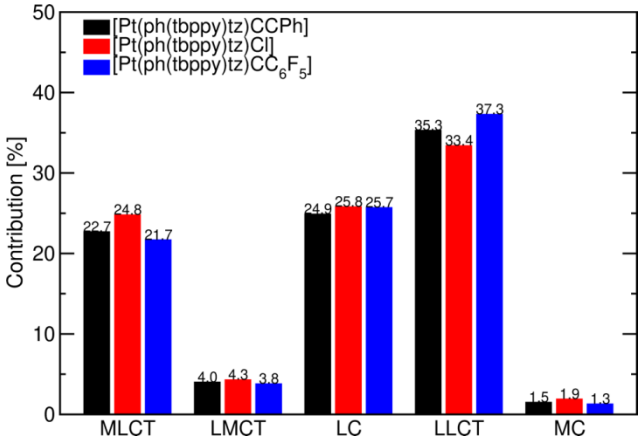

Fig. S112 Decomposition of the emissive T_1 states into MLCT, LMCT, LC, LLCT, and MC contributions for **class A** complexes (black: complex **(3)** [Pt(ph(tbppy)tz)CCPh], red: complex **(2)** [Pt(ph(tbppy)tz)Cl], blue: complex **(4)** [Pt(ph(tbppy)tz)CCC$_6$F$_5$]).

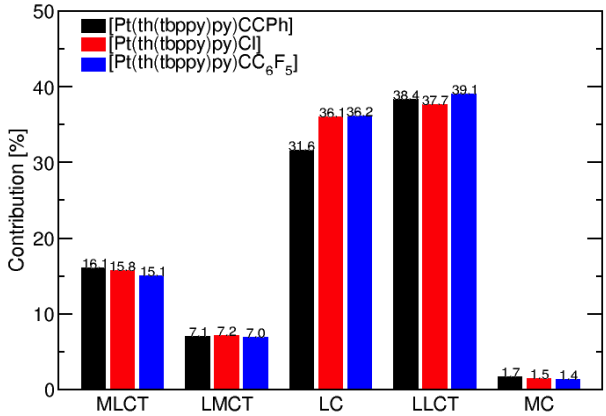

Fig. S113 Decomposition of the emissive T_1 states into MLCT, LMCT, LC, LLCT, and MC contributions for **class B** complexes (black: [Pt(th(tbppy)py)(C≡CPh)] (**12**), red: [Pt(th(tbppy)py)Cl] (**11**), blue: [Pt(th(tbppy)py)(C≡CC$_6$F$_5$)] (**13**).

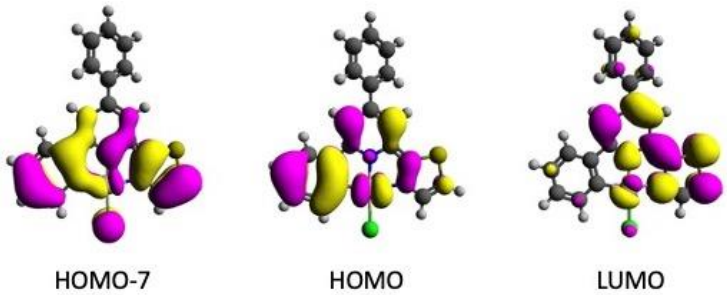

Fig. S114 Molecular orbitals of complex (**1)** with the largest contributions to the emissive T_1 state.

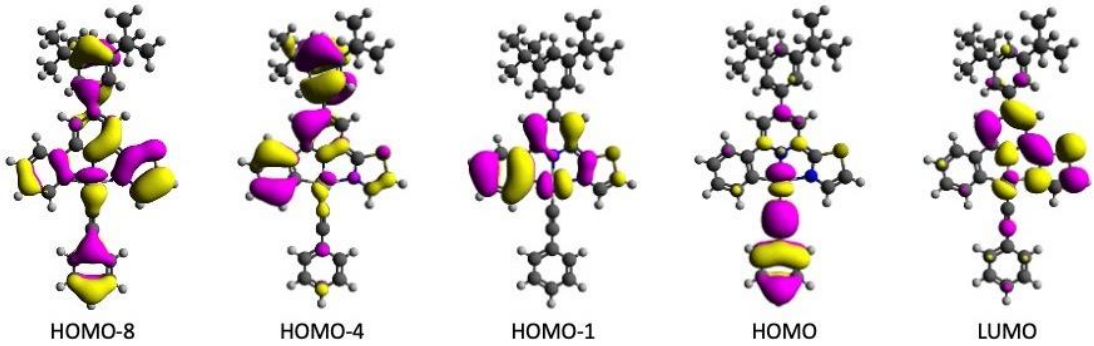

Fig. S115 Molecular orbitals of complex (**3)** with the largest contributions to the emissive T_1 state.

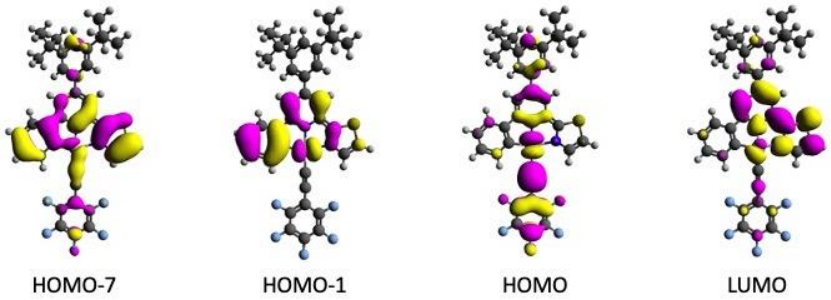

Fig. S116 Molecular orbitals of complex (**4)** with the largest contribitons to the emissive T_1 state.

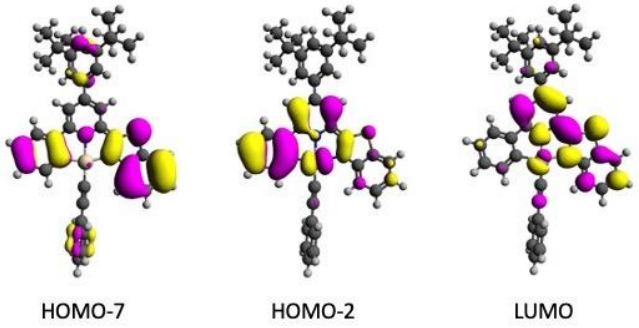

Fig. S117 Molecular orbitals of complex (**9)** with the largest contribitons to the emissive T_1 state.

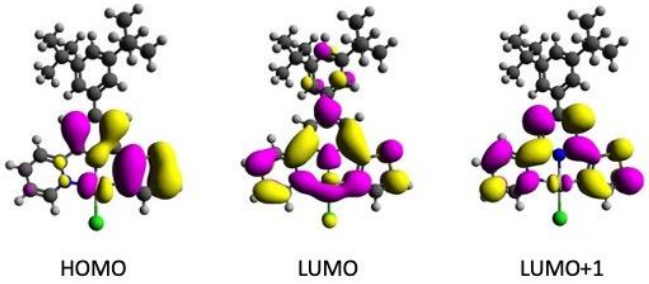

Fig. S118 Molecular orbitals of complex (**11)** with the largest contributions to the emissive T_1 state.

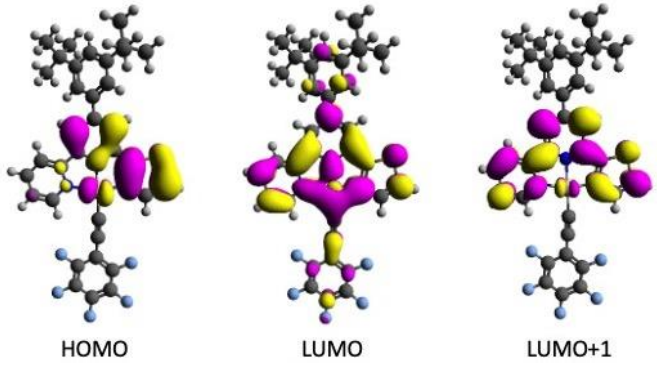

Fig. S119 Molecular orbitals of complex (**12)** with the largest contributions to the emissive T_1 state.

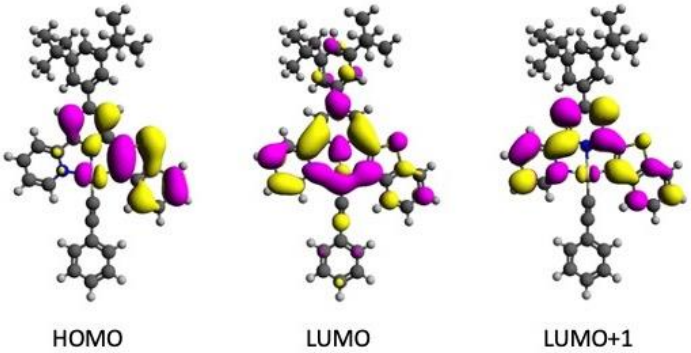

Fig. S120 Molecular orbitals of complex (**16)** with the largest contributions to the emissive T_1 state.

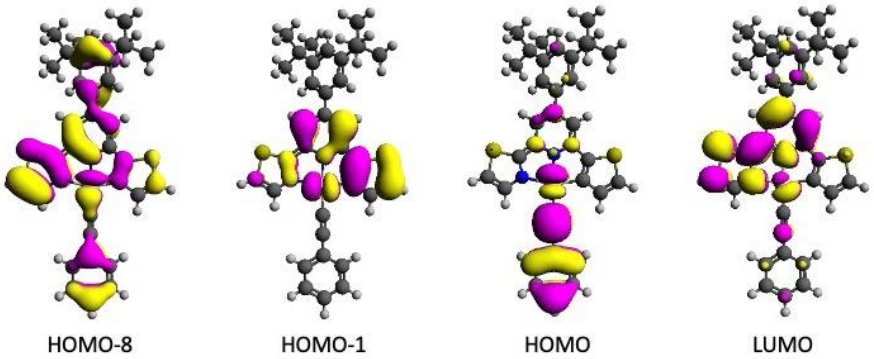

Fig. S121 Molecular orbitals of complex (**18)** with the largest contributions to the emissive T_1 state.

Supporting Tables

Table S1 Selected structure solution and refinement data for [Pt(th(ppy)py)Cl]·CD_2Cl_2 **(10**·CH_2Cl_2**)** and [Pt(ph(tbppy)btz)(CCPh)] **(9)**.

Complex	[Pt(th(ppy)py)Cl]·CH_2Cl_2 **(10**·CH_2Cl_2**)**	[Pt(ph(tbppy)btz)(CCPh)] **(9)** [a]
Formula	$C_{20}H_{13}N_2SPtCl$·CD_2Cl_2	$C_{40}H_{36}N_2PtS$
Molecular weigth	1253.67	771.86
Temperature	170(2) K	100(2) K
Radiation wavelenght	0.71073 Å	0.56076 Å (synchrotron)
Crystal system	triclinic	Monoclinic
Space group	$P\bar{1}$ (No. 2)	$P\ 2_1/c$ (No. 14)
Cell parameters	a = 7.9533(7) Å	a = 13.1805(4) Å
	b = 9.8707(8) Å	b = 37.3146(19) Å
	c = 14.3097(11) Å	c = 6.7184(2) Å
	α = 102.887(6)°	
	β = 103.515(6)°	β = 100.192(3)°
	γ = 102.960(6)°	
Volume	1018.48(15) $Å^3$	3252.1(2) $Å^3$
Z	2	4
Density calculated	2.052 g/cm^3	1.576 g/cm^3
Absorption coefficient	7.397 mm^{-1}	2.400 mm^{-1}
F(000)	601	1536
Theta range for data collection	2.213 to 29.293°	1.729 to 25.650°.
Index ranges	−10≤h≤10, −12≤k≤13, −19≤l≤19	−20≤h≤20, −53≤k≤53, −8≤l≤8
Reflections collected	13115	45728
Independent reflections	5443 [R_{int} = 0.0794]	10542 [R_{int} = 0.0982]
Completeness to theta	theta = 19.661°: 99.8%	theta = 19.661°: 97.0%
Refinement method	Full-matrix least-squares on F^2	Full-matrix least-squares on F^2
Data / restraints / parameters	5443 / 0 / 254	10542 / 0 / 404
Goodness-of-fit on F^2	0.982	1.064
Final R indices [I>2sigma(I)]	R_1 = 0.0493, wR_2 = 0.1175	R_1 = 0.00736, wR_2 = 0.1626
R indices (all data)	R_1 = 0.0709, wR_2 = 0.1300	R_1 = 0.1287, wR_2 = 0.1854
Extinction coefficient	0.0082(9)	0.0015(3)
Largest diff. peak and hole	1.96 and −2.29 e.$Å^{-3}$	3.90 and −4.21 e.$Å^{-3}$
CCDC	2081667	2084095

The dataset for 9 is generally poor and A alerts appeared in the checkcif. The problem is due to poor quality of the crystal.

Table S2 Selected structural data for [Pt(th(ppy)py)Cl]·CH_2Cl_2 **(10**·CH_2Cl_2**)** and [Pt(ph(tbppy)btz)(CCPh)] **(9)**.

distances (Å)	[Pt(th(ppy)py)Cl]·CD_2Cl_2 **(10**·CH_2Cl_2**)**	distances (Å)	[Pt(ph(tbppy)btz)(CCPh)] **(9)**
Pt–C1	1.983(7)	Pt–C1	1.99(1)
Pt–N1	1.957(6)	Pt–N1	2.00(7)
Pt–N2	2.109(5)	Pt–N2	2.13(7)
Pt–Cl	2.293(3)	Pt–C33	1.98(1)
C4–C20	1.45(1)	C12–C11	1.46(1)
C30–C24	1.49(1)	C6–C7	1.47(1)
angles (°)		angles (°)	
Cl–Pt–N1	178.8(2)	C33–Pt–N1	175.3(4)
C1–Pt–N2	161.3(3)	C1–Pt–N2	159.1(3)
C1–Pt–N1	82.2(3)	C1–Pt–N1	81.4(3)
N1–Pt–N2	79.1(2)	N1–Pt–N2	77.6(3)
Cl–Pt–C1	98.6(3)	C33–Pt–C1	93.9(4)
Cl–Pt–N2	100.0(2)	C33–Pt–N2	107.1(4)
C3–S1–C4	90.4(4)	C14–S1–C12	89.3(5)
C1–C4–C20–C21	176.7(9)	C1–C6–C7–C8	175.8(9)
N2–C30–C24–C23	178.0(8)	N2–C12–C11–C10	179.5(9)
C2–C1–C4–C20	175.0(8)	C13–N2–C12–C11	179.6(8)
C21–C22–C40–C45	38.8(11)	C8–C9–C19–C24	33.2(14)
Sum of angles around Pt	360		360

Table S3 Redox potentials of the HC^N^N protoligands.[a]

	$E_{1/2}$ (Red1)	E_{pc} (Red2)	E_{pc} (Red3)
Hth(ppy)py	–2.53	–3.28	
Hth(tbppy)py	–2.57	–3.39	
Hbth(ppy)py	–2.58	–3.04	–3.18
Hbth(tbppy)py	–2.51	–2.92	–3.05
Hph(ppy)tz	–2.44	–3.22	
Hph(tbppy)tz	–2.50	–2.75	–3.43
Hna(ppy)tz	–2.44	–3.02	
Hna(tbppy)tz	–2.45	–3.07	
Hth(tbppy)tz	–2.41		
Hph(ppy)btz	–2.26	–2.76	–3.19
Hph(tbppy)btz	–2.31	–2.89	–3.27

[a] Electrochemical potentials [V], $E_{1/2}$ for reversible redox waves, E_{pc} for irreversible reduction waves, measured in 0.1 M *n* Bu_4NPF_6/THF at 298 K, scan rate 100 mV/s.

Table S4 Selected redox potentials of [Pt(C^N^N)(Cl/R)] complexes.[a]

			Ox (in CH_2Cl_2)		Red (in THF)			ΔE
C^N^N	X	Number	E_{pa} ox 2	E_{pa} ox 1	$E_{1/2}$ red 1	$E_{1/2}$ red 2	red 2–red 1	ox 1–red 1
ph(ppy)tz	Cl	**(1)**	-	0.46	–1.64	–2.32	0.68	2.10
ph(tbppy)tz	Cl	**(2)**	1.14	0.67	–1.64	–2.34	0.70	2.31
ph(tbppy)tz	CCPh	**(3)**	0.60	0.39	–1.66	–2.33	0.67	2.05
ph(tbppy)tz	CCC_6F_5	**(4)**	1.02	0.55	–1.62	–2.25	0.63	2.17
na(ppy)tz	Cl	**(5)**	1.08	0.40	–1.63	–2.28	0.65	2.03
na(tbppy)tz	CCPh	**(6)**	0.62	0.34	–1.66	–2.33	0.67	2.00
ph(ppy)btz	Cl	**(7)**	1.16	0.53	–1.48	–2.13	0.65	2.01
ph(tbppy)btz	Cl	**(8)**	1.16	0.61	–1.51	–2.17	0.66	2.12
ph(tbppy)btz	CCPh	**(9)**	0.57	0.17	–1.54 [b]	–2.20 [b]	0.66	1.71
th(ppy)py	Cl	**(10)**	-	0.55	–1.76	–2.40	0.64	2.28
th(tbppy)py	Cl	**(11)**	1.22	0.86	–1.76	–2.42	0.66	2.62
th(tbppy)py	CCPh	**(12)**	0.74	0.42	–1.74	–2.38	0.64	2.16

th(tbppy)py	CCC_6F_5	**(13)**	0.91	0.32	–1.72	–2.30	0.58	2.04
bth(ppy)py	Cl	**(14)**	-	0.48	–1.65	–2.30	0.62	2.16
bth(tbppy)py	Cl	**(15)**	1.09	0.55	–1.70	–2.35	0.65	2.25
bth(tbppy)py	CCPh	**(16)**	0.42	0.19	–1.71	–2.33	0.62	1.90
th(tbppy)tz	Cl	**(17)**	0.75	0.59	–1.64	–2.33	0.69	2.23
th(tbppy)tz	CCPh	**(18)**	0.76	0.40	–1.64	–2.32	0.68	2.04

[a] Plots in Figs S5-S26, this ESI. Electrochemical potentials [V] with an accuracy of ±0.003 V, vs ferrocene/ferrocenium; $E_{1/2}$ for reversible redox waves, E_{pc} for irreversible reduction waves and E_{pa} for irreversible oxidation waves; measured in 0.1 M nBu$_4$NPF$_6$/CH_2Cl_2 or THF at 298 K, scan rate 100 mV/s, oxidations measured in CH_2Cl_2, reductions in THF. [b] Measured in CH_2Cl_2.

Table S5 UV-vis absorption maxima of HC^N^N protoligands.[a]

HC^N^N	λ_1 (ε)	λ_2 (ε)	λ_3 (ε)	λ_4 (ε)	λ_5 (ε)	λ_6 (ε)
Hph(ppy)tz	257sh (2.96)	266 (3.42)	-	299sh (1.20)	325 (1.13)	344sh (0.46)
Hph(tbppy)tz	-	273 (3.65)	-	-	325 (1.21)	340sh (0.74)
Hna(tbppy)tz	-	266 (4.02)	286 (3.48)	299sh (2.71)	333 (1.14)	347sh (0.69)
Hph(ppy)btz	257 (4.25)	271 (3.99)	-	286sh (3.22)	329 (2.29)	342 (2.05)
Hph(tbppy)btz	258 (2.88)	275 (3.19)	-	-	329 (1.70)	341 (1.60)
Hth(ppy)py	250 (3.67)	280 (3.18)	-	306sh (1.88)	328 (1.46)	350sh (0.56)
Hth(tbppy)py	252 (1.98)	282 (2.63)	-	-	328 (0.92)	350sh (0.27)
Hbth(ppy)py	255 (2.53)	284 (2.22)	-	317sh (1.82)	327 (1.82)	353sh (0.75)
Hbth(tbppy)py	261 (2.39)	284 (2.85)	-	318sh (1.72)	327 (1.69)	354sh (0.44)
Hth(tbppy)tz	-	280 (3.15)	-	-	326 (1.16)	349 (0.45)

[a] Measured in CH_2Cl_2 (298 K), sh = shoulder, wavelength λ in nm, extinction coefficients ε in 10^4 $M^{-1}cm^{-1}$.

Table S6 UV-vis absorption maxima of the [Pt(C^N^N)X] complexes.[a]

C^N^N	X		λ_1 (ε)	λ_2 (ε)	λ_3 (ε)	λ_4 (ε)	λ_5 (ε)	λ_6 (ε)	λ_7 (ε)	λ_8 (ε)	λ_9 (ε)	λ_{10} (ε)
ph(ppy)tz	Cl	**(1)**		-	296 (2.82)	321sh (1.71)	337 (1.86)	373 (1.25)	-	426sh (0.49)	447 (0.44)	501sh (0.09)
ph(tbppy)tz	Cl	**(2)**	271sh (1.99)		297 (2.81)		338 (2.02)	373 (1.04)	-	425sh (0.36)	448 (0.40)	499sh (0.05)
	CCPh	**(3)**	273sh (4.04)	285 (4.24)	298 (4.14)		339 (2.22)	377 (1.58)	-	444sh (0.67)	466 (0.75)	545sh (0.07)
	CCC_6F_5	**(4)**		274sh (2.88)	298 (3.29)		338 (1.95)	371 (1.39)	-	435sh (0.66)	454 (0.68)	509sh (0.06)
na(tbppy)tz	Cl	**(5)**	250 (2.61)		297 (2.96)		337 (2.19)	369 (1.22)		430sh (0.44)	445 (0.49)	500sh (0.02)
	CCPh	**(6)**		284 (5.09)	300 (5.29)	308sh (5.12)	331sh (3.02)	369 (1.88)	398sh (1.32)	413sh (0.81)	463 (0.88)	527sh (0.18)
ph(ppy)btz	Cl	**(7)**		-	305 (2.86)	320sh (2.48)	352 (2.46)	384 (1.26)	-	440sh (0.32)	466 (0.35)	515sh (0.08)
ph(tbppy)btz	Cl	**(8)**		271sh (3.58)	306 (4.34)	323sh (3.07)	350 (3.87)	382sh (1.91)	-	438sh (0.46)	466 (0.51)	514sh (0.10)
	CCPh	**(9)**		270 (3.54)	301 (3.16)	323sh (2.28)	348 (2.28)	384 (1.51)	-	476 (0.56)	505 (0.52)	574sh (0.05)
th(ppy)py	Cl	**(10)**		-	287sh (3.39)	298 (3.58)	335sh (1.86)	367 (1.51)	384sh (1.35)	-	435 (0.41)	491sh (0.04)
th(tbppy)py	Cl	**(11)**		-	284 (2.23)	310 (2.66)	336sh (1.59)	366 (1.19)	380sh (1.11)	-	435 (0.33)	489sh (0.04)
	CCPh	**(12)**		273 (2.42)	290 (2.40)	306 (2.19)	323sh (1.85)	373 (1.26)	-	440 (0.51)	467sh (0.45)	517sh (0.04)
	CCC_6F_5	**(13)**		270sh (2.71)	285 (3.23)	313 (2.87)	341sh (1.89)	371 (1.72)	-	424sh (0.76)	443 (0.79)	501sh (0.05)

bth(ppy)py	Cl	**(14)**		-	291 (3.64)		351 (1.97)	385 (1.66)	-	-	439 (0.27)	495sh (0.06)
bth(tbppy)py	Cl	**(15)**		-	287 (3.96)	310 (3.43)	349 (2.50)	387 (1.96)	-	-	440 (0.34)	496 (0.07)
	CCPh	**(16)**		272sh (2.98)	287 (3.02)	296 (2.91)	355 (1.64)	381 (1.53)	-	407 (1.28)	469 (0.43)	541sh (0.02)
th(tbppy)tz	Cl	**(17)**		-	290sh (2.48)	306 (2.92)	327sh (2.15)	359 (1.64)	380sh (1.15)	-	436 (0.35)	505sh (0.05)
	CCPh	**(18)**		286 (2.86)	299 (2.80)	300 (2.79)	318sh (2.21)	367 (2.18)	381sh (1.55)	441 (0.68)	468 (0.63)	560sh (0.06)

[a] Measured in CH_2Cl_2 (298 K), sh = shoulder, wavelength λ in nm, extinction coefficients ε in 10^4 $M^{-1}cm^{-1}$.

Table S7 Complete emission data and PLYQs, as well as exited state lifetime data for each complex in CH_2Cl_2 at 298 K and in frozen glassy matrix of CH_2Cl_2/MeOH (V:V = 1:1) at 77 K. For multiexponential decays, the amplitude-weighted average lifetimes are given as well as the different components in square brackets with relative amplitudes as percentages in parentheses.

class	Complex	Medium (T/K)	λ_{em}	λ_{exc}	τ_{av} [a]	Φ ± 0.02/± 0.05
B	[Pt(th(ppy)py)Cl] (**10**)	CH_2Cl_2, air (298)	621, 660 sh	341, 450	n.d.	< 0.02
		CH_2Cl_2, Ar (298)			5.04 ± 0.24 [5.49 ± 0.06 (89); 1.3 ± 0.6 (11)]	0.05
		glassy matrix (77)	598, 650, 710	320, 367, 426	11.0 ± 0.4 [12.34 ± 0.10 (79); 6.1 ± 0.5 (21)]	0.39
	[Pt(bth(ppy)py)Cl] (**14**)	CH_2Cl_2, air (298)	675, 745	350, 400, 450sh	n.d.	< 0.02
		CH_2Cl_2, Ar (298)			1.022 ± 0.029 [3.0 ± 0.7 (1); 1.015 ± 0.009 (99)]	0.02
		glassy matrix (77)	655, 720, 800	373, 400	4.71 ± 0.17 [5.60 ± 0.10 (35); 4.23 ± 0.06 (65)]	0.23
	[Pt(th(tbppy)py)Cl] (**11**)	CH_2Cl_2, air (298)	617, 660 sh	315, 370, 440	0.3393 ± 0.0022	< 0.02
		CH_2Cl_2, Ar (298)			1.809 ± 0.013	0.07
		glassy matrix (77)	595, 645, 700	375, 425, 470sh, 490sh	11.6 ± 0.9 [13.17 ± 0.14 (59); 9.32 ± 0.26 (41)]	0.58
	[Pt(bth(tbppy)py)Cl] (**15**)	CH_2Cl_2, air (298)	675, 730	350, 395, 440sh	0.3019 ± 0.0025	< 0.02
		CH_2Cl_2, Ar (298)			1.069 ± 0.008	0.03
		glassy matrix (77)	655, 720, 745	375, 480	4.16 ± 0.16 [5.64 ± 0.12 (21); 3.76 ± 0.05 (79)]	0.13
	[Pt(th(tbppy)py)CCPh] (**12**)	CH_2Cl_2, air (298)	620, 660sh	300, 373, 440, 475sh	0.3146 ± 0.0020	0.04
		CH_2Cl_2, Ar (298)			1.628 ± 0.012	0.14
		glassy matrix (77)	590, 640, 700sh	360, 425sh, 460	8.2 ± 0.3 [9.69 ± 0.15 (37); 7.39 ± 0.11 (63)]	0.79
	[Pt(bth(tbppy)py)CCPh] (**16**)	CH_2Cl_2, air (298)	675, 740	360, 380sh, 405sh, 475	0.2772 ± 0.0021	< 0.02
		CH_2Cl_2, Ar (298)			1.110 ± 0.008	0.04
		glassy	650, 720, 785	365, 400sh, 460	3.57 ± 0.13 [6.00 ± 0.23 (8);	0.24

		matrix (77)			3.34 ± 0.03 (92)]	
	[Pt(th(tbppy)py)CC$_6$F$_5$] (**13**)	CH_2Cl_2, air (298)	620, 660 sh	312, 370, 425sh, 445	0.3513 ± 0.0023	0.03
		CH_2Cl_2, Ar (298)			2.178 ± 0.016	0.15
		glassy matrix (77)	595, 650, 705	350-375, 430	8.7 ± 0.3 [10.08 ± 0.09 (71); 5.5 ± 0.3 (29)]	0.79
A	[Pt(ph(tbppy)btz)Cl] (**8**)	CH_2Cl_2M, air (298)	635, 675sh	353, 464	0.1832 ± 0.0014	< 0.02
		CH_2Cl_2, Ar (298)			0.2057 ± 0.0018	< 0.02
		glassy matrix (77)	600, 656, 710sh	346, 425, 452	1.59 ± 0.06 [1.871 ± 0.022 (53); 1.28 ± 0.03 (47)]	0.07
	[Pt(ph(tbppy)tz)CCPh] (**3**)	CH_2Cl_2, air (298)	626, 645sh	302, 346, 380, 443sh, 473, 495sh	0.1891 ± 0.0014	0.03
		CH_2Cl_2, Ar (298)			0.39 ± 0.04 [0.78 ± 0.04(3); 0.375 ± 0.003 (97)]	0.06
		glassy matrix (77)	558, 605, 660sh	336, 370, 425, 438, 468	3.50 ± 0.12 [5.59 ± 0.24 (8); 3.31 ± 0.03 (92)]	0.62
	[Pt(na(tbppy)tz)CCPh] (**6**)	CH_2Cl_2, air (298)	635	311, 335sh, 370, 398, 420sh, 468	0.200 ± 0.007 [0.2105 ± 0.0016 (84); 0.147 ± 0.011 (16)]	0.05
		CH_2Cl_2, Ar (298)			0.407 ± 0.014 [0.97 ± 0.07 (2); 0.395 ± 0.004 (98)]	0.10
		glassy matrix (77)	555, 595, (650sh)	330, 395, 437, 463	3.97 ± 0.16 [4.29 ± 0.04 (67); 3.33 ± 0.12 (33)]	0.82
	[Pt(ph(tbppy)btz)CCPh] (**9**)	CH_2Cl_2, air (298)	655	360, 470, 500sh	0.089 ± 0.003 [0.116 ± 0.004 (14); 0.0844 ± 0.0008 (86)]	< 0.02
		CH_2Cl_2, Ar (298)			0.112 ± 0.004 [0.262 ± 0.019 (2); 0.1085 ± 0.0010 (98)]	< 0.02
		glassy matrix (77)	600, 650, 700sh	360, 470, 500sh	1.70 ± 0.06 [2.25 ± 0.04 (25); 1.52 ± 0.02 (75)]	0.18
	[Pt(ph(tbppy)tz)CC$_6$F$_5$] (**4**)	CH_2Cl_2, air (298)	605, 635sh	345, 370, 445sh, 465	0.3195 ± 0.0025	0.05
		CH_2Cl_2, Ar (298)			0.91 ± 0.03 [2.7 ± 0.4 (1); 0.899 ± 0.008 (99)]	0.12
		glassy matrix (77)	555, 600, 655sh, 725sh	340, 365, 420, 445	3.53 ± 0.12 [4.61 ± 0.14 (13); 3.37 ± 0.03 (87)]	0.49
C	[Pt(th(tbppy)tz)Cl] (**17**)	CH_2Cl_2, air (298)	655	368, 450	0.1351 ± 0.0009	< 0.02
		CH_2Cl_2, Ar (298)			0.220 ± 0.010 [0.8 ± 0.8 (0.4); 0.2173 ± 0.0020 (99.6)]	< 0.02
		glassy matrix (77)	610, 660, 725sh	364, 430, 503sh	4.17 ± 0.15 [6.25 ± 0.07 (35); 3.04 ± 0.06 (65)]	0.13
	[Pt(th(tbppy)tz)CCPh] (**18**)	CH_2Cl_2, air (298)	658	375, 470	0.1361 ± 0.0009	< 0.02
		CH_2Cl_2, Ar (298)			0.2474 ± 0.0016	< 0.02
		glassy matrix (77)	604, 657, 725sh	365, 425, 454	4.19 ± 0.14 [5.40 ± 0.06 (45); 3.22 ± 0.06 (55)]	0.35

[a] We attribute the biexponential lifetimes in fluid solution to different conformations that can be thermally accessed while possessing comparable excited-state character yet different deactivation rates. Moreover, diverse emitting states could coexist in thermal equilibrium, which might be influenced by the microenvironment affecting the excited states' character (particularly in frozen glassy matrices or in solid samples).

Table S8. Selected photophysical properties of previously reported Pt(II)-complexes.[a]

class	complex	λem (nm)	τ (μs)	Φ_L [b]
	[Pt(ph(tbppy)2-quin)Cl]	624	<0.2 μs	<0.001
D	[Pt(ph(tbppy)1-isoquin)Cl]	621	<0.2	<0.001
	[Pt(ph(tbppy)3-isoquin)Cl]	530, 566(sh)	7.6	0.78
	[Pt(ph(tbppy)3-isoquin)(CCC_6F_5)]	521, 556(sh)	7.6	0.99
	[Pt(2,4-F_2ph(tbppy)3-isoquin)Cl] [c]	528, 565(sh)	2.0	0.14
	[Pt(2-MeOph(tbppy)3-isoquin)Cl] [c]	585	3.3	0.23
	[Pt(2-CF_3ph(tbppy)3-isoquin)Cl] [c]	534, 569(sh)	8.9	0.63
E	[Pt(2,3F_2ph(tbppy)3-isoquin)Cl] [c]	529, 565(sh)	8.9	0.65
	[Pt(1,3-F_2ph(tbppy)3-isoquin)Cl] [c]	529, 561(sh)	10.1	0.69
	[Pt(1-F,3-MeOph(tbppy)3-isoquin)Cl] [c]	529, 561(sh)	9.5	0.73
	[Pt(2-NO_2ph(tbppy)3-isoquin)Cl] [c]	529, 565, 622 (sh)	6.7	0.79
	[Pt(th(tbppy)3-isoquin)Cl]	588, 632, 687(sh)	10.1	0.25
	[Pt(th(tbppy)3-isoquin)(CCC_6F_5)]	591, 636, 680(sh)	8.7	0.66
	[Pt(bth(tbppy)3-isoquin)Cl]	644, 701, 780(sh)	4.5	0.033
	[Pt(bth(tbppy)3-isoquin)(CCC_6F_5)]	653, 710(sh)	4.6	0.082
F	[Pt(na(tbppy)py]	561, 597(sh)	0.7	0.10
	[Pt(ph(tbppy)3-isoquin)(CC4-tolyl)]	573	3.5	0.27

[a] From ref. 1, measured in CH_2Cl_2 solution at 298 K; quin = 2-quinolinyl, 3-isoquin = 3-isoquinolinyl, 1-isoquin = 1-isoquinolyl. [b] Φ_L measured by the optical dilute method with $[Ru(bpy)_3](PF_6)_2$ (bpy = 2,2′-bipyridine) in degassed CH_3CN as standard (Φ_L = 0.062) and calculated by: $\Phi_{Ls} = \Phi_{Lr}\,(B_r/B_s)(n_s/n_r)^2(D_s/D_r)$, s and r refer to sample and reference, n is the refractive index of the solvents, D is the integrated intensity and Φ_L is the emission quantum yield. The excitation intensity B is calculated by: $B = 1-10^{-ad}$, where a is the absorbance at the excitation wavelength and d is the optical path length (d = 1 cm in all cases). Errors for Φ_L values (+/–10%) are estimated. [c] Nomenclature: 1 represents the position *ortho* to the Pt bound C atom.

Table S9 TDDFT calculated transitions contributing to the emissive T_1 state.[a]

complex	transitions	contribution [%]
1	HOMO-7 → LUMO	22.6
	HOMO → LUMO	61.3
2	HOMO-7 → LUMO	19.9
	HOMO-1 → LUMO	28.5
	HOMO → LUMO	27.3
3	HOMO-8 → LUMO	20.5
	HOMO-4 → LUMO	10.4
	HOMO-1 → LUMO	22.7
	HOMO → LUMO	31.2
4	HOMO-7 → LUMO	28.0
	HOMO-1 → LUMO	29.2
	HOMO → LUMO	21.4
6	HOMO-8 → LUMO	25.4
	HOMO-3 → LUMO	17.4
	HOMO → LUMO	35.2
9	HOMO-7 → LUMO	15.2
	HOMO-2 → LUMO	57.6
11	HOMO → LUMO	56.1
	HOMO → LUMO+1	37.9
12	HOMO → LUMO	53.7

	HOMO → LUMO+1	35.0
13	HOMO → LUMO	56.7
	HOMO → LUMO+1	35.1
16	HOMO → LUMO	63.9
	HOMO → LUMO+1	31.9
18	HOMO-8 → LUMO	21.6
	HOMO-1 → LUMO	44.5
	HOMO → LUMO	14.6

[a] Based on the optimised T_1 geometry. Only contributions with a weight > 10% are listed.

References

1. P.-K. Chow, G. Cheng, G. S. M. Tong, W.-P.g To, W.-L. Kwong, K.-H. Low, C.-C. Kwok, C. Ma, C.-M. Che, Luminescent Pincer Platinum(II) Complexes with Emission Quantum Yields up to Almost Unity: Photophysics, Photoreductive C–C Bond Formation, and Materials Applications, *Angew. Chem. Int. Ed.* 2015, **54**, 2084–2089.